

# **R/V Mirai Cruise Report**

## **MR12-03**

*July 17, 2012 – August 29, 2012*  
*Tropical Ocean Climate Study (TOCS)*



Japan Agency for Marine-Earth Science and Technology  
(JAMSTEC)



## Table of contents

1. Cruise name and code	1-1
2. Introduction and observation summary	2-1
2.1 Introduction	2-1
2.2 Overview	2-2
2.3 Observation summary	2-2
2.4 Observed oceanic and atmospheric conditions	2-4
3. Period, ports of call, cruise log and cruise track	3-1
3.1 Period	3-1
3.2 Ports of call	3-1
3.3 Cruise log	3-1
3.4 Cruise track	3-14
4. Chief scientist	4-1
5. Participants list	5-1
5.1 R/V MIRAI scientists and technical staffs	5-1
5.2 R/V MIRAI crew members	5-2
6. General observations	6-1
6.1 Meteorological measurements	6-1
6.1.1 Surface meteorological observations	6-1
6.1.2 Ceilometer	6-10
6.2 CTD/XCTD	6-14
6.2.1 CTD	6-14
6.2.2 XCTD	6-31
6.3 Water sampling	6-36
6.3.1 Salinity	6-36
6.4 Continuous monitoring of surface seawater	6-41
6.4.1 Temperature, salinity and dissolved oxygen	6-41
6.5 Underway pCO <sub>2</sub>	6-45
6.6 Shipboard ADCP	6-47
6.7 Underway geophysics	6-51
6.7.1 Sea surface gravity	6-51
6.7.2 Sea surface magnetic field	6-53
6.7.3 Swath bathymetry	6-55
7. Special observations	7-1
7.1 TRITON buoys	7-1
7.1.1 Operation of the TRITON buoys	7-1
7.1.2 Inter-comparison between shipboard CTD and TRITON transmitted data	7-7
7.1.3 Performance test of pCO <sub>2</sub> sensor	7-11
7.2 Subsurface ADCP moorings	7-13

7.3 Current profile observations using a high frequency lowered acoustic Doppler current profiler	7-21
7.4 Observation of ocean turbulence	7-27
7.5 Argo floats	7-33
7.5.1 Profiling floats for JAMSTEC Argo Project	7-33
7.5.2 ARGO float mission off Papua New Guinea	7-35
7.6 Global Drifter Program – SVP Drifting Buoys	7-38
7.7 Radiosonde observation for the validation of GOSAT and ship-borne sky radiometer products	7-40
7.8 Validation of GOSAT products over sea using a ship-borne compact system for measuring atmospheric trace gas column densities	7-44
7.9 Lidar observations of clouds and aerosol	7-47
7.10 Aerosol optical characteristics measured by Shipborne Sky radiometer	7-49
7.11 Continuous measurement of the water stable isotopes over the Ocean	7-50
7.12 Rock sampling using a dredge	7-55

**Note:**

**This cruise report is a preliminary documentation as of the end of the cruise. It may not be revised even if new findings and others are derived from observation results after publication. It may also be changed without notice. Data on the cruise report may be raw or not processed. Please ask the chief scientist for the latest information before using this report. Users of data or results of this cruise are requested to submit their results to Data Integration and Analysis Group (DIAG), JAMSTEC (e-mail: [diag-dmd@jamstec.go.jp](mailto:diag-dmd@jamstec.go.jp)).**

## **1. Cruise name and code**

Tropical Ocean Climate Study

MR12-03

Ship: R/V Mirai

Captain: Yasushi Ishioka

## **2. Introduction and observation summary**

### **2.1 Introduction**

The purpose of this cruise is to observe ocean and atmosphere in the western tropical Pacific Ocean for better understanding of climate variability involving the ENSO (El Nino/Southern Oscillation) phenomena. Particularly, warm water pool (WWP) in the western tropical Pacific is characterized by the highest sea surface temperature in the world, and plays a major role in driving global atmospheric circulation. Zonal migration of the WWP is associated with El Nino and La Nina which cause drastic climate changes in the world such as 1997-98 El Nino and 1999 La Nina. However, this atmospheric and oceanic system is so complicated that we still do not have enough knowledge about it.

In order to understand the mechanism of the atmospheric and oceanic system, its high quality data for long period is needed. Considering this background, we developed the TRITON (TRIangle Trans-Ocean buoy Network) buoys and have deployed them in the western equatorial Pacific and eastern Indian Ocean since 1998 cooperating with USA, Indonesia, and India. The major mission of this cruise is to maintain the network of TRITON buoys along 147E and 156E lines in the western equatorial Pacific.

During this cruise, we observe the low-latitude western boundary currents in the South Pacific contributing to the SPICE (Southwest Pacific Ocean Circulation and Climate Experiment) project, which was endorsed by CLIVAR in 2008. We conduct observations in the area of north of New Ireland of Papua New Guinea because we focus the New Ireland Coastal Undercurrent (NICU), where observation data is very limited. For this purpose, two subsurface Acoustic Doppler Current Profiler (ADCP) buoys are deployed and one Argo float is launched near the northern coast of New Ireland. Additionally, XCTD and shipboard ADCP observations are conducted in the Papua New Guinea EEZ/territorial water.

We have been observed ocean fine structure in order to understand ocean mixing effect on tropical ocean climate since MR07-07 leg 1 collaborating with International Pacific Research Center (IPRC) of USA. For this purpose, we conducted CTD observations with a Lowered ADCP (LADCP) and ocean turbulence observations along 147E and 156E lines.

During this cruise, 20 surface drifters, which were prepared by Atlantic Oceanographic and Atmospheric Laboratory (AOML) of National Oceanic and Atmospheric Administration (NOAA), are deployed for contribution to the global observational network along 156E between 5S and 14N.

Radiosonde observations were conducted in the Kuroshio Extension region and Tropical region for understanding air-sea interaction in the Kuroshio Extension, and getting support data for CO<sub>2</sub> measurement.

North of Papua New Guinea is also interesting area in geophysics. Particularly, the Early Cretaceous Ontong Java Plateau and neighboring ocean basin flood basalts in the western Pacific constitute the most voluminous Large Igneous Province on the Earth. For further better

understanding of mechanism of generation of Ontong Java Plateau, bottom igneous rocks and sediments on the ocean bottom are sampled using a dredge near the Nuugurigia Island (4-16S, 157-23E) during this cruise.

Except for above, automatic continuous oceanic, meteorological and geophysical observations are also conducted along ship track during this cruise as usual. In particular, a cesium magnetometer is towed in the Lyra Basin (Between 147E and 156E) and near the dredge points.

## **2.2 Overview**

### **1) Ship**

R/V Mirai

Captain Yasushi Ishioka

### **2) Cruise code**

MR12-03

### **3) Project name**

Tropical Ocean Climate Study (TOCS)

### **4) Undertaking institution**

Japan: Japan Agency for Marine-Earth Science and Technology (JAMSTEC)  
2-15, Natsushima-cho, Yokosuka, 237-0061, Japan

### **5) Chief scientist**

Chief Scientist (Japan)

Yuji Kashino, Japan Agency for Marine-Earth Science and Technology (JAMSTEC)

### **6) Period**

July 17, 2012 (Sekinehama, Japan) – August 29, 2012 (Sekinehama, Japan)

### **7) Research participants**

Seven scientists, one engineer, and twenty marine technicians from Japanese Institutes/University/Companies

## **2.3 Observation summary**

TRITON buoy recovery and re-installation:	9 moorings were deployed and 9 moorings were recovered.
Subsurface ADCP moorings:	3 moorings were deployed and

	2 moorings were recovered
CTD (Conductivity, Temperature and Depth) and water sampling:	43 casts
XCTD:	36 casts
Ocean turbulence observation	78 casts
Launch of Argo floats	2 floats
Launch of surface drifters	20 drifters
Radiosonde	45 casts
Rain and surface water sampling for isotope analysis	
	37 casts for rain and 43 casts for surface water
Current measurements by shipboard ADCP:	continuous
Sea surface temperature, salinity, and dissolved oxygen, measurements by intake method:	continuous
CO2 measurement	continuous
Surface meteorology:	continuous
Water vapor observation:	continuous
Underway geophysics observations	continuous
Towing a cesium magnetometer and sub-bottom profiler observations	continuous, 3 times
Rock sampling using a dredge	6 times

At first, engine trouble during this cruise should be noted; one of four engines of R/V Mirai did not work from 25 July to 21 August. and cruise speed reduced to 11 knot during this period. Because of this trouble, we should save ship time and canceled four casts of CTD/ocean turbulence observations between 2.5N and 4N along 147E. Except for these cancel, we conducted all planned observations. Engine was repaired on 21 August.

We recovered and re-installed nine TRITON buoys along 147E and 156E lines during this cruise. Among of them, TRITON buoy #4 started drifting on 28 May 2012, and its float and underwater sensors until 150m depth were recovered by Korean Research Vessel, R/V Onnuri, on 28 June. We found underwater parts of this buoy below 175m on 11 August using acoustic instrument, and recover them on 12 August. Unfortunately, we found that the ADCP installed at the depth of 175m was lost. We did not find severe damages of buoys except for the TRITON buoy #4.

We also successfully recovered and deployed subsurface ADCP buoys. However, data from the ADCPs could not be downloaded. Battery of the ADCP was exhausted when they were recovered because mooring period was extended to 1.5 years although parameters of ADCP were for one-year mooring. From this cruise, we changed ADCP parameters for 1.5-years mooring (the number of pings of ADCP per unit time was reduced).

During this cruise, we conducted shallow CTD casts with a LADCP until 500m or 800m depth and ocean turbulence observation using a Microstructure Profiler (MSP), Turbo-Map L, along 147E and 156 lines. Additionally, we conduct following special observations using CTD/LADCP and

MSP for better understanding of ocean fine structure and its time variability:

- (a) Observations with meridional interval of 15 nautical miles between 2N and equator along 156E. Each station consists of a CTD/LADCP cast to 500m depth followed by 3 MSP casts. .
- (b) A 24-hour station at the equator, 156E with a CTD/LADCP cast every 3hrs with 3 MSP casts in between.

We deployed two Argo floats during this cruise. One was aimed to construct the global ocean dataset under Japan Argo Project. The other was deployed for measuring temperature/salinity profiles in the NICU region. Unfortunately, data communication from the latter float was stopped after sending data of only one profile. We need to check its reason after this cruise.

As shown in 2.1, we carried out rock sampling using a dredge from 6 August to 8 August. During this period, towing of dredge was carried out 6 times around 4-16S, 157-23E on the flanks of the three sea mount. Although fuse wire of the dredge was cut two times, rocks and dredge were successfully recovered.

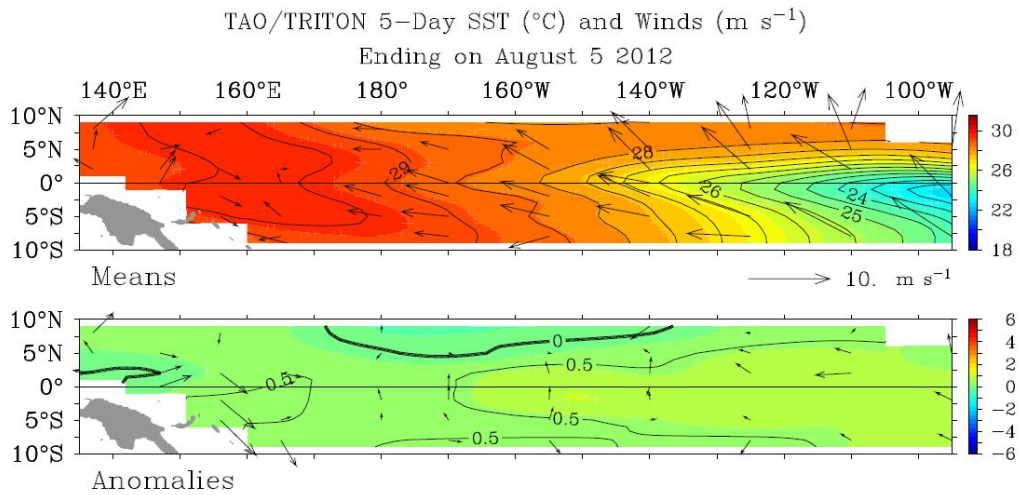
All automatic continuous meteorological, oceanographic and geophysical observations were carried out well.

Thus, we conducted all planed observations on schedule in this cruise except for cancel of four CTD/LADCP and MSP casts along 147E in spite of the engine trouble of R/V Mirai.

## **2.4 Observed oceanic and atmospheric conditions**

In 2012 boreal summer, atmosphere and ocean in the tropical Pacific was under the normal condition. Japan Meteorological Agency suggested possibility of occurrence of El Nino after this summer. Because of this condition, sea surface temperature (SST) anomaly was higher than 1 degree in the whole equatorial Pacific, and westerly wind was observed west of 156E (Figure. 2-1).

During this cruise, sea state was good and suitable for buoy maintenance work in spite of many rainy/cloudy days, which were associating with weak Madden Julian Oscillation. Surface salinity was low because of this condition (Figure 2-2).



TAO Project Office/PMEL/NOAA

Figure 2-1. Maps of sea surface temperature and winds (upper panel), and their anomaly (lower panel) obtained from TAO/TRITON buoy array on 5 August 2012. (<http://www.pmel.noaa.gov/tao/jsdisplay/>)

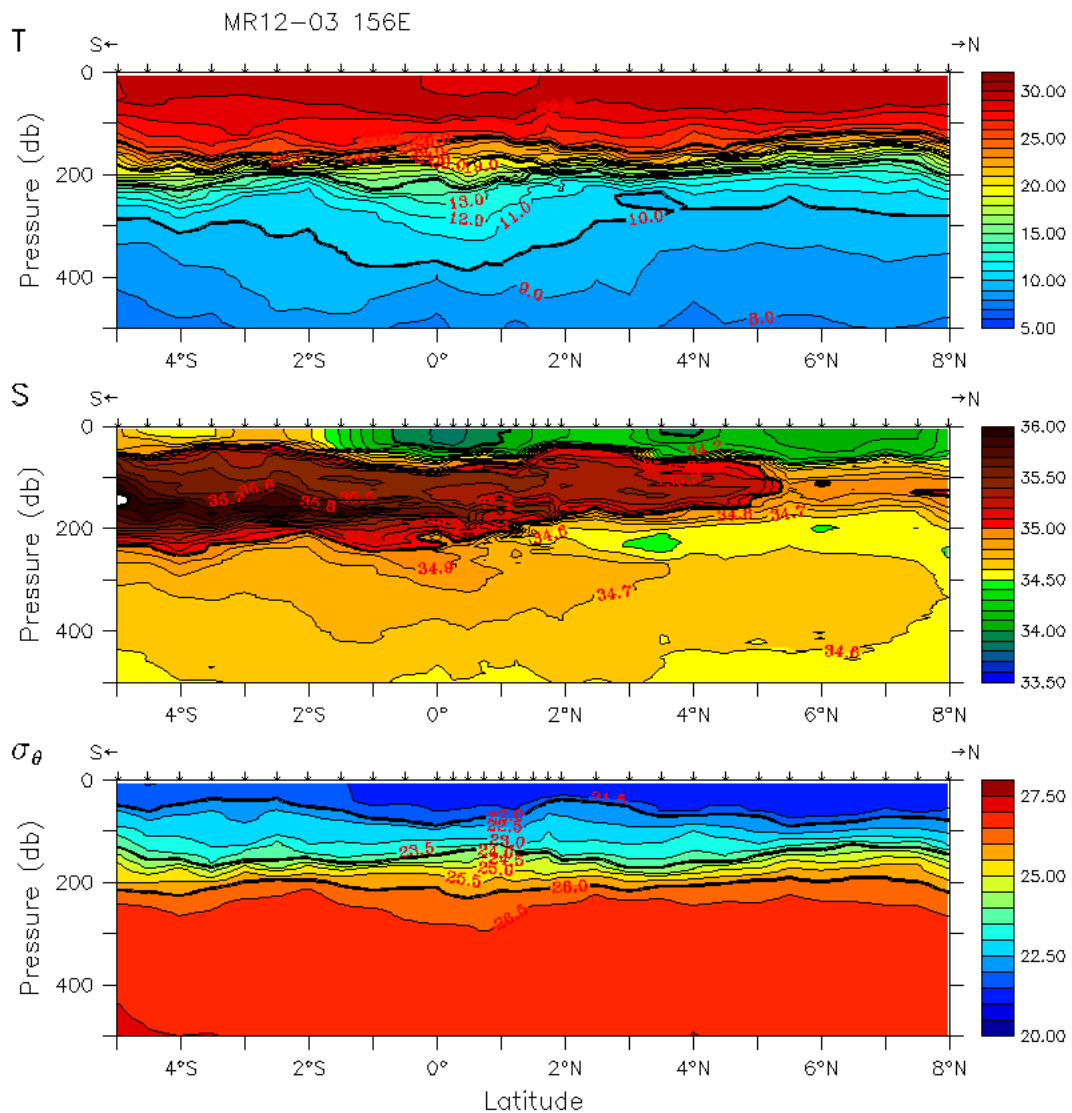


Figure 2-2. Temperature, salinity and potential density sections along 156E line.

### 3. Period, ports of call, cruise log and cruise track

#### 3.1 Period

17th July 2012 – 29th August 2012

#### 3.2 Ports of call

Sekinehama, Japan (Departure: 17th July 2012)

Sekinehama, Japan (Arrival: 29th August 2012)

#### 3.3 Cruise Log

<b>SMT</b>	<b>UTC</b>	<b>Event</b>
Jul. 17th (Tue.) 2012		
08:50	23:50 (-1day)	Departure of Sekinehama [Ship Mean Time (SMT)=UTC+9h]
10:30	01:30	Safety guidance
11:00	02:00	Surface sea water sampling start
13:15	04:15	Emergency drill
15:00	06:00	Observation Meeting
16:45	07:45	Konpira ceremony
Jul. 18th (Wed.) 2012		
05:34	20:34	Radiosonde observation (#1)
11:34	02:34	Radiosonde observation (#2)
17:31	08:31	Radiosonde observation (#3)
23:31	14:31	Radiosonde observation (#4)
Jul. 19th (Thu.) 2012		
05:31	20:31	Radiosonde observation (#5)
Jul. 20th (Fri.) 2012		
12:00	03:00	Radiosonde observation (#6)
12:07 – 12:30	03:07 – 03:30	CO <sub>2</sub> Observation (#1)
Jul. 21st (Sat.) 2012		
23:10	14:10	Radiosonde observation (#7)
Jul. 23rd (Mon.) 2012		
12:10	03:10	Radiosonde observation (#8)
12:11 – 12:40	03:11 – 03:40	CO <sub>2</sub> observation (#2)
Jul. 24th (Tue.) 2012		
22:00	13:00	Time adjustment +1h (SMT=UTC+10h)
Jul. 25th (Wed.) 2012		
00:25	14:25	Radiosonde observation (#9)
10:00	00:00	Arrival at St. 1 (TR#7; 05-00N, 147-00E)

<b>SMT</b>	<b>UTC</b>	<b>Event</b>
12:42	02:42	Radiosonde observation (#10)
12:42 – 13:12	02:42 – 03:12	CO <sub>2</sub> observation (#3)
13:06 – 15:46	03:06 – 15:46	Deployment of TRITON buoy TR#7 (#1) (Fixed Position: 04-57.8151N, 147-01.6231E)
16:49	06:49	XCTD observation X-01 (#1)
18:03 – 18:41	08:03 – 08:41	CTD dC01M01 (800m)
18:44 – 19:17	08:44 – 09:17	MSP observation (#1)
19:17 – 19:47	09:17 – 09:47	MSP observation (#2)
Jul. 26th (Thu.) 2012		
07:57 – 11:20	21:57 – 01:20	Recovery of TRITON buoy TR#7 (#1)
11:24	01:24	Departure of St. 1
14:42	04:42	Arrival at St. 2 (04-30N, 147-00E)
14:45 – 15:13	04:45 – 05:13	CTD dC02M01 (500m)
15:17 – 15:54	05:17 – 05:54	MSP observation (#3)
15:54	05:54	Departure of St. 2
18:42	08:42	XCTD observation X-02 (#2)
21:21	11:21	XCTD observation X-03 (#3)
Jul. 27th (Fri.) 2012		
00:03	14:03	XCTD observation X-04 (#4)
02:40	16:40	XCTD observation X-05 (#5)
05:18	19:18	Arrival at St. 3 (TR#8; 02-00N, 147-00E)
05:30 – 06:11	19:30 – 20:11	CTD dC03M01 (800m; near the TR#8 Recovery point)
06:16 – 06:54	20:16 – 20:54	MSP observation (#4)
08:04 – 11:35	22:04 – 01:35	Recovery of TRITON buoy TR#8 (#2)
11:36	01:36	Departure of St. 3
14:42	04:42	Arrival at St. 4 (01-30N, 147-00E)
14:45 – 15:13	04:45 – 05:13	CTD dC04M01 (500m)
15:17 – 15:55	05:17 – 05:55	MSP observation (#5)
16:00	06:00	Departure of St. 4
18:36	08:36	Arrival at St. 5 (01-00N, 147-00E)
18:40 – 19:09	08:40 – 09:09	CTD dC05M01 (500m)
19:15 – 19:54	09:15 – 09:54	MSP observation (#6)
20:00	10:00	Departure of St. 5
Jul. 28th (Sat.) 2012		
00:05	14:25	Radiosonde observation (#11)
04:48	18:48	Arrival at St. 3 (TR#8; 02-00N, 147-00E)
05:07 – 05:30	19:07 – 19:30	Figure-8 turn for Three-components magnetometer calibration (02-04.9N, 146-59.6E, #1)

<b>SMT</b>	<b>UTC</b>	<b>Event</b>
08:06 – 11:00	22:06 – 01:00	Deployment of TRITON buoy TR#8 (#2) (Fixed Position: 02-04.4521N, 146-57.1186E)
12:40	02:40	Radiosonde observation (#12)
13:35	03:35	XCTD observation X-06 (#6)
13:36	03:36	Departure of St. 3
Jul. 29th (Sun.) 2012		
05:12	19:12	Arrival at St. 7 (TR#9; EQ, 147-00E)
08:05 – 10:29	22:05 – 00:29	Deployment of TRITON buoy TR#9 (#3) (Fixed Position: 00-03.5409N, 147-00.6787E)
11:18	01:18	XCTD observation X-07 (#7)
12:59 – 14:53	02:59 – 04:53	Recovery of ADCP buoy (#1)
16:12	06:12	Departure of St. 7
18:30	08:30	Arrival at St. 6 (00-30N, 147-00E)
18:35 – 19:06	08:35 – 09:06	CTD dC06M01 (500m)
19:10 – 19:45	09:10 – 09:45	MSP observation (#7)
19:48	09:48	Departure of St. 6
Jul. 30th (Mon.) 2012		
02:00	16:00	Arrival at St. 7 (TR#9; EQ, 147-00E)
05:14 – 05:58	19:14 – 19:58	CTD dC07M01 (1000m; near the TR#9 Recovery point)
06:04 – 06:38	20:04 – 20:38	MSP observation (#8)
07:57 – 11:06	21:57 – 01:06	Recovery of TRITON buoy TR#9 (#3)
11:38	01:38	Departure of St. 7
11:23	01:23	Start of Cesium magnetometer observation (#1)
13:02	03:02	Suspend of Cesium magnetometer observation
13:44	03:44	Re-start of Cesium magnetometer observation
Jul. 31st (Tue.) 2012		
00:25	14:25	Radiosonde observation (#13)
12:40	02:25	Radiosonde observation (#14)
12:40 – 13:10	02:40 – 03:10	CO <sub>2</sub> observation (#4)
22:00	12:00	Time adjustment +1h (SMT=UTC+11h)
Aug. 1st (Wed.) 2012		
05:56	18:56	End of Cesium magnetometer observation (#1)
09:11	22:11	XCTD observation X-08 (#8)
11:05	00:05	XCTD observation X-09 (#9)
11:48	00:48	Arrival at St. ADCP#1 (02-38.1S, 153-20.1E)
12:58 – 14:16	01:58 – 03:16	Deployment of ADCP buoy (#1) (Fixed Position: 02-38.1725S, 153-21.0438E)
14:54	03:54	Departure of St. ADCP#1
15:36	04:36	Arrival at St.8 (02-43.2S, 153-16.65E)

<b>SMT</b>	<b>UTC</b>	<b>Event</b>
15:40 – 16:24	04:40 – 05:24	CTD dC08M01 (1000m)
16:29	05:29	Deployment of Argo float (#1)
16:30	05:30	Departure of St. 8
17:04	06:04	XCTD observation X-10 (#10)
18:48	07:48	XCTD observation X-11 (#11)
20:43	09:43	XCTD observation X-12 (#12)
22:38	11:38	XCTD observation X-13 (#13)
Aug. 2nd (Thu.) 2012		
04:12	17:12	Arrival at St. ADCP#2 (2-48.3S, 153-13.2E)
07:57 – 09:21	20:57 – 22:21	Deployment of ADCP buoy (#2) (Fixed Position: 02-48.3474S, 153-13.1757E)
10:00	23:00	Departure of St. ADCP#2
13:11	02:11	Radiosonde observation (#15)
13:11 – 13:41	02:11 – 02:41	CO <sub>2</sub> observation (#5)
16:03	05:03	XCTD observation X-14 (#14)
18:08	07:07	XCTD observation X-15 (#15)
20:18	09:18	XCTD observation X-16 (#16)
22:25	11:25	XCTD observation X-17 (#17)
Aug. 3rd (Fri.) 2012		
00:18	13:18	XCTD observation X-18 (#18)
01:25	14:25	Radiosonde observation (#16)
02:19	15:19	XCTD observation X-19 (#19)
04:14	17:14	XCTD observation X-20 (#20)
06:00	19:00	XCTD observation X-21 (#21)
07:45	20:45	XCTD observation X-22 (#22)
09:27	22:27	XCTD observation X-23 (#23)
18:12	07:12	Arrival at St. 12 (03-30S, 156-00E)
18:17 – 18:52	07:17 – 07:52	CTD dC12M01 (500m)
18:56 – 19:32	07:56 – 08:32	MSP observation (#9)
19:36	08:36	Departure of St. 12
Aug. 4th (Sat.) 2012		
05:18	18:18	Arrival at St. 9 (TR#6; 05-00S, 156-00E)
05:28 – 05:53	18:28 – 18:18	Figure-8 turn for Three-components magnetometer calibration (05-01.6S, 156-01.0E, #2)
08:04 – 09:38	22:04 – 23:38	Deployment of TRITON buoy TR#6 (#4) (Fixed Position: 05-02.0108S, 156-01.5378E)
13:01 – 13:43	02:01 – 02:43	CTD dC09M01 (800m)
13:47 – 14:23	02:47 – 02:23	MSP observation (#10)
14:24	03:24	Departure of St. 9

<b>SMT</b>	<b>UTC</b>	<b>Event</b>
17:36	06:36	Arrival at St. 10 (04-30S, 156-00E)
17:39 – 18:07	06:39 – 07:07	CTD dC10M01 (500m)
18:10 – 18:46	07:10 – 07:46	MSP observation (#11)
18:48	07:48	Departure of St. 10
21:36	10:36	Arrival at St. 9 (TR#6; 05-00S, 156-00E)
21:37	10:37	XCTD observation X-24 (#24)
Aug. 5th (Sun.) 2012		
07:56 – 10:26	20:56 – 00:26	Recovery of TRITON buoy TR#6 (#4)
10:33	00:33	Deployment of Drifter buoy (#1)
10:36	00:36	Departure of St. 9
13:12	02:12	Radiosonde observation (#17)
16:12	05:12	Arrival at St. 11 (04-00S, 156-00E)
16:17 – 16:49	05:17 – 05:49	CTD dC11M01 (500m)
16:49 – 17:25	05:49 – 06:25	MSP observation (#12)
17:28	06:28	Deployment of Drifter buoy (#2)
17:28	06:28	Start of OTJ site survey (MBES and Sub-bottom profiler)
17:30	06:30	Departure of St. 11
21:42	10:42	XCTD observation X-D1 (#25)
Aug. 6th (Mon.) 2012		
01:25	14:25	Radiosonde observation (#18)
03:03	16:03	XCTD observation X-D2 (#26)
06:19	19:19	End of OTJ site survey (MBES and Sub-bottom profiler)
06:42	19:42	Arrival at St. Dredge (04-16S, 157-24E)
08:00 – 10:27	21:00 – 23:27	Dredge (#1)
12:54 – 15:22	01:54 – 04:22	Dredge (#2)
15:43	04:43	Start of Cesium magnetometer observation (#2)
15:54	04:54	Departure of St. Dredge
15:54	04:54	Start of OTJ site survey (MBES and Sub-bottom profiler)
19:04	08:04	XCTD observation X-D3 (#27)
Aug. 7th (Tue.) 2012		
06:28	19:28	End of Cesium magnetometer observation (#2)
06:29	19:29	End of OTJ site survey (MBES and Sub-bottom profiler)
06:42	19:42	Arrival at St. Dredge
07:57 – 10:20	20:57 – 23:20	Dredge (#3)
12:54 – 15:32	01:54 – 04:32	Dredge (#4)
15:51	04:51	Start of Cesium magnetometer observation (#3)
15:54	04:54	Departure of St. Dredge
16:06 – 16:52	05:06 – 05:52	Figure-8 turn for Three-components magnetometer calibration (04-16.0S, 157-26.3E, #3)

<b>SMT</b>	<b>UTC</b>	<b>Event</b>
16:56	05:56	Start of OTJ site survey (MBES and Sub-bottom profiler)
Aug. 8th (Wed.) 2012		
02:10	15:10	Radiosonde observation (#19)
06:29	19:29	End of OTJ site survey (MBES and Sub-bottom profiler)
06:30	19:30	End of Cesium magnetometer observation (#3)
07:00	20:00	Arrival at St. Dredge
07:56 – 10:27	20:56 – 23:27	Dredge (#5)
12:22 – 15:31	01:22 – 04:31	Dredge (#6)
13:10	02:10	Radiosonde observation (#20)
13:10 – 13:40	02:10 – 02:40	CO <sub>2</sub> observation (#6)
15:36	04:36	Departure of St. Dredge
15:53	04:53	Start of OTJ site survey (MBES and Sub-bottom profiler)
Aug. 9th (Thu.) 2012		
01:25	14:25	Radiosonde observation (#21)
05:30	18:30	Arrival at St. 15 (TR#9; 02-00S, 156-00E)
		End of OTJ site survey (MBES and Sub-bottom profiler)
05:35 – 06:18	18:35 – 19:18	CTD dC15M01 (800m)
06:21 – 06:59	19:21 – 19:59	MSP observation (#13)
07:57 – 10:36	20:57 – 00:36	Recovery of TRITON buoy TR#5 (#5)
10:42	23:42	Departure of St. 15
13:24	02:24	Arrival at St. 14 (02-30S, 156-00E)
13:28 – 13:56	02:28 – 02:56	CTD dC14M01 (500m)
14:02 – 14:36	03:02 – 03:36	MSP observation (#14)
14:36	03:36	Departure of St. 14
17:24	06:24	Arrival at St. 13 (03-00S, 156-00E)
17:26 – 17:55	06:26 – 06:55	CTD dC13M01 (500m)
17:58 – 18:33	06:58 – 07:33	MSP observation (#15)
18:50 – 19:22	07:50 – 08:22	MSP observation (#16)
19:25	08:25	Deployment of Drifter buoy (#3)
19:30	08:30	Departure of St. 14
Aug. 10th (Fri.) 2012		
06:12	19:12	Arrival at St. 15 (TR#9; 02-00S, 156-00E)
08:05 – 10:04	21:05 – 23:04	Deployment of TRITON buoy TR#5 (#5) (Fixed Position: 02-01.0319S, 155-57.5176E)
12:25	01:25	Deployment of Drifter buoy (#3)
12:26	01:26	XCTD observation X-25 (#28)
12:30	01:30	Departure of St. 15
14:09	03:09	Radiosonde observation (#22)
15:24	04:24	Arrival at St. 16 (01-30S, 156-00E)

<b>SMT</b>	<b>UTC</b>	<b>Event</b>
15:25 – 15:56	04:25 – 04:56	CTD dC16M01 (500m)
16:01 – 16:35	05:01 – 05:35	MSP observation (#17)
16:36	05:36	Departure of St. 16
19:30	08:30	Arrival at St. 17 (01-00S, 156-00E)
19:32 – 20:02	08:32 – 09:02	CTD dC17M01 (500m)
20:05 – 20:42	09:05 – 09:42	MSP observation (#18)
20:51	09:51	Deployment of Drifter buoy (#3)
20:54	09:54	Departure of St. 17
Aug. 11th (Sat.) 2012		
00:50	13:50	Radiosonde observation (#23)
05:30	18:30	Arrival at St. 19 (TR#4; EQ, 156-00E)
08:05 – 09:49	21:05 – 22:49	Deployment of TRITON buoy TR#4 (#6) (Fixed Position: 00-00.9741N, 156-02.4995E)
10:21	23:21	XCTD observation X-26 (#29)
11:10	00:10	Radiosonde observation (#24)
12:53 – 14:10	01:53 – 03:10	Recovery of ADCP buoy (#2)
13:10	02:10	Radiosonde observation (#25)
15:11	04:11	Radiosonde observation (#26)
15:38 – 16:01	04:38 – 05:01	Search for TRITON buoy TR#4 & SSBL Calibration (Fixed Position: 00-01.0636S, 155-57.3603E)
17:58 – 18:24	06:58 – 07:24	Figure-8 turn for Three-components magnetometer calibration (00-03.2S, 155-58.6E, #4)
Aug. 12th (Sun.) 2012		
08:02 – 10:00	21:02 – 23:00	Recovery of TRITON buoy TR#4 (#6)
12:54 – 13:49	01:54 – 02:49	Deployment of ADCP buoy (#3) (Fixed Position: 00-02.2110S, 156-07.9543E)
14:10	03:10	Radiosonde observation (#27)
14:12	03:12	Departure of St. 19
17:18	06:18	Arrival at St. 18 (00-30S, 156-00E)
17:23 – 17:54	06:23 – 06:54	CTD dC18M01 (500m)
17:57 – 18:37	06:57 – 07:37	MSP observation (#19)
18:42	07:42	Departure of St. 18
Aug. 13th (Mon.) 2012		
01:00	14:00	Arrival at St. 19 (TR#4; EQ, 156-00E)
02:30	15:30	Radiosonde observation (#28)
05:58 – 06:30	18:58 – 19:30	CTD dC19M01 (500m)
06:33 – 07:09	19:33 – 20:09	MSP observation (#20)
07:11 – 07:45	20:11 – 20:45	MSP observation (#21)
07:47 – 08:24	20:47 – 21:24	MSP observation (#22)

<b>SMT</b>	<b>UTC</b>	<b>Event</b>
08:58 – 09:27	21:58 – 22:27	CTD dC19M02 (500m)
09:31 – 10:05	22:31 – 23:05	MSP observation (#23)
10:06 – 10:38	23:06 – 23:38	MSP observation (#24)
10:39 – 11:16	23:39 – 00:16	MSP observation (#25)
11:56 – 12:23	00:56 – 01:23	CTD dC19M03 (500m)
12:26 – 13:03	01:26 – 02:03	MSP observation (#26)
13:05 – 13:37	02:05 – 02:37	MSP observation (#27)
13:40 – 14:25	02:40 – 03:25	MSP observation (#28)
14:56 – 15:23	03:56 – 04:23	CTD dC19M04 (500m)
15:27 – 16:04	04:27 – 05:04	MSP observation (#29)
16:06 – 16:41	05:06 – 05:41	MSP observation (#30)
16:42 – 17:20	05:42 – 06:20	MSP observation (#31)
17:56 – 18:26	06:56 – 07:26	CTD dC19M05 (500m)
18:30 – 19:03	07:30 – 08:03	MSP observation (#32)
19:04 – 19:34	08:04 – 08:34	MSP observation (#33)
19:35 – 20:09	08:35 – 09:09	MSP observation (#34)
20:56 – 21:25	09:56 – 10:25	CTD dC19M06 (500m)
21:29 – 22:04	10:29 – 11:04	MSP observation (#35)
22:05 – 22:37	11:05 – 11:37	MSP observation (#36)
22:38 – 23:15	11:38 – 12:15	MSP observation (#37)
23:55 – 00:24	12:55 – 13:24	CTD dC19M07 (500m)
Aug. 14th (Tue.) 2012		
00:28 – 01:00	13:28 – 14:00	MSP observation (#38)
00:50	13:50	Radiosonde observation (#29)
01:01 – 01:31	14:01 – 14:31	MSP observation (#39)
01:32 – 02:08	14:32 – 15:08	MSP observation (#40)
02:55 – 03:23	15:55 – 16:23	CTD dC19M08 (500m)
03:27 – 03:57	16:27 – 16:57	MSP observation (#41)
03:58 – 04:30	16:58 – 17:30	MSP observation (#42)
04:31 – 05:06	17:31 – 18:06	MSP observation (#43)
05:55 – 06:26	18:55 – 19:26	CTD dC19M09 (500m)
06:30 – 07:06	19:30 – 20:06	MSP observation (#44)
07:07 – 07:40	20:07 – 20:40	MSP observation (#45)
07:41 – 08:19	20:41 – 21:19	MSP observation (#46)
08:22	21:22	Deployment of Drifter buoy (#6)
08:24	21:24	Departure of St. 19
09:48	22:48	Arrival at St. 20 (00-15N, 156-00E)
09:50 – 10:19	22:50 – 23:19	CTD dC20M01 (500m)
10:23 – 10:56	23:23 – 23:56	MSP observation (#47)

<b>SMT</b>	<b>UTC</b>	<b>Event</b>
10:57 – 11:30	23:57 – 00:30	MSP observation (#48)
11:31 – 12:09	00:31 – 01:09	MSP observation (#49)
12:12	01:12	Departure of St. 20
13:10	02:10	Radiosonde observation (#30)
13:10 – 13:40	02:10 – 03:40	CO <sub>2</sub> observation (#7)
13:36	02:36	Arrival at St. 21 (00-30N, 156-00E)
13:40 – 14:07	02:40 – 03:07	CTD dC21M01 (500m)
14:11 – 14:42	03:11 – 03:42	MSP observation (#50)
14:43 – 15:13	03:43 – 04:13	MSP observation (#51)
15:13 – 15:45	04:13 – 04:45	MSP observation (#52)
15:47 – 16:21	04:47 – 05:21	MSP observation (#53)
16:24	05:24	Departure of St. 21
17:42	06:42	Arrival at St. 22 (00-45N, 156-00E)
17:45 – 18:16	06:45 – 07:16	CTD dC22M01 (500m)
18:19 – 18:49	07:19 – 07:49	MSP observation (#54)
18:50 – 19:18	07:50 – 08:18	MSP observation (#55)
19:19 – 19:51	08:19 – 08:51	MSP observation (#56)
19:54	08:54	Departure of St. 22
21:12	10:12	Arrival at St. 23 (01-00N, 156-00E)
21:13 – 21:45	10:13 – 10:45	CTD dC23M01 (500m)
21:49 – 22:19	10:49 – 11:19	MSP observation (#57)
22:20 – 22:50	11:20 – 11:50	MSP observation (#58)
22:51 – 23:23	11:51 – 12:23	MSP observation (#59)
23:26	12:26	Deployment of Drifter buoy (#7)
23:30	12:30	Departure of St. 23
Aug. 15th (Wed.) 2012		
00:36	13:36	Arrival at St. 24 (01-15N, 156-00E)
00:40 – 01:07	13:40 – 14:07	CTD dC24M01 (500m)
01:10 – 01:40	14:10 – 14:40	MSP observation (#60)
01:25	14:25	Radiosonde observation (#31)
01:41 – 02:09	14:41 – 15:09	MSP observation (#61)
02:10 – 02:42	15:10 – 15:42	MSP observation (#62)
02:48	15:48	Departure of St. 24
04:06	17:06	Arrival at St. 25 (01-30N, 156-00E)
04:08 – 04:39	17:08 – 17:39	CTD dC25M01 (500m)
04:43 – 05:14	17:43 – 18:14	MSP observation (#63)
05:15 – 05:44	18:15 – 18:44	MSP observation (#64)
05:45 – 06:17	18:45 – 19:17	MSP observation (#65)
06:18	19:18	Departure of St. 25

<b>SMT</b>	<b>UTC</b>	<b>Event</b>
07:30	20:30	Arrival at St. 26 (01-45N, 156-00E)
07:35 – 08:05	20:35 – 21:05	CTD dC26M01 (500m)
08:10 – 08:45	21:10 – 21:45	MSP observation (#66)
08:46 – 09:22	21:46 – 22:22	MSP observation (#67)
09:23 – 09:59	22:23 – 22:59	MSP observation (#68)
10:00	23:00	Departure of St. 26
11:00	00:00	Arrival at St. 27 (TR#3; 02-00N, 156-00E)
11:04 – 11:44	00:04 – 00:44	CTD dC27M01 (800m)
11:47 – 12:19	00:47 – 01:19	MSP observation (#69)
12:20 – 12:50	01:20 – 01:50	MSP observation (#70)
12:51 – 13:24	01:51 – 02:24	MSP observation (#71)
13:24	02:24	Departure of St. 27
16:06	05:06	Arrival at St. 28 (02-30N, 156-00E)
16:11 – 16:41	05:11 – 05:41	CTD dC28M01 (500m)
16:44 – 17:23	05:44 – 06:23	MSP observation (#72)
17:24	06:24	Departure of St. 28
23:30	12:30	Arrival at St. 27 (TR#3; 02-00N, 156-00E)
Aug. 16th (Thu.) 2012		
08:03 – 09:55	21:03 – 22:55	Deployment of TRITON buoy TR#3 (#7) (Fixed Position: 02-02.2565N, 156-01.2636E)
12:28	01:28	XCTD observation X-27 (#30)
12:30	01:30	Departure of St. 27
17:18	06:18	Arrival at St. 29 (03-00N, 156-00E)
17:24 – 17:56	06:24 – 06:56	CTD dC29M01 (500m)
18:00 – 18:33	07:00 – 07:33	MSP observation (#73)
18:37	07:37	Deployment of Drifter buoy (#8)
18:42	07:42	Departure of St. 29
Aug. 17th (Fri.) 2012		
00:51	13:51	Radiosonde observation (#32)
05:30	18:30	Arrival at St. St. 27 (TR#3; 02-00N, 156-00E)
07:56 – 10:48	20:56 – 23:48	Recovery of TRITON buoy TR#3 (#7)
10:50	23:50	Deployment of Drifter buoy (#9)
10:54	23:54	Departure of St. 27
13:11	02:11	Radiosonde observation (#33)
18:42	07:42	Arrival at St. 30 (03-30N, 156-00E)
18:45 – 19:14	07:45 – 08:14	CTD dC30M01 (500m)
19:18 – 19:54	08:18 – 08:54	MSP observation (#74)
19:54	08:54	Departure of St. 30

<b>SMT</b>	<b>UTC</b>	<b>Event</b>
Aug. 18th (Sat.) 2012		
04:12	17:12	Arrival at St. St. 33 (TR#2; 05-00N, 156-00E)
05:26 – 06:05	18:26 – 19:05	CTD dC33M01 (800m)
06:09 – 06:47	19:09 – 19:47	MSP observation (#375)
07:57 – 11:42	20:57 – 00:42	Recovery of TRITON buoy TR#2 (#8)
11:42	00:42	Departure of St. 33
14:42	03:42	Arrival at St. St. 32 (04-30N, 156-00E)
14:45 – 15:15	03:45 – 04:14	CTD dC32M01 (500m)
15:19 – 15:53	04:19 – 04:53	MSP observation (#76)
15:54	04:54	Departure of St. 32
18:36	07:36	Arrival at St. St. 31 (04-00N, 156-00E)
18:42 – 19:15	03:45 – 04:14	CTD dC31M01 (500m)
19:18 – 19:53	08:18 – 08:53	MSP observation (#77)
19:55	08:55	Deployment of Drifter buoy (#10)
20:00	09:00	Departure of St. 31
Aug. 19th (Sun.) 2012		
05:30	18:30	Arrival at St. St. 33 (TR#2; 05-00N, 156-00E)
08:04 – 10:27	21:04 – 23:27	Deployment of TRITON buoy TR#2 (#8) (Fixed Position: 05-01.2108N, 155-58.0056E)
12:22	01:22	Deployment of Drifter buoy (#11)
12:23	01:23	XCTD observation X-28 (#31)
12:24	01:24	Departure of St. 33
14:10	03:10	Radiosonde observation (#34)
15:10	04:10	XCTD observation X-29 (#32)
17:55	06:55	Deployment of Drifter buoy (#12)
17:56	06:56	XCTD observation X-30 (#33)
20:34	09:34	XCTD observation X-31 (#34)
23:08	12:08	Deployment of Drifter buoy (#13)
23:09	12:09	XCTD observation X-32 (#35)
Aug. 20th (Mon.) 2012		
00:55	13:55	Radiosonde observation (#35)
01:52	14:52	XCTD observation X-33 (#36)
04:30	17:30	Arrival at St. St. 34 (TR#1; 08-00N, 156-00E)
05:30 – 06:10	18:30 – 19:10	CTD dC34M01 (800m)
05:40	18:40	XCTD observation X-34 (#37)
05:51	18:51	XCTD observation X-35 (#38)
06:13 – 06:48	19:13 – 19:48	MSP observation (#78)
07:57 – 11:25	20:57 – 00:25	Recovery of TRITON buoy TR#1 (#9)
13:10	02:10	Radiosonde observation (#36)

<b>SMT</b>	<b>UTC</b>	<b>Event</b>
13:10 – 13:40	02:10 – 02:40	CO <sub>2</sub> observation (#8)
13:40 – 14:17	02:40 – 03:17	Figure-8 turn for Three-components magnetometer calibration (07-57.3N, 155-59.9E, #5)
Aug. 21st (Tue.) 2012		
08:03 – 10:27	21:03 – 23:27	Deployment of TRITON buoy TR#1 (#9) (Fixed Position: 07-58.0164N, 156-01.9061E)
12:38	01:38	Deployment of Drifter buoy (#14)
12:39	01:39	XCTD observation X-36 (#39)
12:42	01:42	Departure of St. 34
18:30	07:30	Deployment of Drifter buoy (#15)
23:32	12:32	Deployment of Drifter buoy (#16)
Aug. 22nd (Wed.) 2012		
04:35	17:35	Deployment of Drifter buoy (#17)
09:36	22:36	Arrival at St. St. 35 (12-00N, 154-18E)
09:41 – 10:52	22:41 – 23:52	CTD dC35M01 (2000m)
10:56	23:56	Deployment of ARGO float (#2)
10:57	23:57	Deployment of Drifter buoy (#18)
11:00	00:00	Departure of St. 358
15:57	04:58	Deployment of Drifter buoy (#19)
21:00	10:00	Deployment of Drifter buoy (#20)
Aug. 23rd (Thu.) 2012		
00:57	13:57	Radiosonde observation (#37)
05:30	18:30	Arrival at Freefall point (15-12N, 152-46E)
06:02 – 09:37	19:02 – 22:37	CTD winch cable Freefall
09:42	22:42	Departure of Freefall point
Aug. 24th (Fri.) 2012		
01:31	14:31	Radiosonde observation (#38)
13:35	02:35	Radiosonde observation (#39)
22:00	11:00	Time adjustment -1h (SMT=UTC+10h)
Aug. 25th (Sat.) 2012		
13:05	03:05	Radiosonde observation (#40)
13:05 – 13:35	03:05 – 03:35	CO <sub>2</sub> observation (#9)
Aug. 27th (Mon.) 2012		
00:31	14:31	Radiosonde observation (#41)
06:30	18:30	Radiosonde observation (#42)
12:30	02:30	Radiosonde observation (#43)
18:30	08:30	Radiosonde observation (#44)
22:00	12:00	Time adjustment -1h (SMT=UTC+9h)
23:30	14:30	Radiosonde observation (#45)

<b>SMT</b>	<b>UTC</b>	<b>Event</b>
Aug. 28th (Tue.) 2012		
13:01	04:01	Surface sea water sampling stop
Dec. 29th (Wed.) 2012		
09:10	00:10	Arrival of Sekinehama

### 3.4 Cruise track

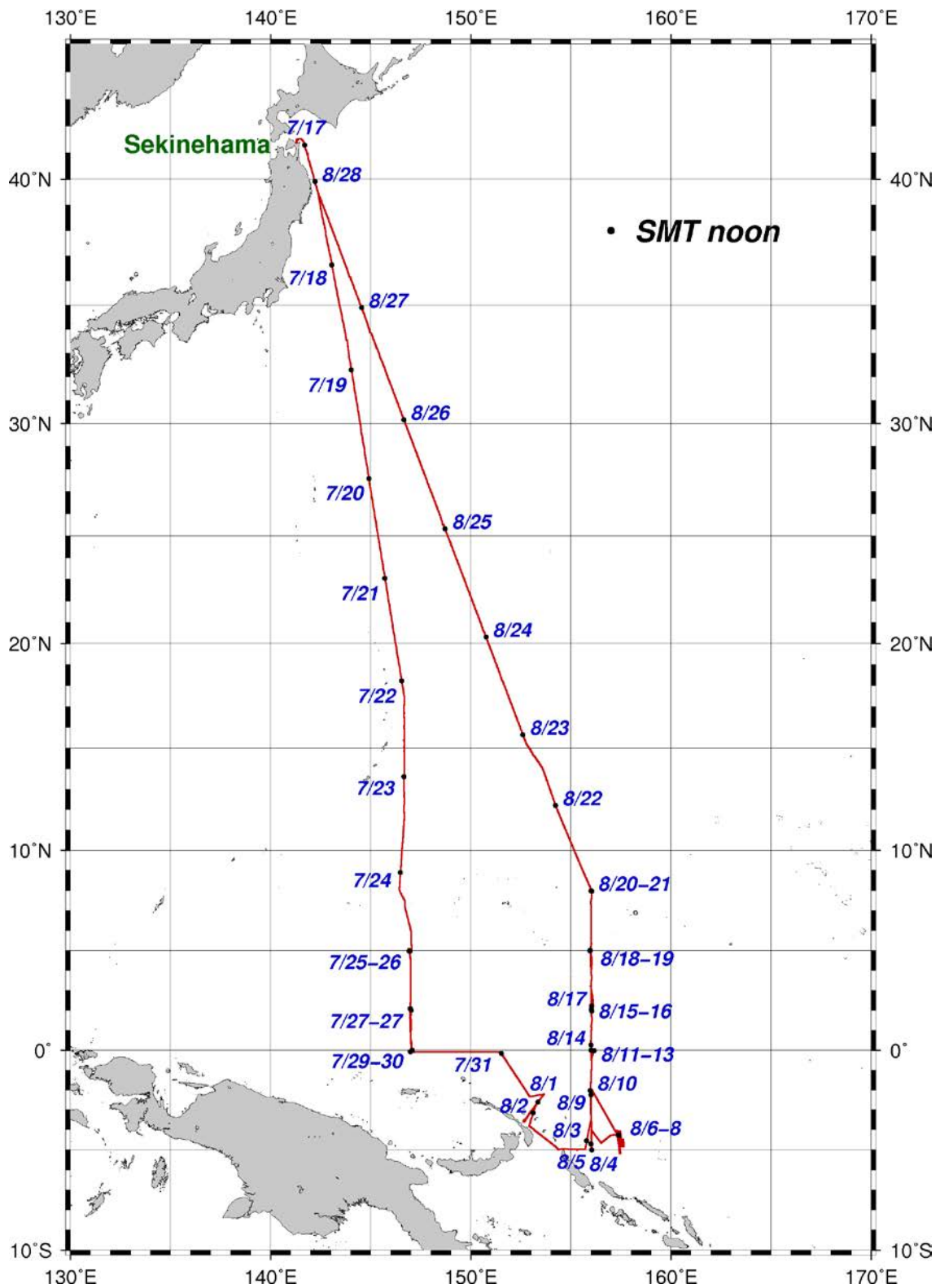


Fig 3-4-1. MR12-03 Cruise track and noon positions

#### **4. Chief scientist**

Chief Scientist

Yuji Kashino

Senior Research Scientist

Research Institute for Global Change (RIGC),

Japan Agency for Marine-Earth Science and Technology (JAMSTEC)

2-15, Natsushima-cho, Yokosuka, 237-0061, Japan

Tel: +81-468-67-9459, FAX: +81-468-67-9255

e-mail: [kashinoy@jamstec.go.jp](mailto:kashinoy@jamstec.go.jp)

## 5. Participants list

### 5.1 R/V MIRAI scientist and technical staff

Name	Affiliation	Occupation
Yuji Kashino	JAMSTEC	Chief Scientist
Takuya Hasegawa	JAMSTEC	Scientist
Takeshi Hanyu	JAMSTEC	Scientist
Kenji Shimizu	JAMSTEC	Scientist
Maria Luisa Tejada	JAMSTEC	Scientist
Shuji Kawakami	JAXA	Engineer
Miho Ishizu	IPRC, University of Hawaii	Scientist
Makoto Nakamura	University of Chiba	Scientist
Tomohide Noguchi	Marine Works Japan Ltd.	Technical Staff
Hiroshi Matunaga	Marine Works Japan Ltd.	Technical Staff
Hiroki Ushiromura	Marine Works Japan Ltd.	Technical Staff
Akira Watanabe	Marine Works Japan Ltd.	Technical Staff
Shungo Oshitani	Marine Works Japan Ltd.	Technical Staff
Tamami Ueno	Marine Works Japan Ltd.	Technical Staff
Rei Ito	Marine Works Japan Ltd.	Technical Staff
Tetsuharu Iino	Marine Works Japan Ltd.	Technical Staff
Minoru Kamata	Marine Works Japan Ltd.	Technical Staff
Hatsumi Aoyama	Marine Works Japan Ltd.	Technical Staff
Shoko Tatamisashi	Marine Works Japan Ltd.	Technical Staff
Yohei Taketomo	Marine Works Japan Ltd.	Technical Staff
Yuki Miyajima	Marine Works Japan Ltd.	Technical Staff
Tetsuya Nagahama	Marine Works Japan Ltd.	Technical Staff
Masaki Yamada	Marine Works Japan Ltd.	Technical Staff
Kazuma Takahashi	Marine Works Japan Ltd.	Technical Staff
Shihomi Saito	Marine Works Japan Ltd.	Technical Staff
Wataru Tokunaga	Global Ocean Development Inc.	Technical Staff
Harumi Ota	Global Ocean Development Inc.	Technical Staff
Koichi Inagaki	Global Ocean Development Inc.	Technical Staff

JAMSTEC: Japan Agency for Marine-Earth Science and Technology

JAXA: Japan Aerospace Exploration Agency

IPRC: International Pacific Research Center

## 5.2 R/V MIRAI crew member

Name	Rank or rating
Yasushi Ishioka	Master
Takeshi Isohi	Chief Officer
Hajime Matsuo	1st Officer
Yoshiharu Tsutsumi	Jr. 1st Officer
Haruka Wakui	2nd Officer
Hiroki Kobayashi	3rd Officer
Yoichi Furukawa	Chief Engineer
Hiroyuki Tohken	1st Engineer
Toshio Kiuchi	2nd Engineer
Koji Manako	3rd Engineer
Ryo Oyama	Technical Officer
Yosuke Kuwahara	Boatswain
Tsuyoshi Sato	Able Seaman
Takeharu Aisaka	Able Seaman
Tsuyoshi Monzawa	Able Seaman
Masashige Okada	Able Seaman
Hideyuki Okubo	Ordinary Seaman
Masaya Tanikawa	Ordinary Seaman
Shohei Uehara	Ordinary Seaman
Kazunari Mitsunaga	Ordinary Seaman
Akiya Chishima	Ordinary Seaman
Tetsuya Sakamoto	Ordinary Seaman

Name	Rank or rating
Yoshihiro Sugimoto	No.1 Oiler
Nobuo Boshita	Oiler
Kazumi Yamashita	Oiler
Shintaro Abe	Ordinary Oiler
Keisuke Yoshida	Ordinary Oiler
Hiromi Ikuta	Ordinary Oiler
Hitoshi Ota	Chief Steward
Ryotaro Baba	Cook
Masao Hosoya	Cook
Michihiro Mori	Cook
Shigenori Yamaguchi	Cook
Shohei Maruyama	Steward

## 6. General observations

### 6.1 Meteorological measurements

#### 6.1.1 Surface meteorological observations

Yuji Kashino	(JAMSTEC) : Principal Investigator
Wataru Tokunaga	(Global Ocean Development Inc., GODI)
Harumi Ota	(GODI)
Koichi Inagaki	(GODI)
Ryo Ohyama	(MIRAI Crew)

##### (1) Objectives

Surface meteorological parameters are observed as a basic dataset of the meteorology. These parameters bring us the information about the temporal variation of the meteorological condition surrounding the ship.

##### (2) Methods

Surface meteorological parameters were observed throughout the MR12-03 cruise. During this cruise, we used two systems for the observation.

- i. MIRAI Surface Meteorological observation (SMet) system
  - ii. Shipboard Oceanographic and Atmospheric Radiation (SOAR) system
- 
- i. MIRAI Surface Meteorological observation (SMet) system  
Instruments of SMet system are listed in Table.6.1.1-1 and measured parameters are listed in Table.6.1.1-2. Data were collected and processed by KOAC-7800 weather data processor made by Koshin-Denki, Japan. The data set consists of 6-second averaged data.
  - ii. Shipboard Oceanographic and Atmospheric Radiation (SOAR) measurement system  
SOAR system designed by BNL (Brookhaven National Laboratory, USA) consists of major three parts.
    - a) Portable Radiation Package (PRP) designed by BNL – short and long wave downward radiation.
    - b) Zeno Meteorological (Zeno/Met) system designed by BNL – wind, air temperature, relative humidity, pressure, and rainfall measurement.
    - c) Scientific Computer System (SCS) developed by NOAA (National Oceanic and Atmospheric Administration, USA) – centralized data acquisition and logging of all data sets.SCS recorded PRP data every 6 seconds, while Zeno/Met data every 10 seconds. Instruments and their locations are listed in Table.6.1.1-3 and measured parameters are listed in Table.6.1.1-4.

For the quality control as post processing, we checked the following sensors, before and after the cruise.

- i. Young Rain gauge (SMet and SOAR)  
Inspect of the linearity of output value from the rain gauge sensor to change Input value

- by adding fixed quantity of test water.
- ii. Barometer (SMet and SOAR)
  - Comparison with the portable barometer value, PTB220CASE, VAISALA.
- iii. Thermometer (air temperature and relative humidity) (SMet and SOAR)
  - Comparison with the portable thermometer value, HMP41/45, VAISALA.

(3) Preliminary results

Figure 6.1.1-1 shows the time series of the following parameters;

- Wind (SOAR)
- Air temperature (SMet)
- Sea surface temperature (SMet)
- Relative humidity (SMet)
- Precipitation (SOAR, Rain gauge)
- Short/long wave radiation (SOAR)
- Pressure (SMet)
- Significant wave height (SMet)

(4) Data archives

These meteorological data will be submitted to the Data Management Group (DMG) of JAMSTEC just after the cruise.

(5) Remarks

- i. Following period, SST (Sea Surface Temperature) data was available.
  - 02:01UTC 17 Jul. 2012 – 04:01UTC 28 Aug. 2012
- ii. In the following time, SMet rain gauge amount values were increased because of test transmitting for MF/HF radio
  - 05:50UTC – 05:55UTC 17 Jul. 2012
  - 03:54UTC – 04:00UTC 27 Aug. 2012

Table.6.1.1-1 Instruments and installations of MIRAI Surface Meteorological observation system

<u>Sensors</u>	<u>Type</u>	<u>Manufacturer</u>	<u>Location (altitude from surface)</u>
Anemometer	KE-500	Koshin Denki, Japan	foremast (24 m)
Tair/RH	HMP45A	Vaisala, Finland	
with 43408 Gill aspirated radiation shield		R.M. Young, USA	compass deck (21 m) starboard side and port side
Thermometer: SST	RFN1-0	Koshin Denki, Japan	4th deck (-1m, inlet -5m)
Barometer	Model-370	Setra System, USA	captain deck (13 m) weather observation room
Rain gauge	50202	R. M. Young, USA	compass deck (19 m)
Optical rain gauge	ORG-815DR	Osi, USA	compass deck (19 m)
Radiometer (short wave)	MS-802	Eiko Seiki, Japan	radar mast (28 m)
Radiometer (long wave)	MS-202	Eiko Seiki, Japan	radar mast (28 m)
Wave height meter	WM-2	Tsurumi-seiki, Japan	bow (10 m)

Table.6.1.1-2 Parameters of MIRAI Surface Meteorological observation system

Parameter	Units	Remarks
1 Latitude	degree	
2 Longitude	degree	
3 Ship's speed	knot	MIRAI log, DS-30 Furuno
4 Ship's heading	degree	MIRAI gyro, TG-6000, Tokimec
5 Relative wind speed	m/s	6sec./10min. averaged
6 Relative wind direction	degree	6sec./10min. averaged
7 True wind speed	m/s	6sec./10min. averaged
8 True wind direction	degree	6sec./10min. averaged
9 Barometric pressure	hPa	adjusted to sea surface level 6sec. averaged
10 Air temperature (starboard side)	degC	6sec. averaged
11 Air temperature (port side)	degC	6sec. averaged
12 Dewpoint temperature (starboard side)	degC	6sec. averaged
13 Dewpoint temperature (port side)	degC	6sec. averaged
14 Relative humidity (starboard side)	%	6sec. averaged
15 Relative humidity (port side)	%	6sec. averaged
16 Sea surface temperature	degC	6sec. averaged
17 Rain rate (optical rain gauge)	mm/hr	hourly accumulation
18 Rain rate (capacitive rain gauge)	mm/hr	hourly accumulation
19 Down welling shortwave radiation	W/m <sup>2</sup>	6sec. averaged
20 Down welling infra-red radiation	W/m <sup>2</sup>	6sec. averaged
21 Significant wave height (bow)	m	hourly
22 Significant wave height (aft)	m	hourly
23 Significant wave period (bow)	second	hourly
24 Significant wave period (aft)	second	hourly

Table.6.1.1-3 Instruments and installation locations of SOAR system

Sensors (Zeno/Met)	Type	Manufacturer	Location (altitude from surface)
Anemometer	05106	R.M. Young, USA	foremast (25 m)
Tair/RH	HMP45A	Vaisala, Finland	
with 43408 Gill aspirated radiation shield		R.M. Young, USA	foremast (23 m)
Barometer	61202V	R.M. Young, USA	
with 61002 Gill pressure port		R.M. Young, USA	foremast (23 m)
Rain gauge	50202	R.M. Young, USA	foremast (24 m)
Optical rain gauge	ORG-815DA	Osi, USA	foremast (24 m)
Sensors (PRP)	Type	Manufacturer	Location (altitude from surface)
Radiometer (short wave)	PSP	Epply Labs, USA	foremast (25 m)
Radiometer (long wave)	PIR	Epply Labs, USA	foremast (25 m)
Fast rotating shadowband radiometer		Yankee, USA	foremast (25 m)

Table.6.1.1-4 Parameters of SOAR system

Parameter	Units	Remarks
1 Latitude	degree	
2 Longitude	degree	
3 SOG	knot	
4 COG	degree	
5 Relative wind speed	m/s	
6 Relative wind direction	degree	
7 Barometric pressure	hPa	
8 Air temperature	degC	
9 Relative humidity	%	
10 Rain rate (optical rain gauge)	mm/hr	
11 Precipitation (capacitive rain gauge)	mm	reset at 50 mm
12 Down welling shortwave radiation	W/m2	
13 Down welling infra-red radiation	W/m2	
14 Defuse irradiance	W/m2	

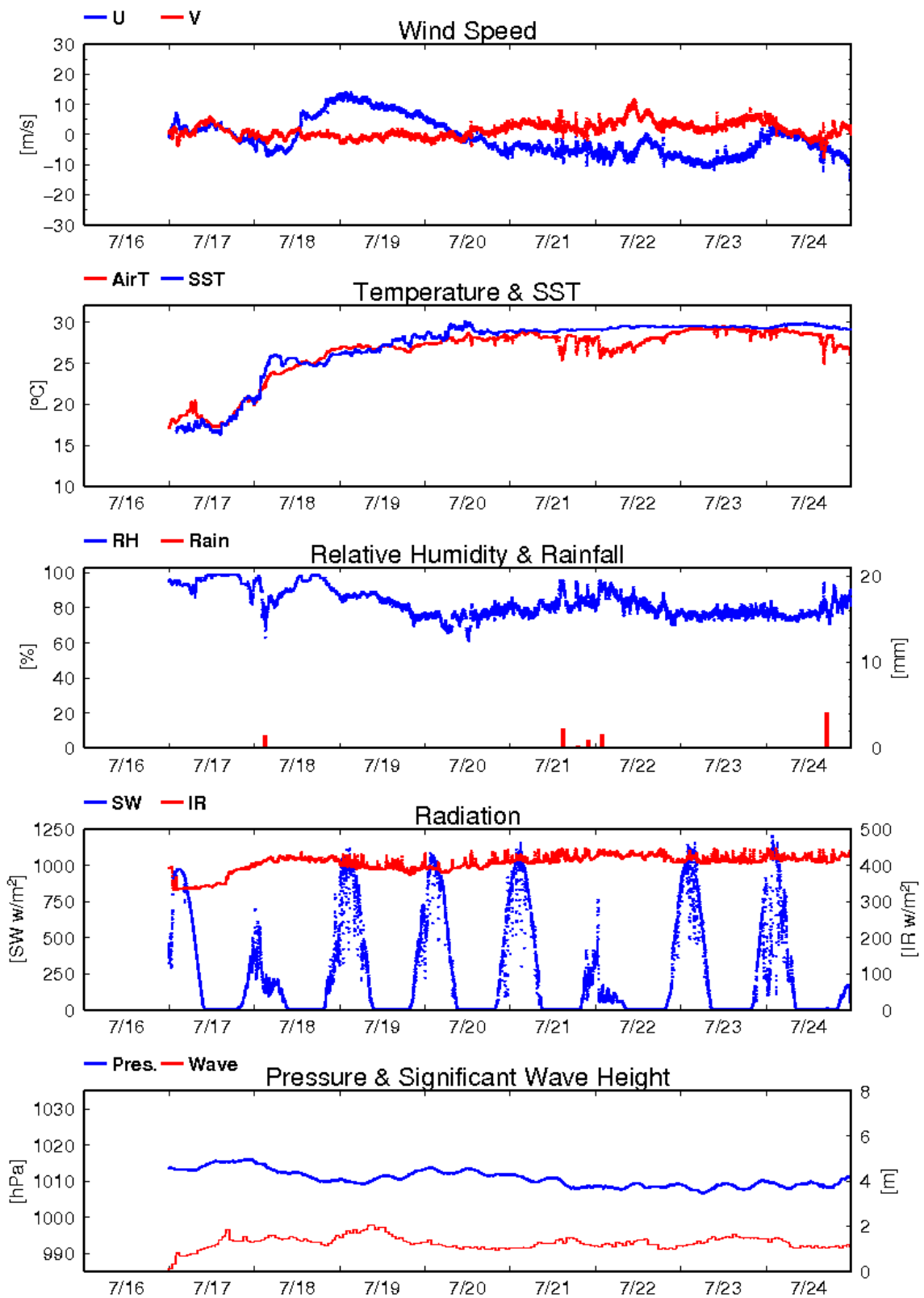


Fig.6.1.1-1 Time series of surface meteorological parameters during the MR12-03 cruise

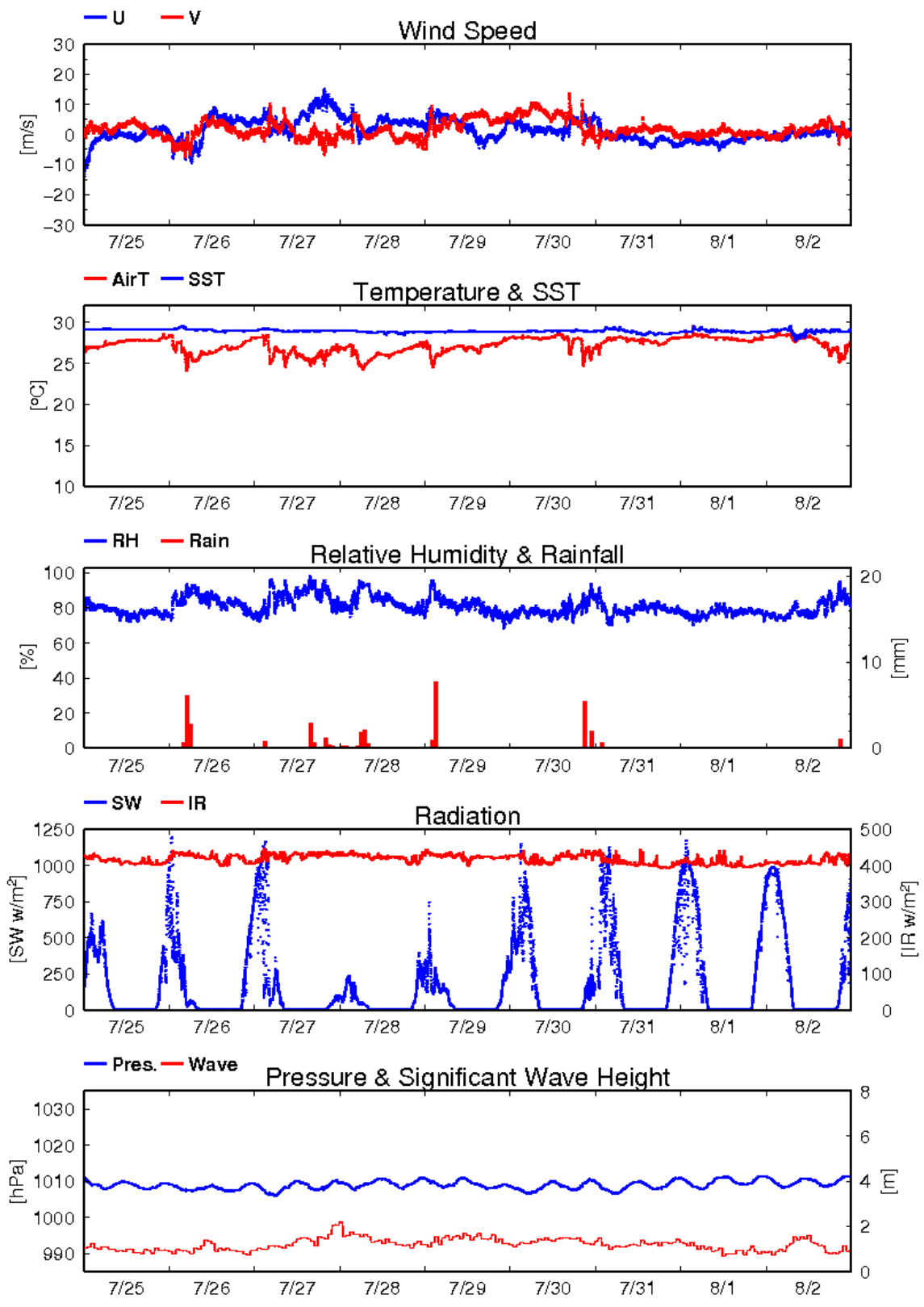


Fig. 6.1.1-1 (Continued)

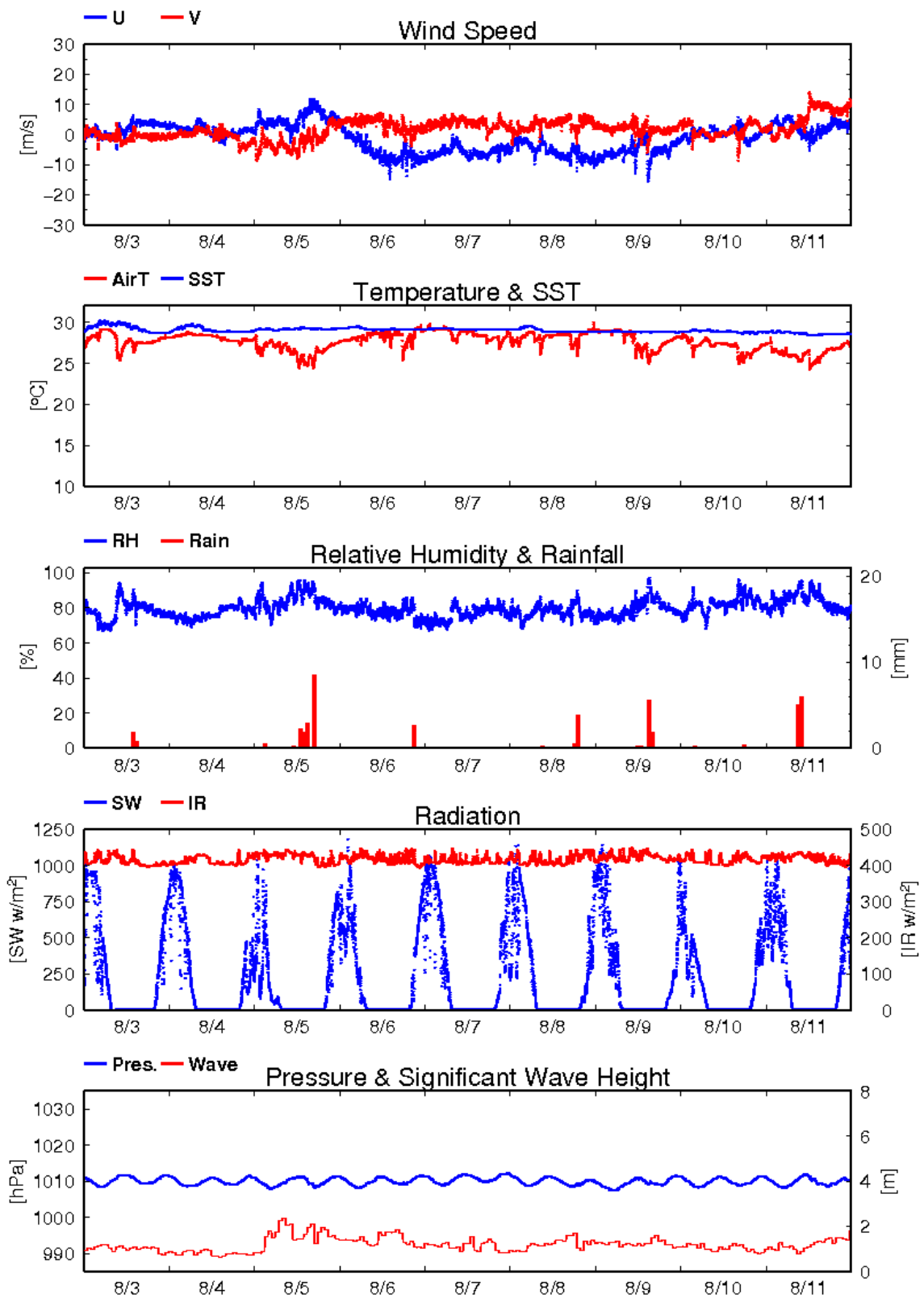


Fig. 6.1.1-1 (Continued)

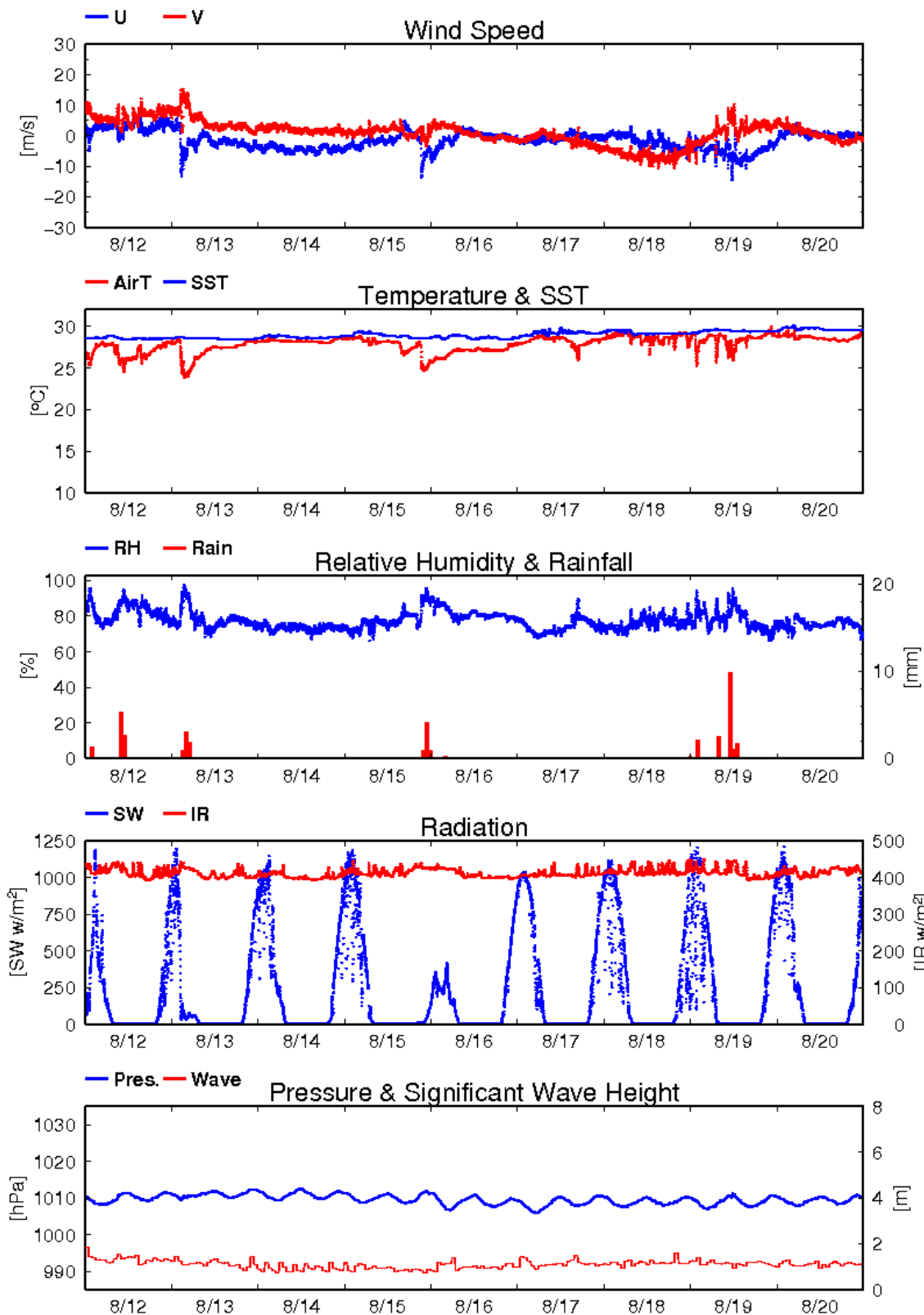


Fig. 6.1.1-1 (Continued)

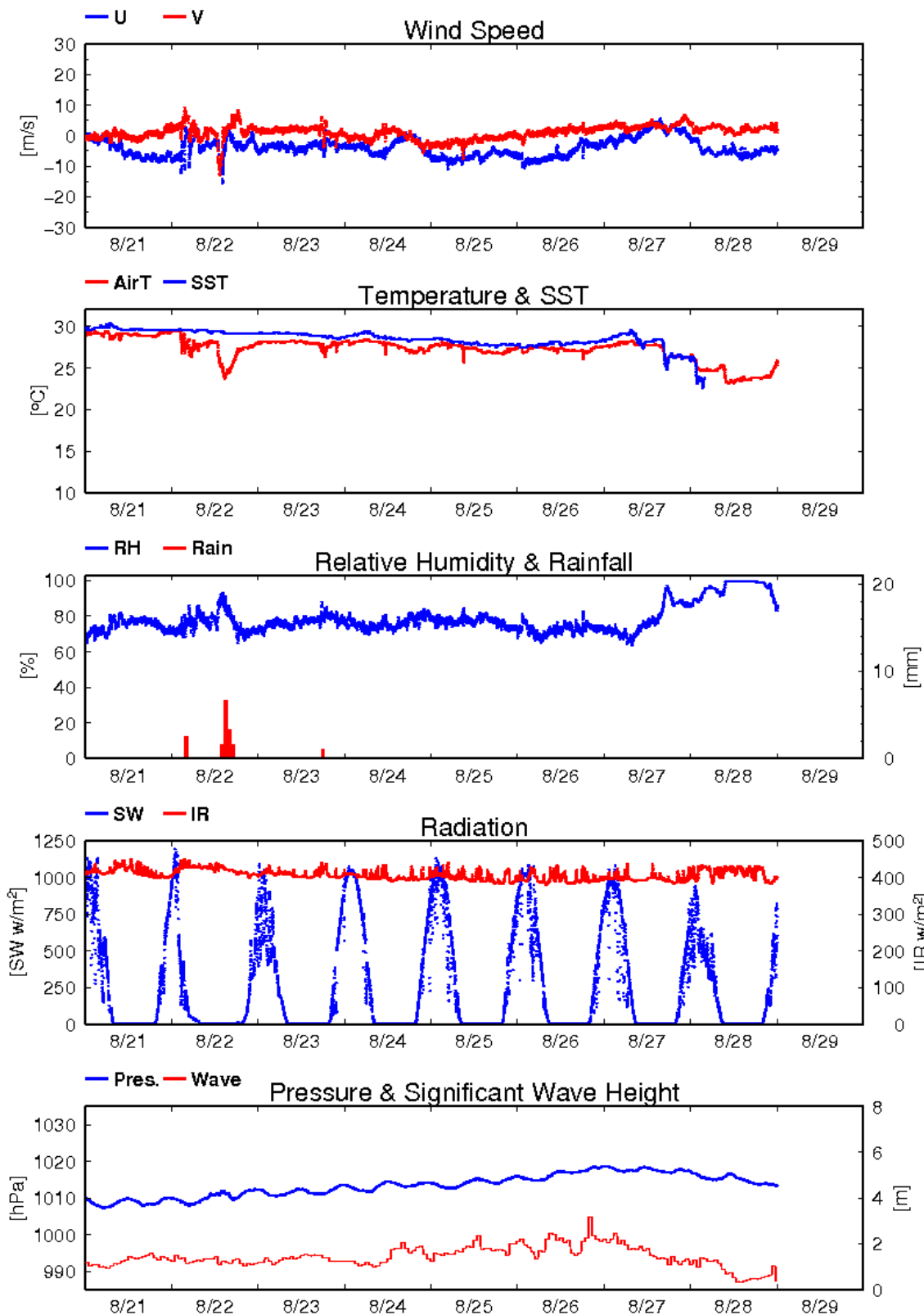


Fig. 6.1.1-1 (Continued)

## 6.1.2 Ceilometer

Yuji Kashino	(JAMSTEC) : Principal Investigator
Wataru Tokunaga	(Global Ocean Development Inc., GODI)
Harumi Ota	(GODI)
Koichi Inagaki	(GODI)
Ryo Ohyama	(MIRAI Crew)

### (1) Objectives

The information of cloud base height and the liquid water amount around cloud base is important to understand the process on formation of the cloud. As one of the methods to measure them, the ceilometer observation was carried out.

### (2) Parameters

1. Cloud base height [m].
2. Backscatter profile, sensitivity and range normalized at 30 m resolution.
3. Estimated cloud amount [oktas] and height [m]; Sky Condition Algorithm.

### (3) Methods

We measured cloud base height and backscatter profile using ceilometer (CT-25K, VAISALA, Finland) throughout the MR12-03 cruise.

Major parameters for the measurement configuration are as follows;

Laser source:	Indium Gallium Arsenide (InGaAs) Diode
Transmitting wavelength:	905±5 nm at 25 degC
Transmitting average power:	8.9 mW
Repetition rate:	5.57 kHz
Detector:	Silicon avalanche photodiode (APD) Responsibility at 905 nm: 65 A/W
Measurement range:	0 ~ 7.5 km
Resolution:	50 ft in full range
Sampling rate:	60 sec
Sky Condition	0, 1, 3, 5, 7, 8 oktas (9: Vertical Visibility) (0: Sky Clear, 1:Few, 3:Scattered, 5-7: Broken, 8: Overcast)

On the archive dataset, cloud base height and backscatter profile are recorded with the resolution of 30 m (100 ft).

### (4) Preliminary results

Fig.6.1.2-1 shows the time series of the lowest, second and third cloud base height during the cruise.

### (5) Data archives

The raw data obtained during this cruise will be submitted to the Data Management Group

(DMG) in JAMSTEC.

(7) Remarks

1. Window cleaning;

23:20UTC 16 Jul. 2012, 04:52UTC 23 Jul. 2012, 03:49UTC 25 Jul. 2012,  
21:10UTC 28 Jul. 2012, 03:03UTC 31 Jul. 2012, 03:01UTC 02 Aug. 2012  
02:30UTC 11 Aug. 2012, 01:37UTC 17 Aug. 2012, 03:59UTC 24 Aug. 2012

2. Following period, data acquisition was suspended because of PC trouble.

00:00UTC 22 Jul. 2012 - 00:22UTC 23 Jul. 2012

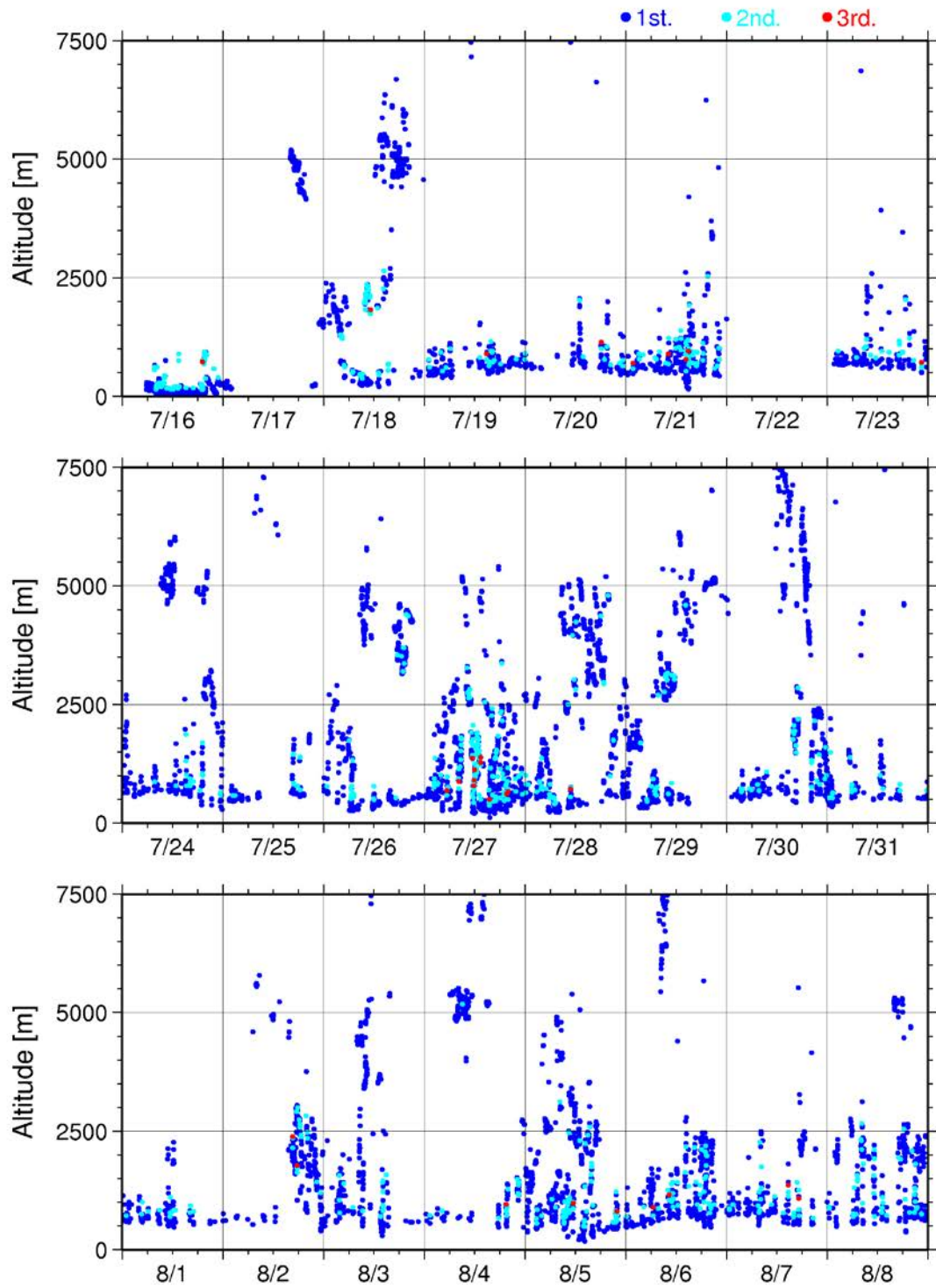


Fig. 6.1.2-1 Lowest, 2nd and 3rd cloud base height during the MR12-03 cruise

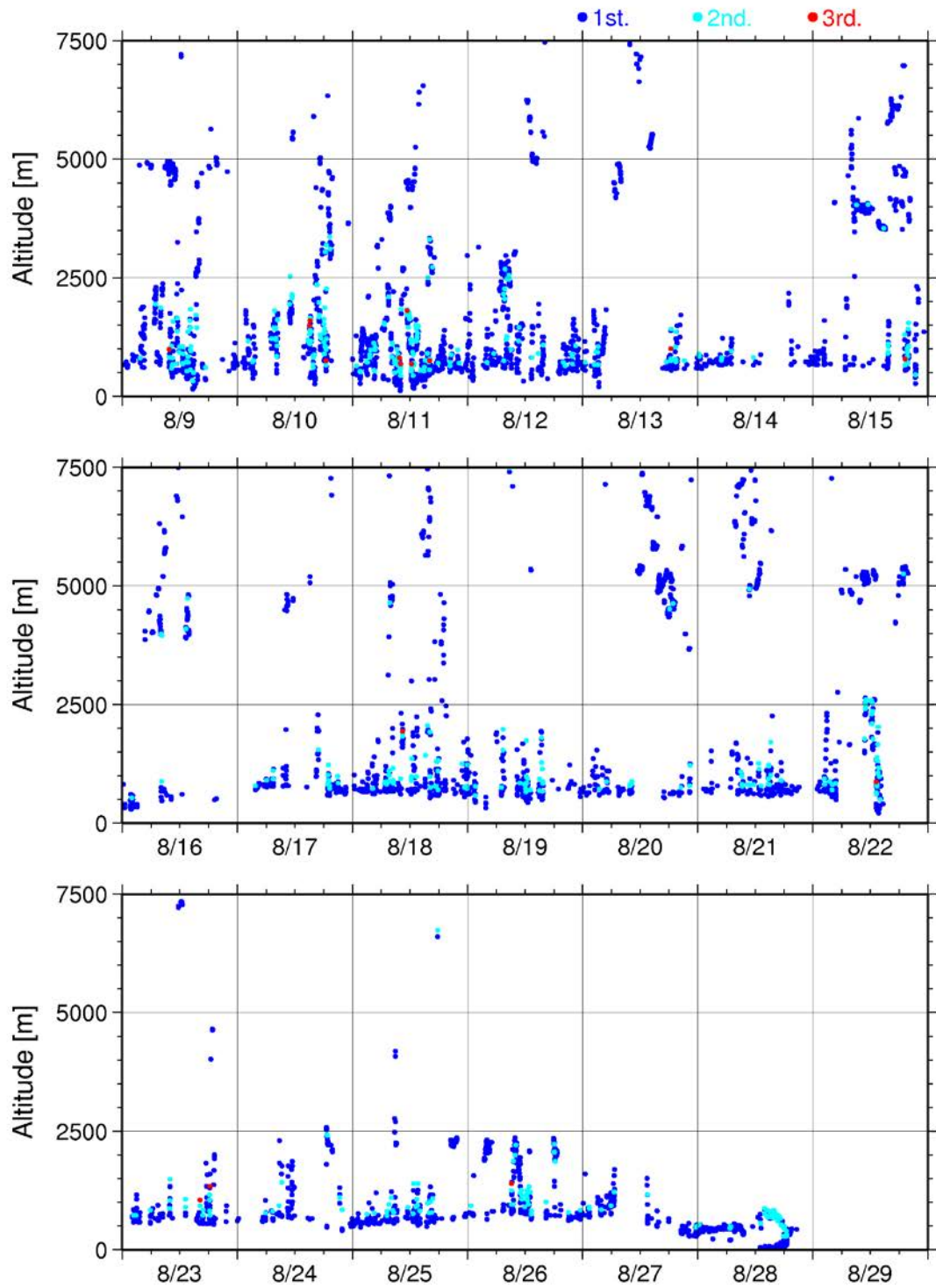


Fig. 6.1.2-1 (Continued)

## 6.2 CTD/XCTD

### 6.2.1 CTD

#### (1) Personnel

Yuji Kashino	(JAMSTEC): Principal investigator
Shungo Oshitani	(MWJ): Operation leader
Hiroshi Matsunaga	(MWJ)
Tomohide Noguchi	(MWJ)
Tamami Ueno	(MWJ)
Rei Ito	(MWJ)
Minoru Kamata	(MWJ)
Shoko Tatamisashi	(MWJ)
Hatsumi Aoyama	(MWJ)

#### (2) Objective

Investigation of oceanic structure and water sampling.

#### (3) Parameters

Temperature (Primary and Secondary)  
Conductivity (Primary and Secondary)  
Pressure  
Dissolved Oxygen (Primary only)

#### (4) Instruments and Methods

CTD/Carousel Water Sampling System, which is a 36-position Carousel water sampler (CWS) with Sea-Bird Electronics, Inc. CTD (SBE9plus), was used during this cruise. 12-liter Niskin Bottles were used for sampling seawater. The sensors attached on the CTD were temperature (Primary and Secondary), conductivity (Primary and Secondary), and pressure and dissolved oxygen (Primary). Salinity was calculated by measured values of pressure, conductivity and temperature. The CTD/CWS was deployed from starboard on working deck.

The CTD raw data were acquired on real time using the Seasave-Win32 (ver.7.21h) provided by Sea-Bird Electronics, Inc. and stored on the hard disk of the personal computer. Seawater was sampled during the up cast by sending fire commands from the personal computer. We usually stop for 30 seconds to stabilize then fire.

43 casts of CTD measurements were conducted (Table 6.2.1-1).

Data processing procedures and used utilities of SBE Data Processing-Win32 (ver.7.18d) and SEASOFT were as follows:

(The process in order)

DATCNV: Convert the binary raw data to engineering unit data. DATCNV also extracts bottle information where scans were marked with the bottle confirm bit during acquisition. The duration was set to 3.0 seconds, and the offset was set to 0.0

seconds.

**BOTTLESUM:** Create a summary of the bottle data. The data were averaged over 3.0 seconds.

**ALIGNCTD:** Convert the time-sequence of sensor outputs into the pressure sequence to ensure that all calculations were made using measurements from the same parcel of water. Dissolved oxygen data are systematically delayed with respect to depth mainly because of the long time constant of the dissolved oxygen sensor and of an additional delay from the transit time of water in the pumped plumbing line. This delay was compensated by 6 seconds advancing dissolved oxygen sensor output (dissolved oxygen voltage) relative to the temperature data.

**WILDEDIT:** Mark extreme outliers in the data files. The first pass of WILDEDIT obtained an accurate estimate of the true standard deviation of the data. The data were read in blocks of 1000 scans. Data greater than 10 standard deviations were flagged. The second pass computed a standard deviation over the same 1000 scans excluding the flagged values. Values greater than 20 standard deviations were marked bad. This process was applied to pressure, depth, temperature, conductivity dissolved oxygen voltage and decent rate.

**CELLTM:** Remove conductivity cell thermal mass effects from the measured conductivity. Typical values used were thermal anomaly amplitude  $\alpha = 0.03$  and the time constant  $1/\beta = 7.0$ .

**FILTER:** Perform a low pass filter on pressure with a time constant of 0.15 second. In order to produce zero phase lag (no time shift) the filter runs forward first then backward

**SECTIONU** (original module of SECTION): Select a time span of data based on scan number in order to reduce a file size. The minimum number was set to be the starting time when the CTD package was beneath the sea-surface after activation of the pump. The maximum number of was set to be the end time when the package came up from the surface.

**LOOPEDIT:** Mark scans where the CTD was moving less than the minimum velocity of 0.0 m/s (traveling backwards due to ship roll).

**DERIVE:** Compute dissolved oxygen (SBE43).

**BINAVG:** Average the data into 1-dbar pressure bins.

DERIVE: Compute salinity, potential temperature, and sigma-theta.

SPLIT: Separate the data from an input .cnv file into down cast and up cast files.

Configuration file: MR1203A.con

Specifications of the sensors are listed below.

CTD: SBE911plus CTD system

Under water unit:

SBE9plus

S/N 09P38273-0786 (Sea-Bird Electronics, Inc.)

Pressure sensor: Digiquartz pressure sensor (S/N 94766)

Calibrated Date: 30 Jun. 2012

Temperature sensors:

Primary: SBE03-04/F (S/N 031464, Sea-Bird Electronics, Inc.)

Calibrated Date: 15 Dec. 2011

Secondary: SBE03Plus (S/N 03P2730, Sea-Bird Electronics, Inc.)

Calibrated Date: 18 Apr. 2012

Conductivity sensors:

Primary: SBE04-04/0 (S/N 041203, Sea-Bird Electronics, Inc.)

Calibrated Date: 18 Apr. 2012

Secondary: SBE04-04/0 (S/N 041172, Sea-Bird Electronics, Inc.)

Calibrated Date: 18 Apr. 2012

Dissolved Oxygen sensors:

Primary: SBE43 (S/N 43330, Sea-Bird Electronics, Inc.)

Calibrated Date: 01 May. 2012

Carousel water sampler:

SBE32 (S/N 3221746-0278, Sea-Bird Electronics, Inc.)

Deck unit: SBE11plus (S/N 11P7030-0272, Sea-Bird Electronics, Inc.)

##### (5) Preliminary Results

During this cruise, 43casts of CTD observation were carried out. Date, time and locations of the CTD casts are listed in Table 6.2.1-1.

Vertical profile (down cast) of primary temperature, salinity and dissolved oxygen with pressure are shown in Figure 6.2.1-1 - 6.2.1-11

In the down cast of Stn.C21 (filename: C21M01) and Stn.C31 (filename: C31M01), spike was observed in the dissolved oxygen sensor.

##### (6) Data archive

All raw and processed data files were copied onto HD provided by Data Management Office (DMO); JAMSTEC will be opened to public via "R/V MIRAI Data Web Page" in the JAMSTEC home page.

Table 6.2.1-1 MR12-03 CTD Cast table

Stnbr	Castno	Date(UTC)	Time(UTC)		Bottom Position		Depth	Wire Out	Max Depth	Max Pressure	CTD Filename	Remark
		(mmddy)	Start	End	Latitude	Longitude						
C01	1	072512	08:08	08:38	05-03.70N	146-55.54E	4215.0	799.3	801.0	807.0	C01M01	LADCP Recovery point of T07
C02	1	072612	04:50	05:11	04-30.30N	146-59.90E	4087.0	498.9	501.6	505.0	C02M01	LADCP
C03	1	072612	19:35	20:07	02-05.26N	146-58.72E	4496.0	800.9	803.0	809.0	C03M01	LADCP Recovery point of T08
C04	1	072712	04:50	05:11	01-29.88N	147-00.15E	4506.0	500.7	501.6	505.0	C04M01	LADCP
C05	1	072712	08:45	09:06	00-59.95N	146-59.99E	4512.0	500.0	502.6	506.0	C05M01	LADCP
C06	1	072912	08:40	09:03	00-29.89N	147-00.16E	4473.0	500.0	501.6	505.0	C06M01	LADCP
C07	1	072912	19:19	19:55	00-01.47S	147-02.00E	4532.0	1001.6	1002.0	1010.0	C07M01	LADCP Recovery point of T09
C08	1	080112	04:45	05:21	02-43.21S	153-16.59E	2820.0	998.5	1002.0	1010.0	C08M01	LADCP Argo float
C12	1	080312	07:24	07:48	03-30.13S	155-59.96E	1895.0	500.7	503.6	507.0	C12M01	LADCP
C09	1	080412	02:07	02:40	04-58.66S	156-02.30E	1490.0	799.1	802.0	808.0	C09M01	LADCP Recovery point of T06
C10	1	080412	06:43	07:04	04-30.08S	156-00.07E	1717.0	501.2	503.6	507.0	C10M01	LADCP
C11	1	080512	05:22	05:43	04-00.17S	156-00.07E	1781.0	498.9	500.6	504.0	C11M01	LADCP
C15	1	080812	18:41	19:13	02-00.85S	156-00.44E	1761.0	799.8	802.0	808.0	C15M01	LADCP Recovery point of T05

C14	1	080912	02:33	02:54	02-30.06S	156-00.06E	1740.0	496.5	500.6	504.0	C14M01	LADCP
C13	1	080912	06:31	06:52	03-00.02S	156-00.02E	1815.0	498.7	501.6	505.0	C13M01	LADCP
C16	1	081012	04:31	04:53	01-30.10S	155-59.98E	1803.0	501.8	502.6	506.0	C16M01	LADCP
C17	1	081012	08:37	08:59	01-00.05S	156-00.04E	2083.0	499.8	501.6	505.0	C17M01	LADCP
C18	1	081212	06:29	06:51	00-30.15S	156-00.09E	1953.0	499.2	501.6	505.0	C18M01	LADCP
C19	1	081212	19:03	19:27	00-00.00S	155-59.97E	1953.0	499.6	500.6	504.0	C19M01	LADCP
C19	2	081212	22:03	22:25	00-00.11N	156-00.59E	1954.0	499.6	501.6	505.0	C19M02	LADCP
C19	3	081312	01:00	01:21	00-00.07N	155-59.62E	1953.0	499.4	501.6	505.0	C19M03	LADCP
C19	4	081312	04:01	04:21	00-00.14N	156-00.00E	1953.0	500.3	500.6	504.0	C19M04	LADCP
C19	5	081312	07:01	07:23	00-00.00N	155-59.96E	1953.0	500.0	500.6	504.0	C19M05	LADCP
C19	6	081312	10:01	10:23	00-00.15S	155-59.80E	1950.0	500.7	502.6	506.0	C19M06	LADCP
C19	7	081312	13:00	13:21	00-00.12N	155-59.38E	1952.0	502.3	501.6	505.0	C19M07	LADCP
C19	8	081312	16:00	16:21	00-00.25S	155-59.26E	1949.0	500.5	501.6	505.0	C19M08	LADCP
C19	9	081312	19:01	19:23	00-00.20S	155-59.57E	1952.0	499.0	500.6	504.0	C19M09	LADCP
C20	1	081312	22:56	23:17	00-15.05N	156-00.10E	1985.0	499.8	502.6	506.0	C20M01	LADCP
C21	1	081412	02:45	03:06	00-30.07N	156-00.01E	2143.0	502.0	501.6	505.0	C21M01	LADCP
C22	1	081412	06:50	07:13	00-45.14N	156-00.14E	2152.0	502.5	502.6	506.0	C22M01	LADCP
C23	1	081412	10:19	10:42	01-00.13N	156-00.15E	2264.0	500.5	501.6	505.0	C23M01	LADCP
C24	1	081412	13:44	14:05	01-14.94N	156-00.04E	2409.0	499.8	501.6	505.0	C24M01	LADCP
C25	1	081412	17:13	17:36	01-30.19N	156-02.66E	2372.0	501.1	501.6	505.0	C25M01	LADCP
C26	1	081412	20:39	21:02	01-45.20N	156-00.21E	2428.0	500.9	500.6	504.0	C26M01	LADCP
C27	1	081512	00:10	00:41	01-57.49N	156-01.57E	2555.0	799.3	802.0	808.0	C27M01	LADCP Recovery point of T03
C28	1	081512	05:16	05:38	02-30.05N	156-00.10E	2676.0	498.9	501.6	505.0	C28M01	LADCP
C29	1	081612	06:29	06:52	02-59.94N	156-00.06E	2875.0	500.5	502.7	506.0	C29M01	LADCP

C30	1	081712	07:49	08:11	03-30.12N	156-00.05E	3251.0	499.8	501.6	505.0	C30M01	LADCP
C33	1	081712	18:31	19:02	05-01.00N	155-59.33E	3610.0	799.7	801.0	807.0	C33M01	LADCP Recovery point of T02
C32	1	081812	03:51	04:12	04-29.90N	156-02.75E	3571.0	501.1	503.6	507.0	C32M01	LADCP
C31	1	081812	07:48	08:11	03-59.97N	156-00.04E	3476.0	498.9	501.6	505.0	C31M01	LADCP
C34	1	081912	18:35	19:07	07-58.61N	156-00.75E	4839.0	799.5	800.9	807.0	C34M01	LADCP Recovery point of T01
C35	1	082112	22:46	23:49	12-00.04N	154-18.05E	5923.0	2002.0	2001.8	2023.0	C35M01	

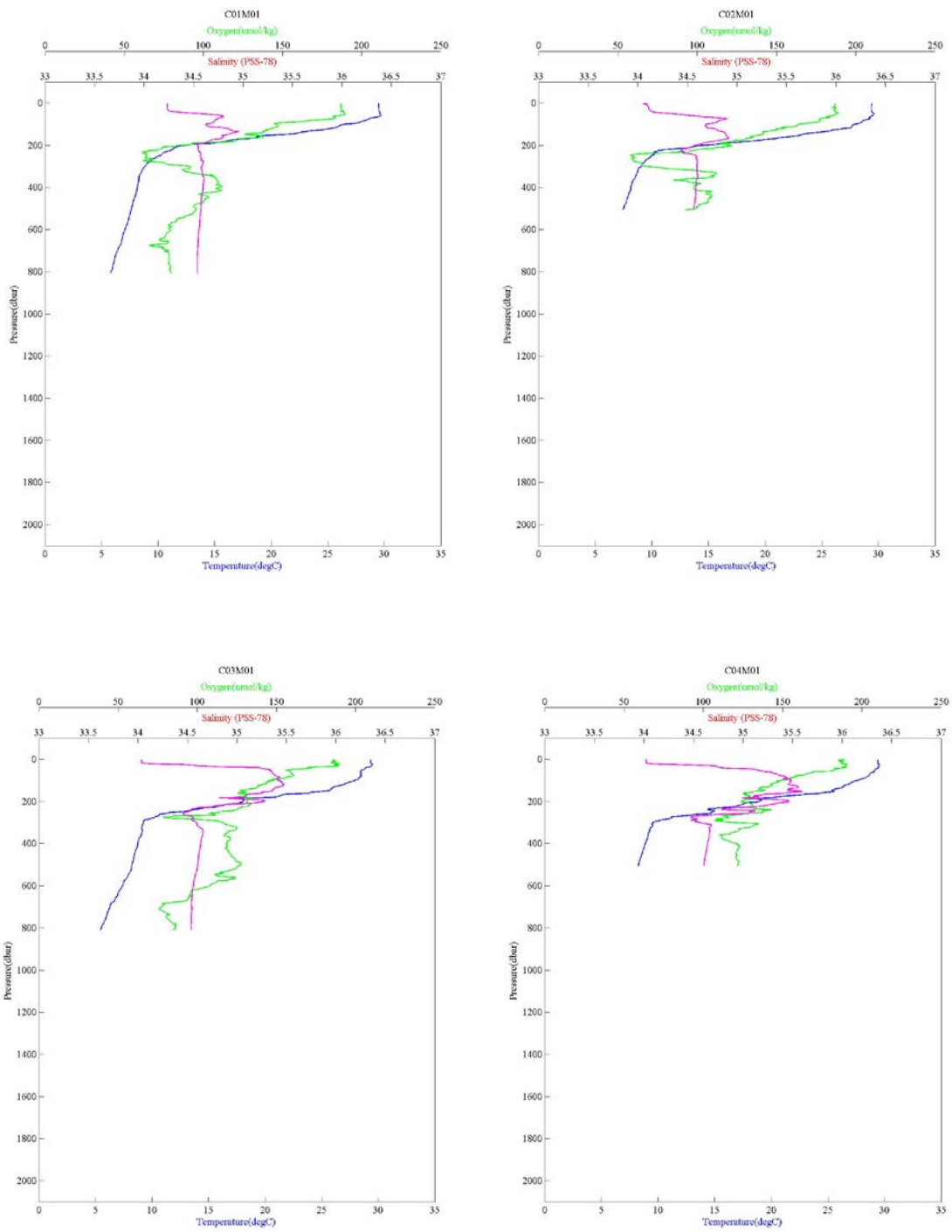


Figure 6.2.1-1 CTD profile (C01M01, C02M01, C03M01 and C04M01)

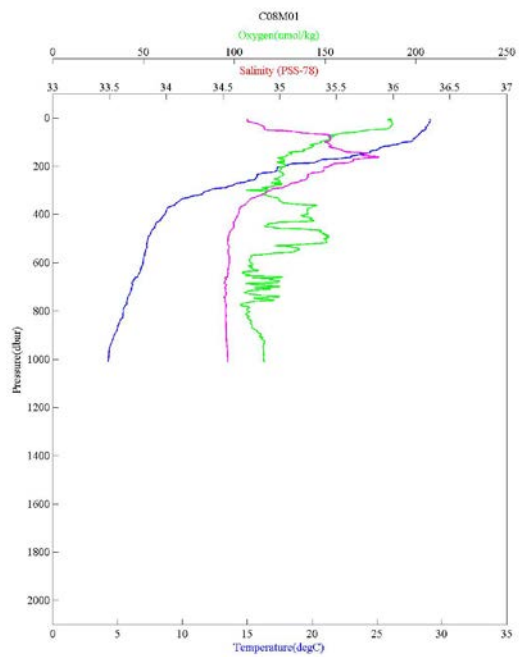
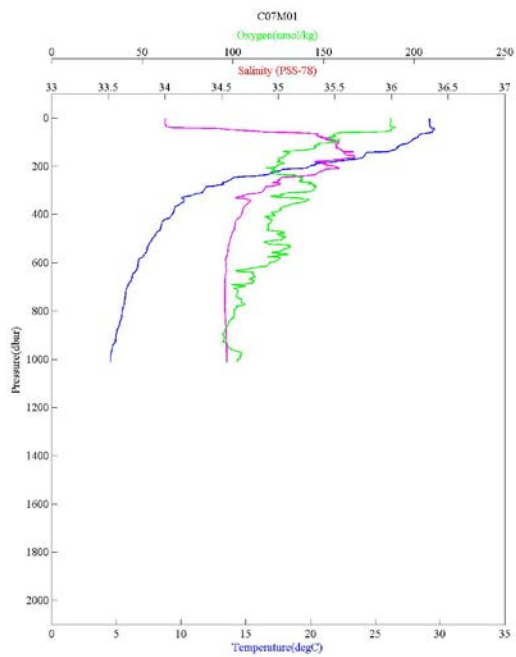
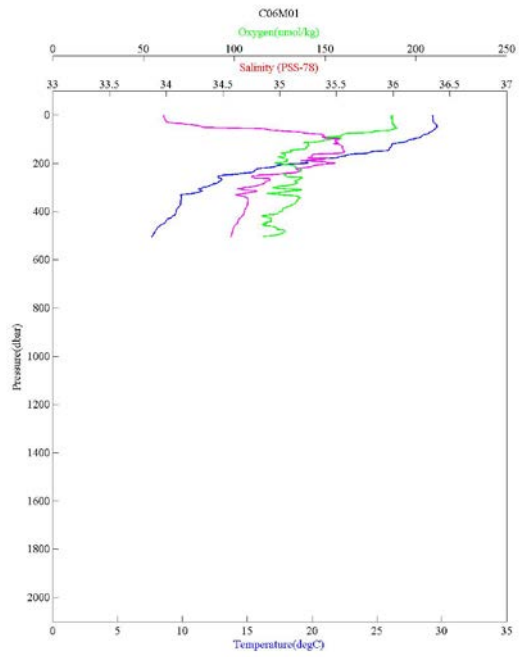
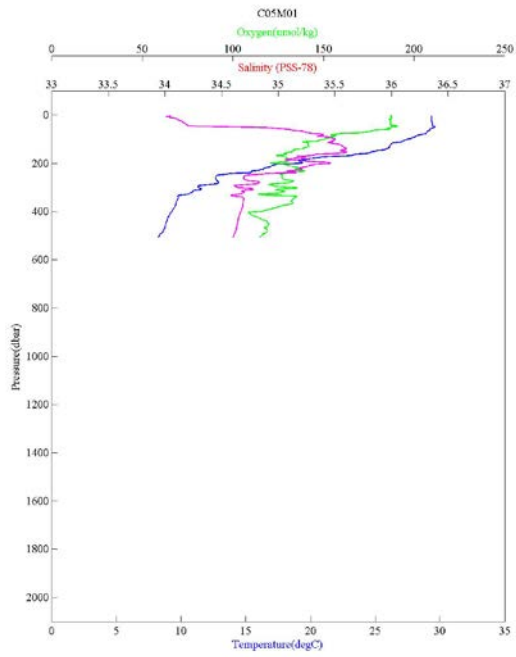


Figure 6.2.1-2 CTD profile (C05M01, C06M01, C07M01 and C08M01)

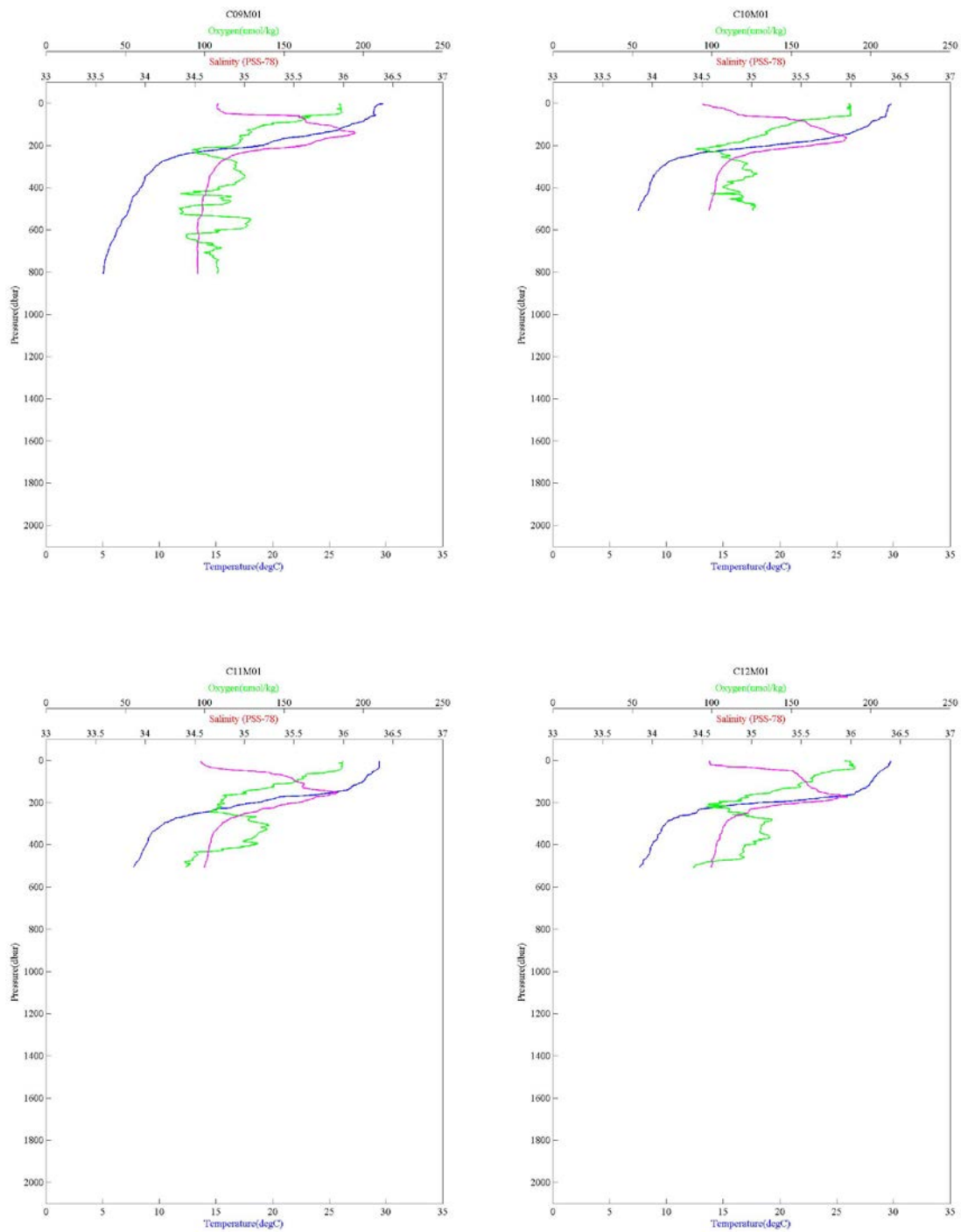


Figure 6.2.1-3 CTD profile (C09M01, C10M01, C11M01 and C12M01)

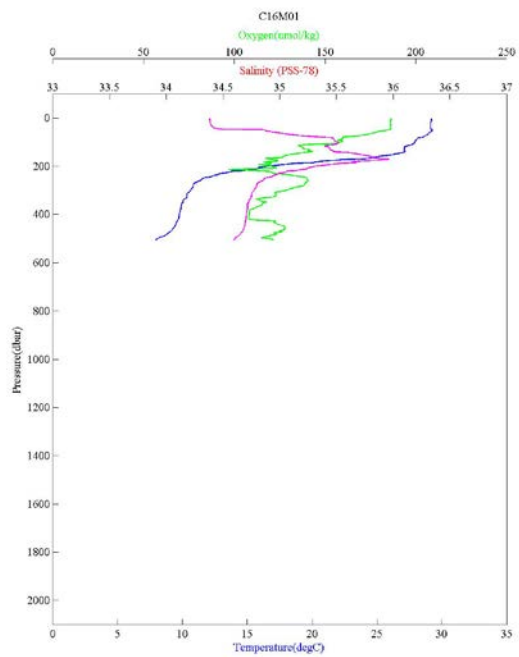
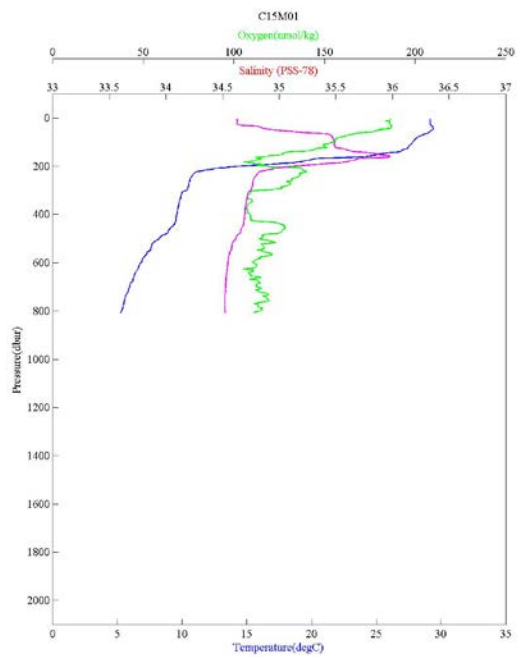
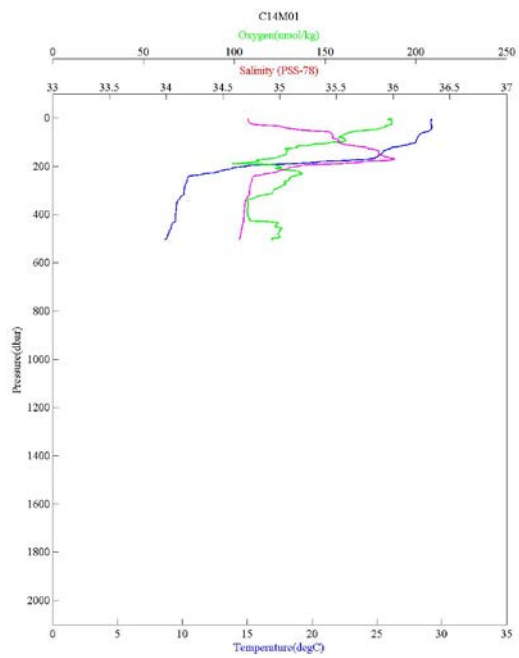
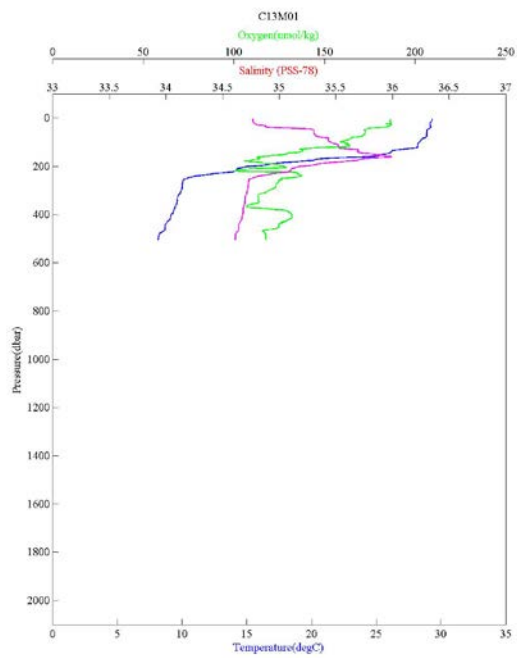


Figure 6.2.1-4 CTD profile (C13M01, C14M01, C15M01 and C16M01)

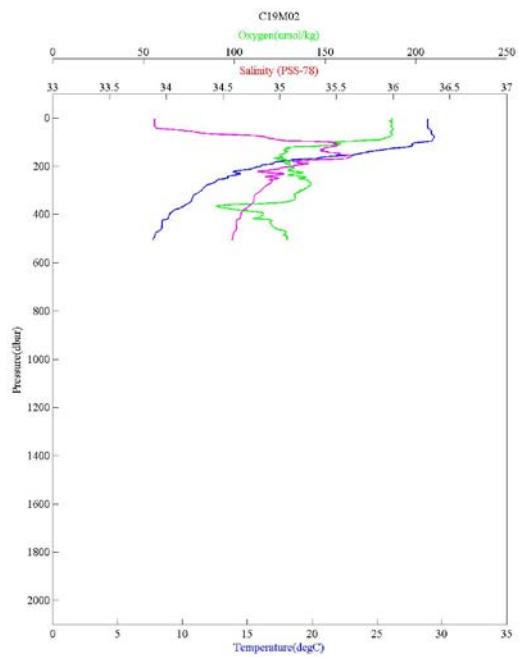
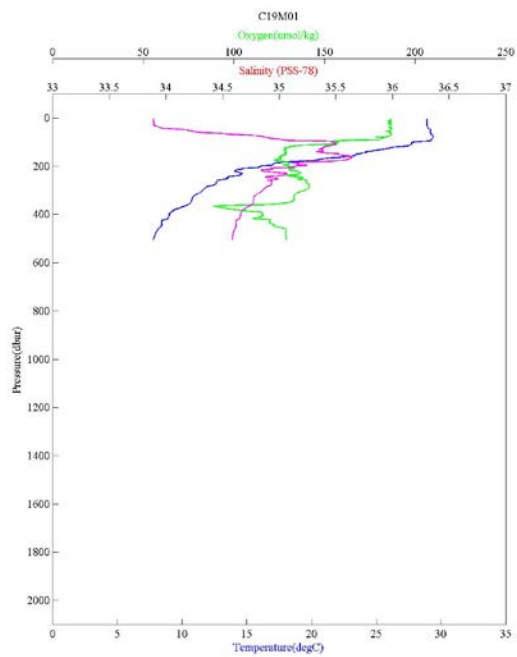
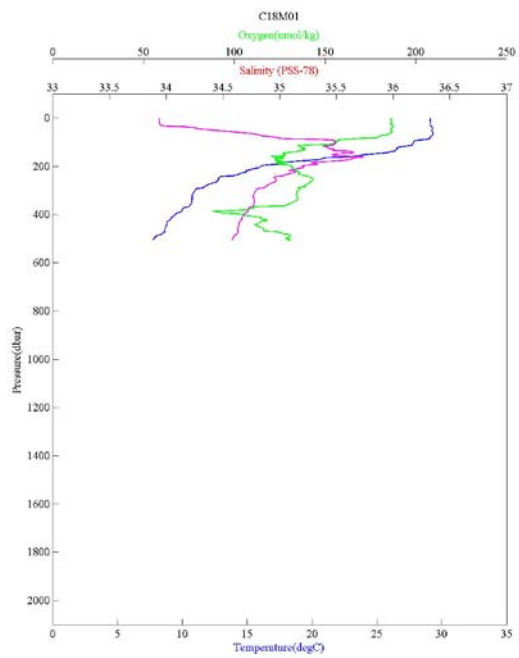
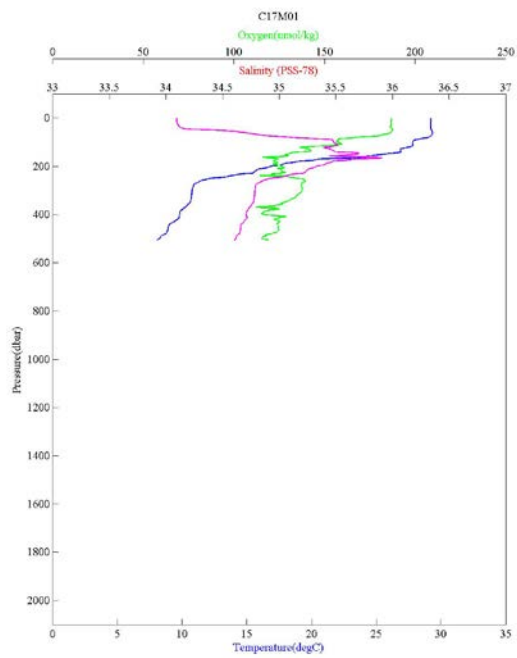


Figure 6.2.1-5 CTD profile (C17M01, C18M01, C19M01 and C19M02)

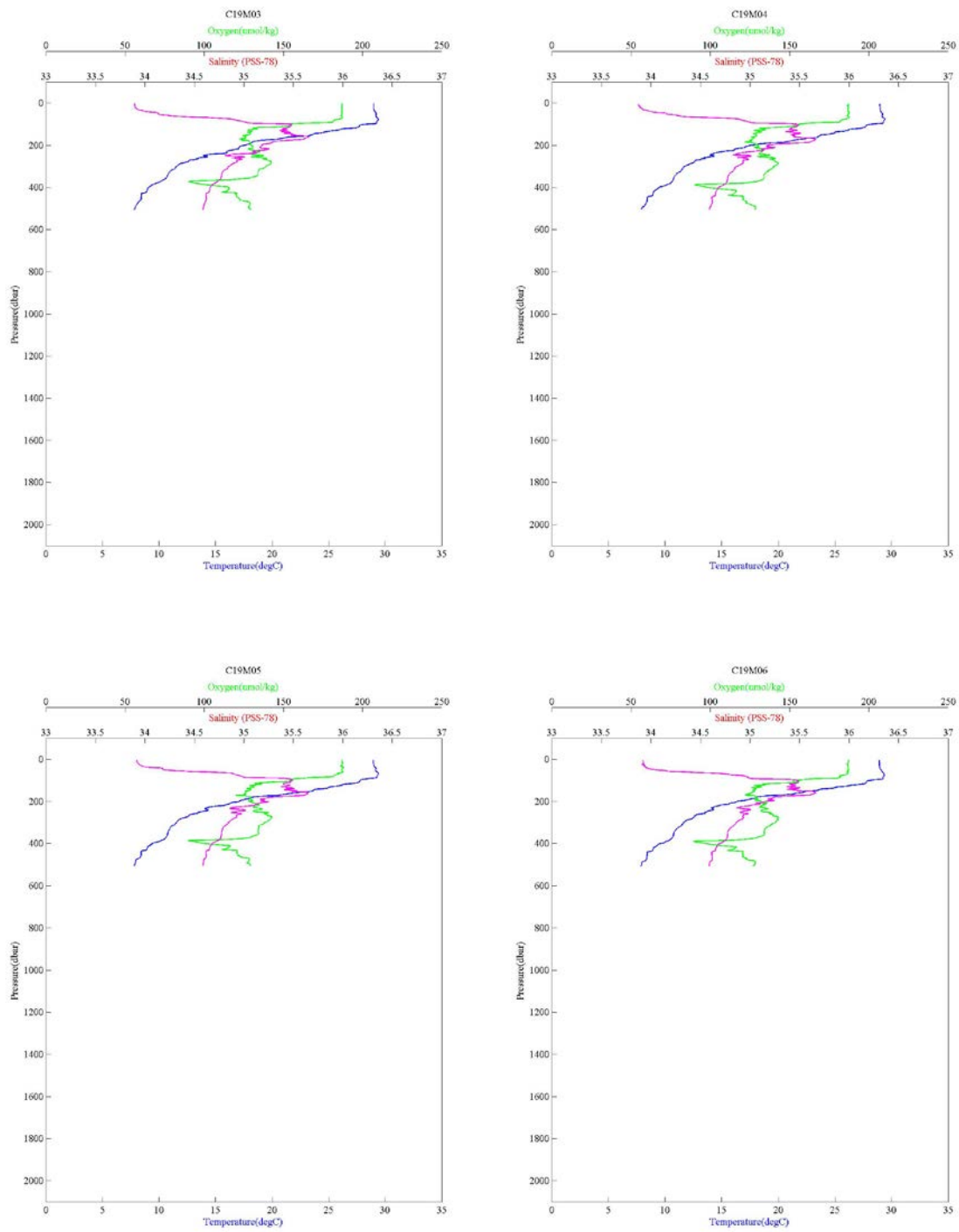


Figure 6.2.1-6 CTD profile (C19M03, C19M04, C19M05 and C19M06)

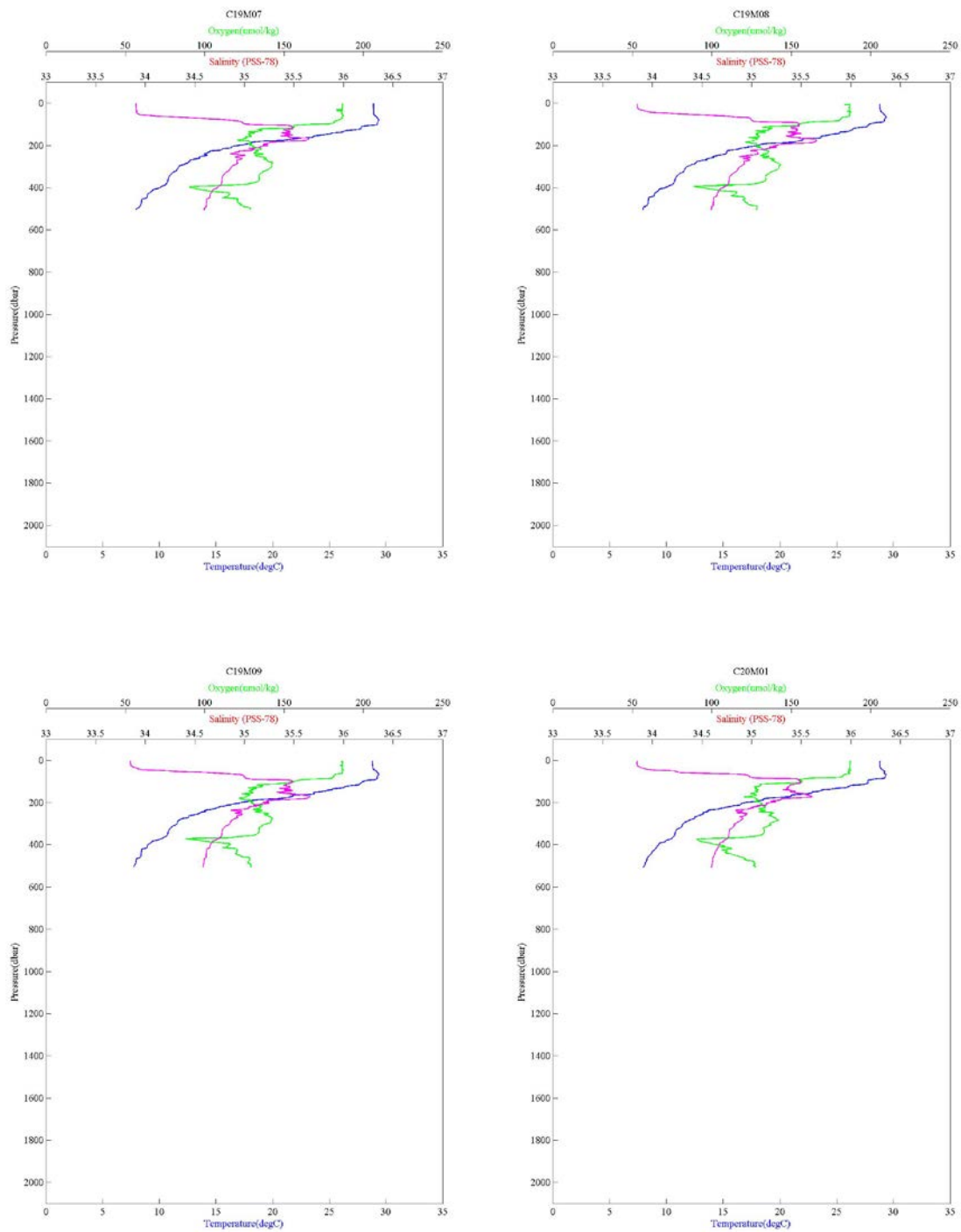


Figure 6.2.1-7 CTD profile (C19M07, C19M08, C19M09 and C20M01)

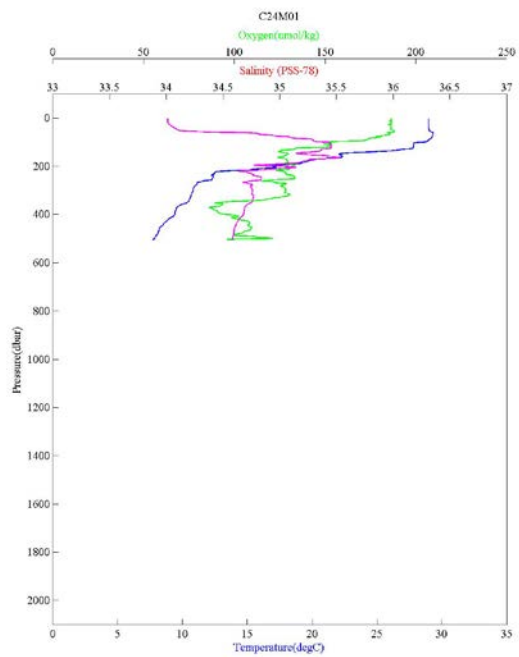
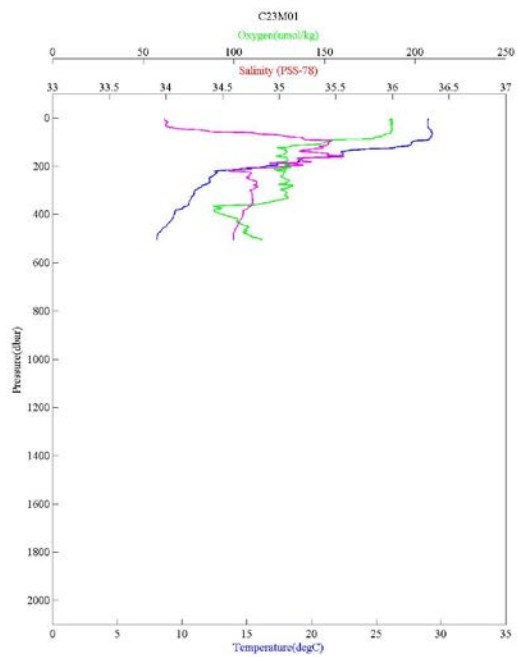
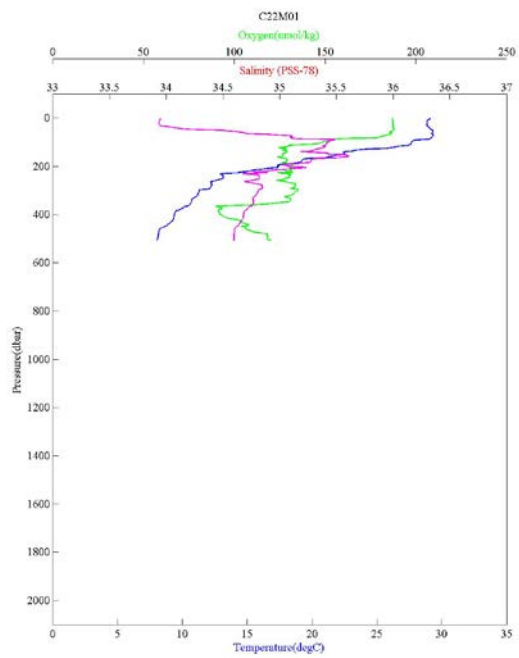
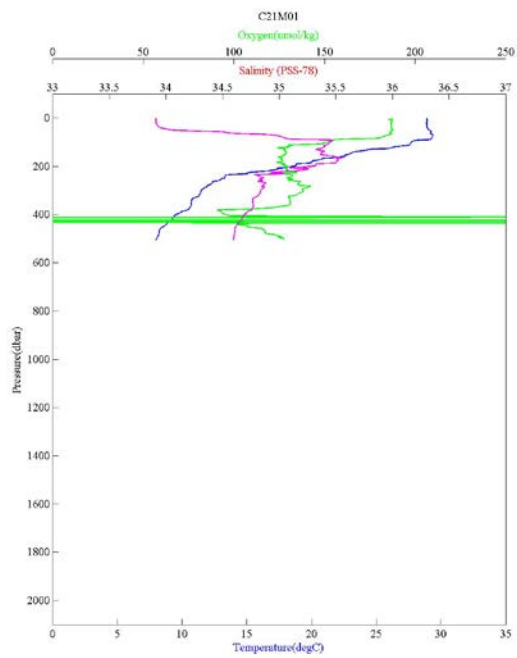


Figure 6.2.1-8 CTD profile (C21M01, C22M01, C23M01 and C24M01)

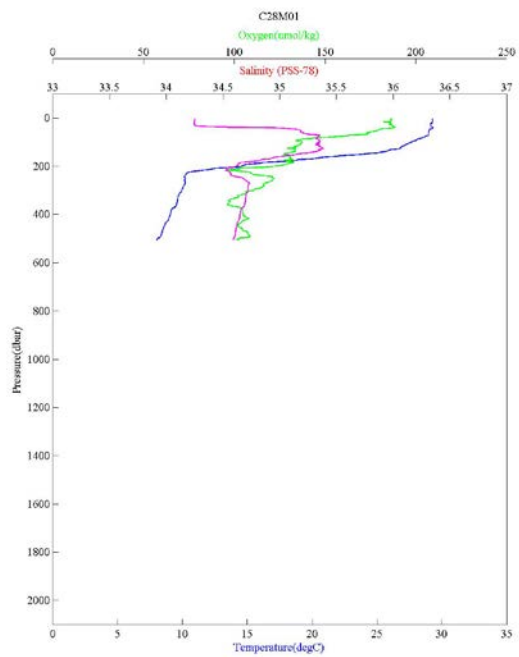
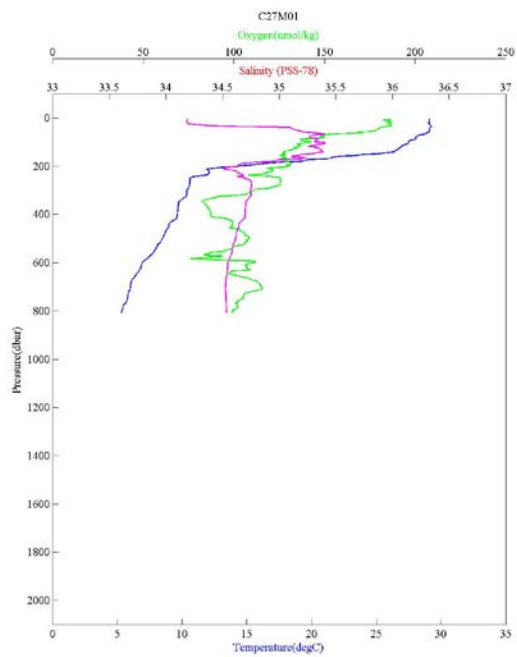
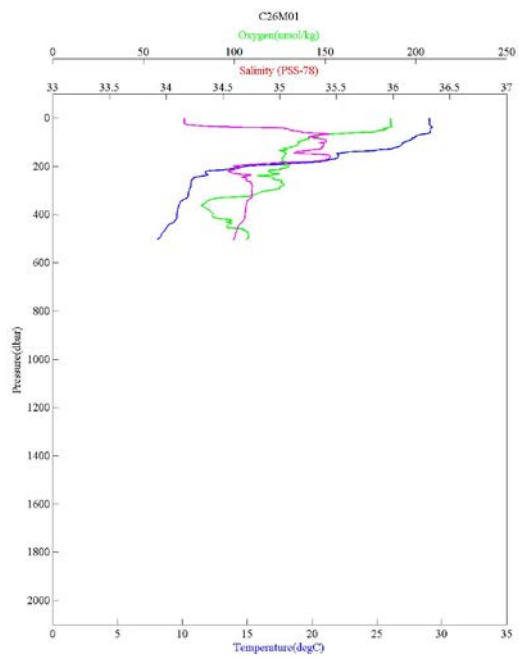
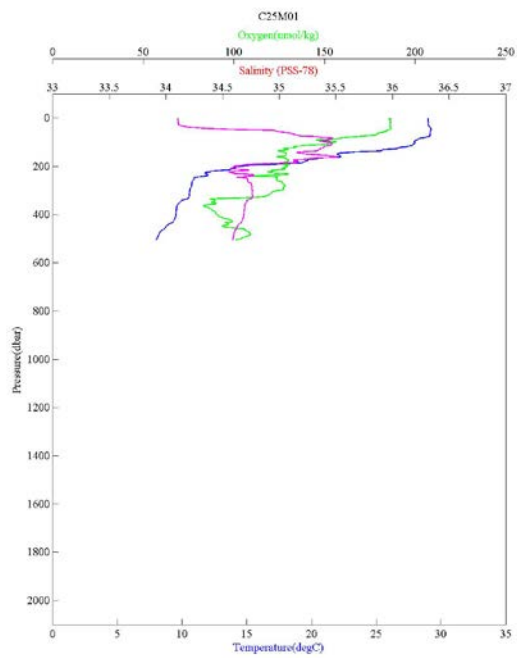


Figure 6.2.1-9 CTD profile (C25M01, C26M01, C27M01 and C28M01)

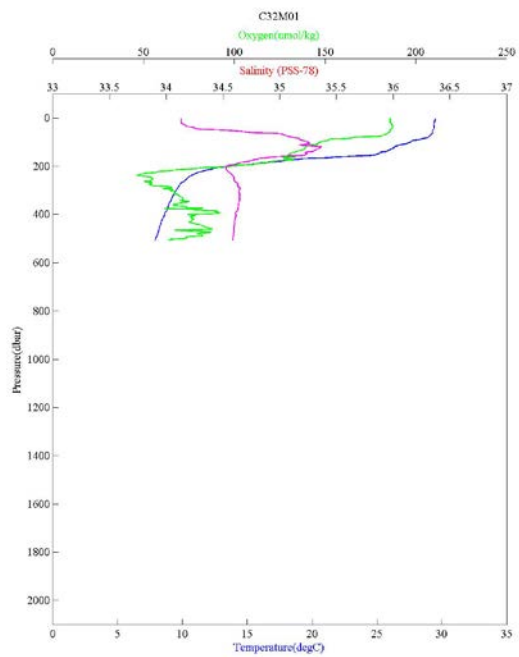
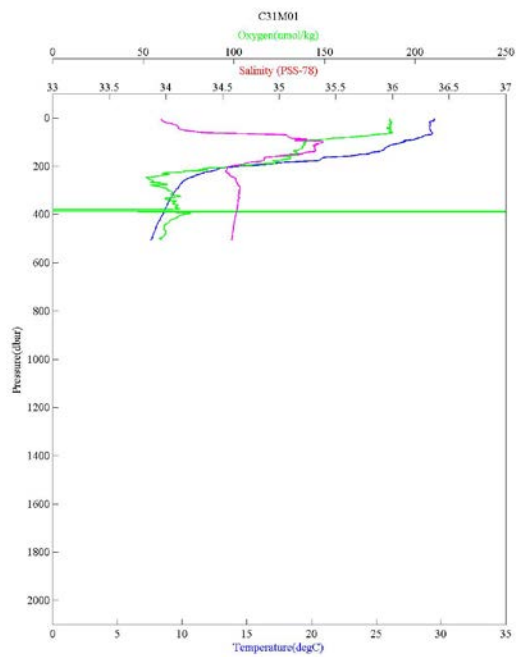
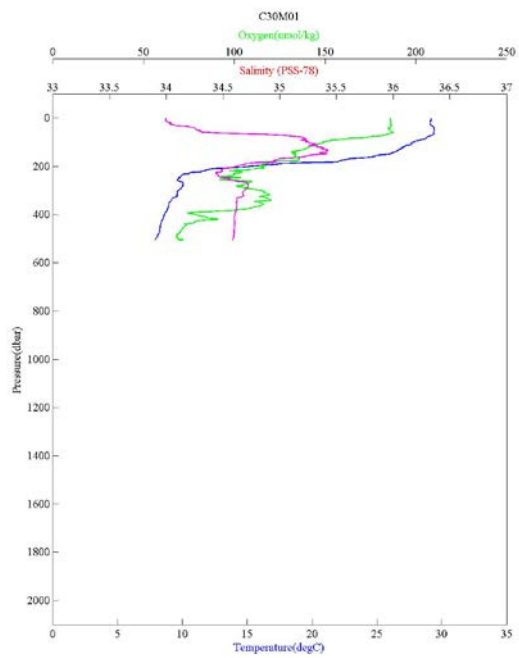
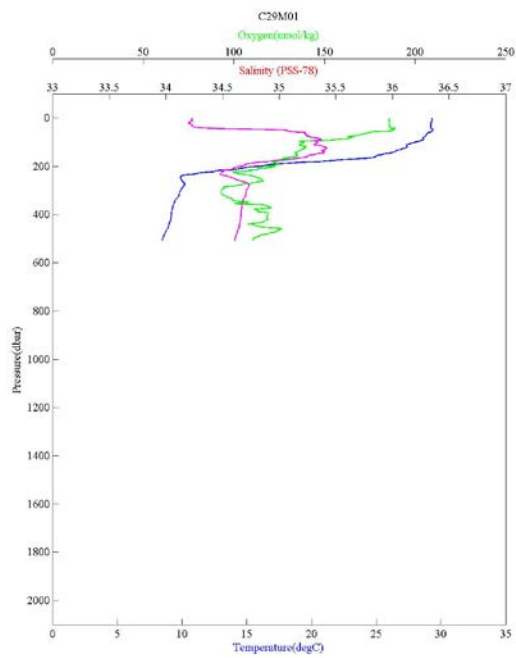


Figure 6.2.1-10 CTD profile (C29M01, C30M01, C31M01 and C32M01)

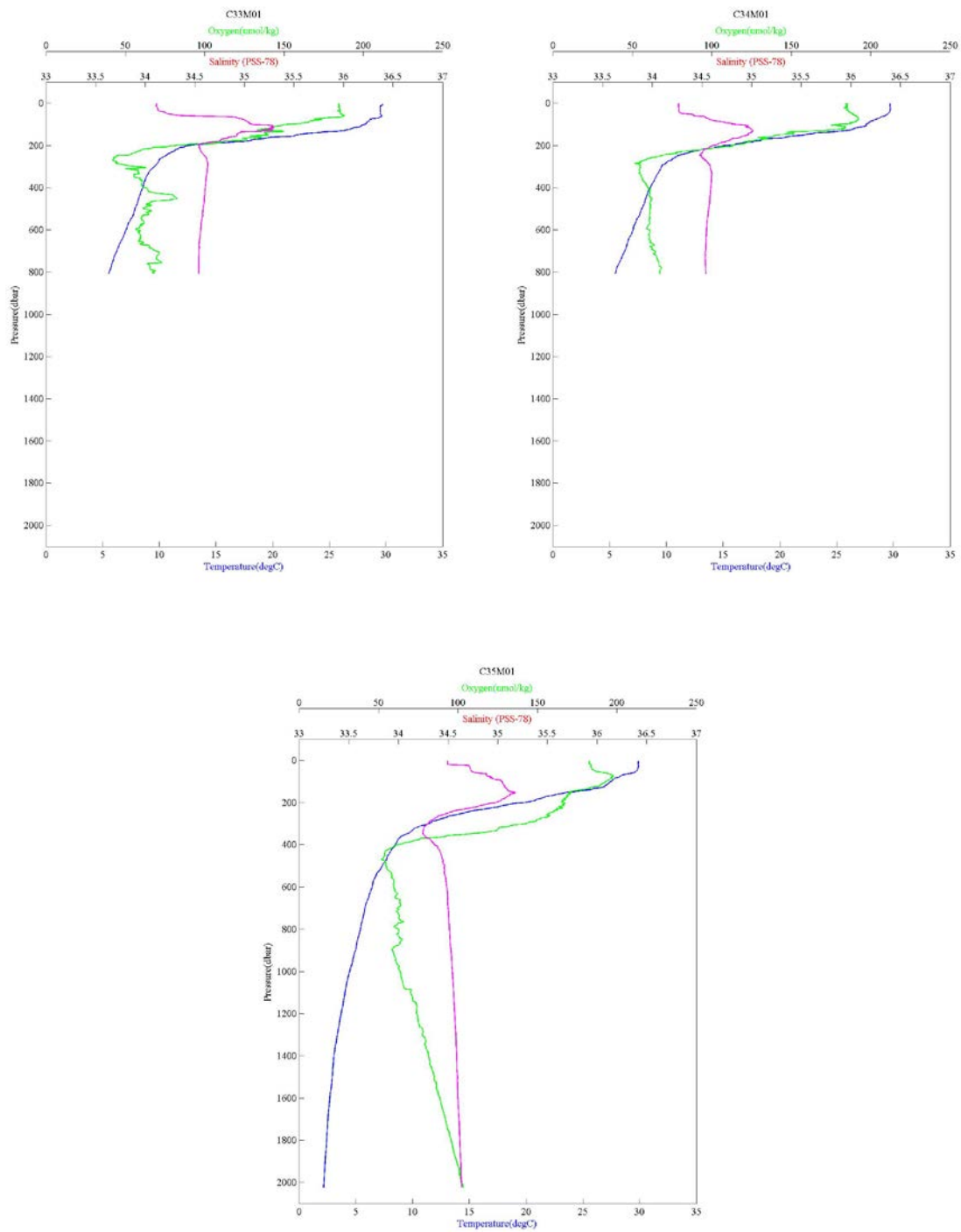


Figure 6.2.1-11 CTD profile (C33M01, C34M01, and C35M01)

## 6.2.2 XCTD

### (1) Personnel

Yuji Kashino	(JAMSTEC): Principal Investigator
Takuya Hasegawa	(JAMSTEC)
Wataru Tokunaga	(Global Ocean Development Inc.: GODI)
Harumi Ota	(GODI)
Koichi Inagaki	(GODI)
Ryo Ohyama	(MIRAI Crew)

### (2) Objectives

Investigation of oceanic structure.

### (3) Parameters

According to the manufacturer's nominal specifications, the range and accuracy of parameters measured by the XCTD (eXpendable Conductivity, Temperature & Depth profiler) are as follows;

<u>Parameter</u>	<u>Range</u>	<u>Accuracy</u>
Conductivity	0 ~ 60 [mS/cm]	+/- 0.03 [mS/cm]
Temperature	-2 ~ 35 [deg-C]	+/- 0.02 [deg-C]
Depth	0 ~ 1000 [m]	5 [m] or 2 [%] (either of them is major)

### (4) Methods

We observed the vertical profiles of the sea water temperature and salinity measured by XCTD-1 manufactured by Tsurumi-Seiki Co.. The signal was converted by MK-150N, Tsurumi-Seiki Co. and was recorded by AL12 software (Ver.1.1.4) provided by Tsurumi-Seiki Co.. We launched 36 probes (X01-X36) by an automatic launcher. The summary of XCTD observations and launching log were shown in Table 6.2.2. SST (Sea Surface Temperature) and SSS (Sea Surface Salinity) in the table were got from TSG (ThermoSalinoGraph) at launching.

### (5) Preliminary results

Position map of XCTD observations was shown in Fig. 6.2.2-1. Vertical section of temperature and salinity were shown in Fig.6.2.2-2 and Fig.6.2.2-3.

### (6) Data archive

These data obtained in this cruise will be submitted to the Data Management Group (DMG) of JAMSTEC, and will be opened to the public via "R/V MIRAI Data Web Page" in JAMSTEC home page.

Table 6.2.2 Summary of XCTD observation and launching log

Station No.	Date (UTC)	Time (UTC)	Latitude	Longitude	Depth [m]	SST [deg-C]	SSS [PSU]	Probe S/N
X01	2012/07/25	06:51	04-58.00N	147-00.70E	4290	29.578	34.178	12057601
X02	2012/07/26	08:41	03-59.96N	147-00.01E	4668	29.473	34.148	12057604
X03	2012/07/26	11:21	03-29.98N	146-59.98E	4281	29.503	34.148	12057605
X04	2012/07/26	14:03	03-00.00N	146-59.97E	4428	29.199	33.866	12057603
X05	2012/07/26	16:40	02-30.00N	146-59.93E	4423	29.338	34.040	12057602
X06	2012/07/28	03:35	02-04.35N	146-56.82E	4490	29.384	34.151	12057606
X07	2012/07/29	01:18	00-03.21N	147-02.00E	4479	29.091	33.831	12057607
X08	2012/07/31	22:11	02-14.02S	153-38.01E	3830	29.021	34.677	12057609
X09	2012/08/01	00:05	02-30.02S	153-25.99E	4507	29.153	34.725	12057608
X10	2012/08/01	06:03	02-48.31S	153-13.21E	3473	29.451	34.615	12057612
X11	2012/08/01	07:48	03-03.00S	153-01.03E	2337	29.236	34.825	12057611
X12	2012/08/01	09:43	03-20.00S	152-49.02E	2266	29.198	34.823	12057610
X13	2012/08/01	11:37	03-35.97S	152-37.00E	1065	29.222	34.820	12057613
X14	2012/08/02	05:03	03-50.24S	152-56.01E	2412	29.502	34.855	12057614
X15	2012/08/02	07:08	04-05.28S	153-15.02E	2638	29.271	34.811	12057618
X16	2012/08/02	09:17	04-19.92S	153-34.00E	3532	28.575	34.591	12057617
X17	2012/08/02	11:25	04-34.31S	153-53.01E	3817	29.002	34.753	12057621
X18	2012/08/02	13:18	04-47.44S	154-09.00E	2931	29.043	34.777	12057622
X19	2012/08/02	15:19	04-59.88S	154-25.00E	1052	29.299	34.696	12057615
X20	2012/08/02	17:13	04-57.97S	154-44.01E	2343	29.160	34.695	12057616
X21	2012/08/02	19:00	05-00.00S	155-03.00E	3298	29.511	34.588	12057619
X22	2012/08/02	20:45	05-00.00S	155-22.00E	3013	29.410	34.726	12057620
X23	2012/08/02	22:27	05-00.00S	155-41.00E	2053	29.195	34.673	12057623
X24	2012/08/04	10:37	05-01.93S	156-02.49E	1509	29.429	34.697	12057624
X25	2012/08/10	01:26	02-01.02S	155-57.96E	1758	29.223	34.646	12036649
X26	2012/08/10	23:21	00-00.22N	156-03.29E	1950	19.129	33.825	12036650
X27	2012/08/16	01:28	02-02.23N	156-00.74E	2579	29.147	34.003	12057627
X28	2012/08/19	01:23	05-01.06N	155-58.54E	3607	29.694	34.152	12057628
X29	2012/08/19	04:09	05-30.00N	156-00.00E	3737	29.869	34.051	12057630
X30	2012/08/19	06:55	06-00.15N	156-00.00E	4150	29.979	34.092	12057629
X31	2012/08/19	09:34	06-29.97N	156-00.03E	4413	29.877	34.087	12057631
X32	2012/08/19	12:08	07-00.20N	156-00.00E	4435	29.739	34.085	12057632
X33	2012/08/19	14:52	07-30.00N	155-59.99E	4396	29.802	34.088	12057635
X34	2012/08/19	18:19	07-58.60N	156-00.75E	4838	29.722	34.241	12057634
X35	2012/08/19	18:51	07-58.61N	156-00.75E	4839	29.716	34.241	12057633
X36	2012/08/21	01:39	07-57.89N	156-02.62E	4830	29.951	34.199	12057636

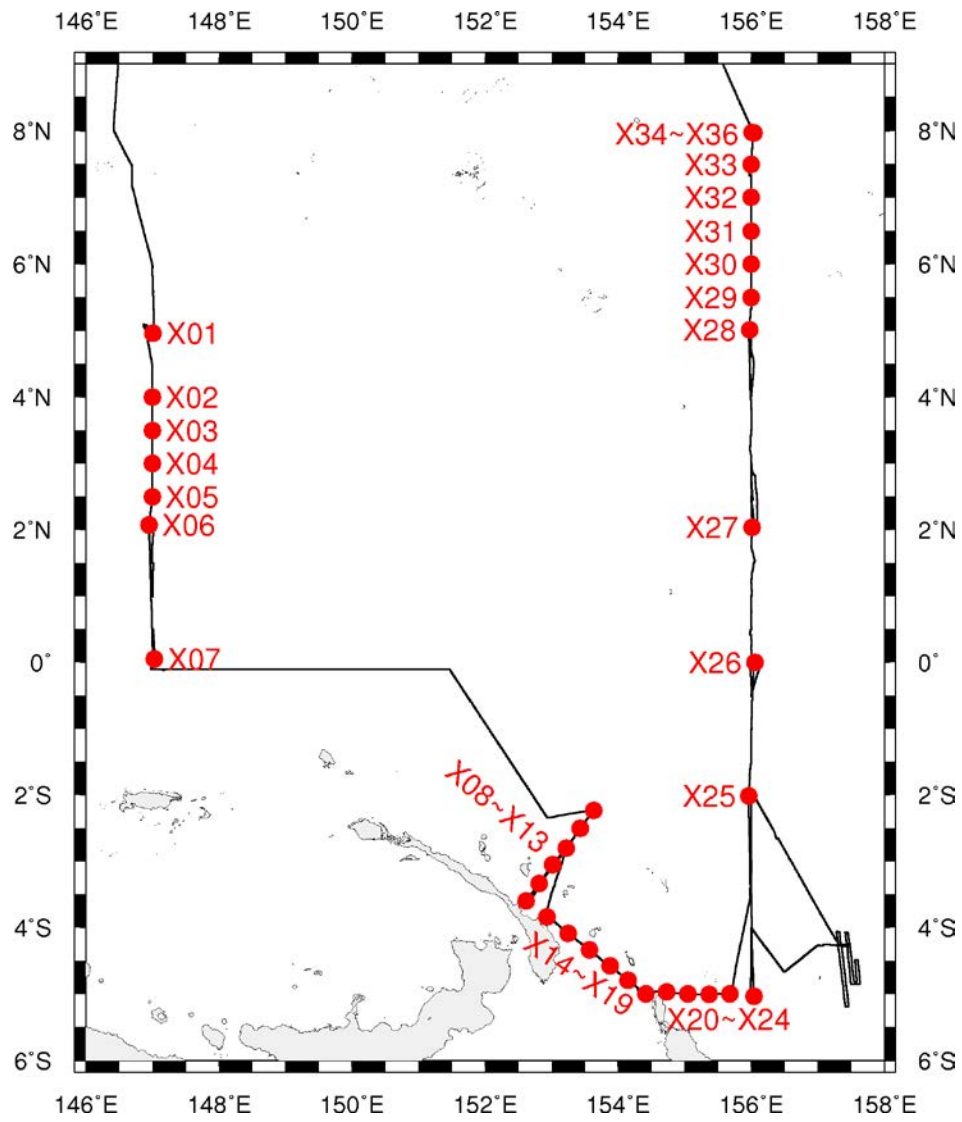


Fig. 6.2.2-1 Position map of XCTD observations.

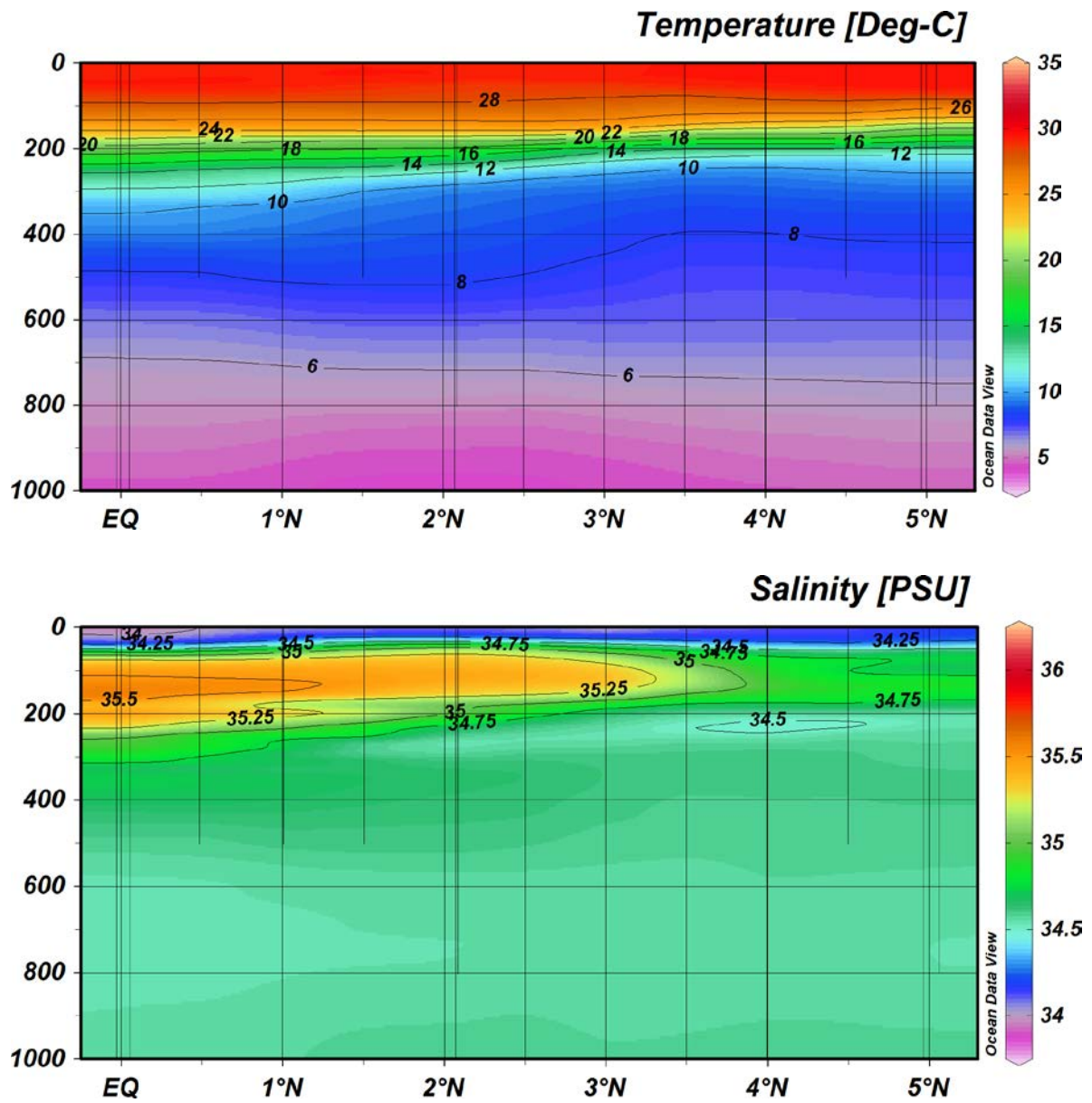


Fig. 6.2.2-2 Vertical section of temperature (upper) and salinity (lower) along 147E(X01 to X07)

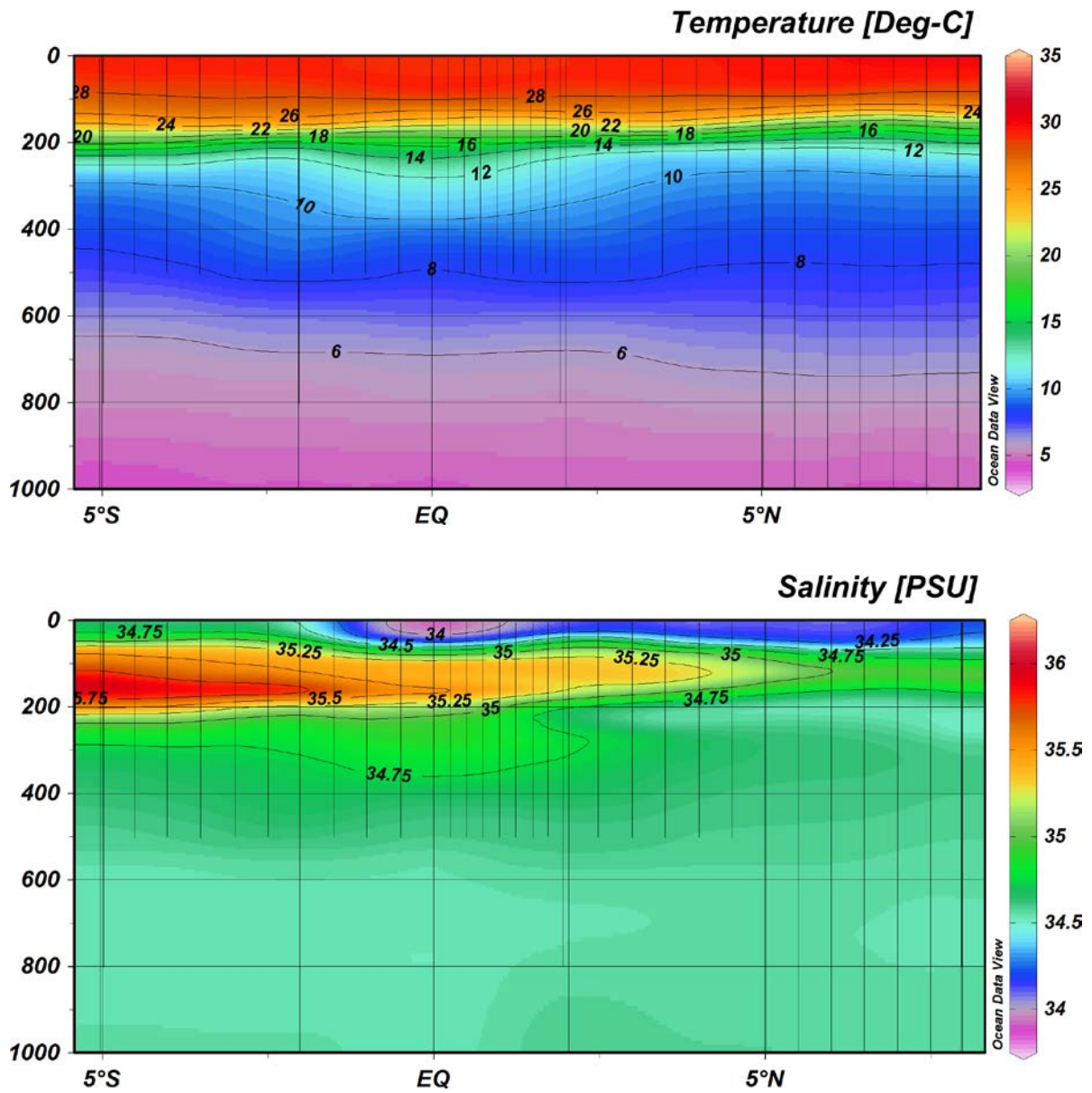


Fig. 6.2.2-3 Vertical section of temperature (upper) and salinity (lower) along 156E(X24 to X36)

## 6.3 Water sampling

### 6.3.1 Salinity

#### (1) Personnel

Yuji Kashino (JAMSTEC) : Principal Investigator  
Tamami Ueno (MWJ) : Technical Staff (Operation Leader)  
Hiroki Ushiomura (MWJ) : Technical Staff

#### (2) Objective

To measure bottle salinity obtained by CTD casts and The Continuous Sea Surface Water Monitoring System (TSG).

#### (3) Method

##### a. Salinity Sample Collection

Seawater samples were collected with 12 liter Niskin-X bottles and TSG. The salinity sample bottle of the 250ml brown glass with screw cap was used collecting the sample seawater. Each bottle was rinsed three times with the sample seawater, and was filled with sample seawater to the bottle shoulder. In this cruise, each bottle sealed with a plastic insert cap and a screw cap because we took into consideration the possibility of storage for about two weeks. These caps were rinsed three times with the sample seawater before its use. Each bottle was stored for more than 12 hours in the laboratory before the salinity measurement.

The kind and number of samples taken are shown as follows ;

Table 6.3.1-1 Kind and number of samples

Kind of Samples	Number of Samples
Samples for CTD	86
Samples for TSG	41
Total	127

##### b. Instruments and Method

The salinity measurement was carried out on R/V MIRAI during the cruise of MR12-03 using the salinometer (Model 8400B “AUTOSAL” ; Guildline Instruments Ltd.: S/N 62556) with an additional peristaltic-type intake pump (Ocean Scientific International, Ltd.). A pair of precision digital thermometers (Model 9540 ; Guildline Instruments Ltd.) were used. One thermometer monitored the ambient temperature and the other monitored the bath temperature of the salinometer.

The specifications of the AUTOSAL salinometer and thermometer are shown as follows ;

Salinometer (Model 8400B “AUTOSAL” ; Guildline Instruments Ltd.)

Measurement Range : 0.005 to 42 (PSU)

Accuracy : Better than  $\pm 0.002$  (PSU) over 24 hours

without re-standardization

Maximum Resolution : Better than  $\pm 0.0002$  (PSU) at 35 (PSU)

Thermometer (Model 9540 ; Guildline Instruments Ltd.)

Measurement Range : -40 to +180 deg C  
Resolution : 0.001  
Limits of error  $\pm$ deg C : 0.01 (24 hours @ 23 deg C  $\pm$ 1 deg C)  
Repeatability :  $\pm$ 2 least significant digits

The measurement system was almost the same as Aoyama *et al.* (2002). The salinometer was operated in the air-conditioned ship's laboratory at a bath temperature of 24 deg C. The ambient temperature varied from approximately 22 deg C to 25 deg C, while the bath temperature was very stable and varied within  $\pm$  0.002 deg C on rare occasion. The measurement for each sample was done with a double conductivity ratio and defined as the median of 31 readings of the salinometer. Data collection was started 10 seconds after filling the cell with the sample and it took about 15 seconds to collect 31 readings by a personal computer. Data were taken for the sixth and seventh filling of the cell. In the case of the difference between the double conductivity ratio of these two fillings being smaller than 0.00002, the average value of the double conductivity ratio was used to calculate the bottle salinity with the algorithm for the practical salinity scale, 1978 (UNESCO, 1981). If the difference was greater than or equal to 0.00003, an eighth filling of the cell was done. In the case of the difference between the double conductivity ratio of these two fillings being smaller than 0.00002, the average value of the double conductivity ratio was used to calculate the bottle salinity. In the case of the double conductivity ratio of eighth filling did not satisfy the criteria, we measured a ninth filling of the cell and calculated the bottle salinity. The measurement was conducted in about 5 hours per day and the cell was cleaned with soap after the measurement of the day.

#### (4) Preliminary Results

##### a. Standard Seawater

Standardization control of the salinometer was set to 696 at 26th July. But soon the value of SSW was off the point. So standardization control of the salinometer was set again to 693 at 28th July. After the day, the value of STANDBY was 24+5200~5201 and that of ZERO was 0.0-0001~0000.

In this cruise, the conductivity ratio of IAPSO Standard Seawater batch P154 was 0.99990 (the double conductivity ratio was 1.99980) and was used as the standard for salinity.

The specifications of SSW used in this cruise are shown as follows ;

Batch : P154  
Conductivity Ratio : 0.99990  
Salinity : 34.996  
Use By : 20<sup>th</sup> October 2014

Fig.6.3.1 shows the double conductivity ratio of the Standard Seawater. Figure (a) shows before correction. The average of the double conductivity ratio was 1.99986 and the standard deviation was 0.00003, which is equivalent to 0.0006 in salinity. Figure (b) shows after correction. The average of the double conductivity ratio was 1.99980 and the standard deviation was 0.00001, which is equivalent to 0.0002 in salinity.

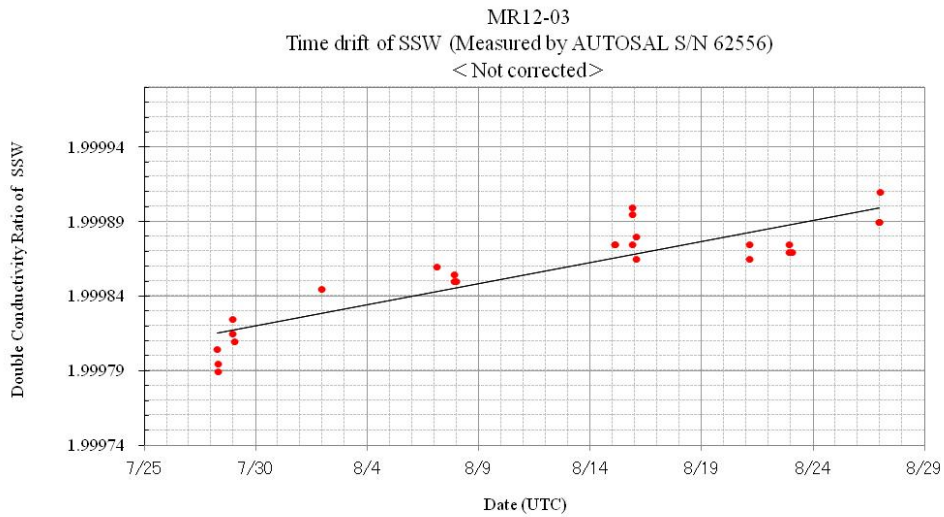


Fig. 6.3.1(a) Time series of double conductivity ratio for the Standard Seawater (before correction)

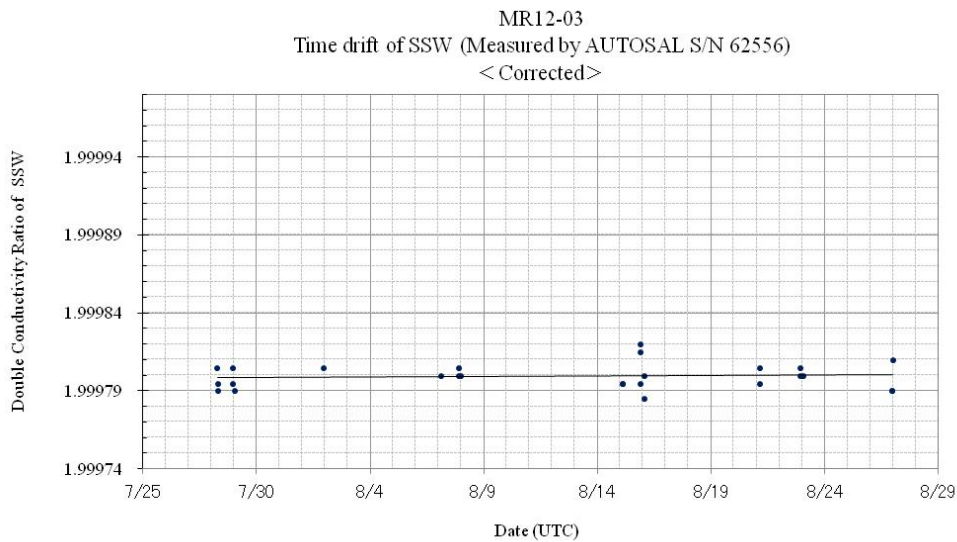


Fig.6.3.1(b) Time series of double conductivity ratio for the Standard Seawater (after correction)

b. Sub-Standard Seawater

Sub-standard seawater was made from deep-sea water filtered by a pore size of 0.45 micrometer and stored in a 20 liter container made of polyethylene and stirred for at least 24 hours before measuring. It was measured about every 6 samples in order to check for the possible sudden drifts of the salinometer.

c. Replicate Samples

We estimated the precision of this method using 43 pairs of replicate samples taken from the same Niskin bottle. Fig.6.3.2 shows the histogram of the absolute difference between each pair of the replicate samples. The average and the standard deviation of absolute difference among 43 pairs of replicate samples were 0.0003 and 0.0003 in salinity, respectively.

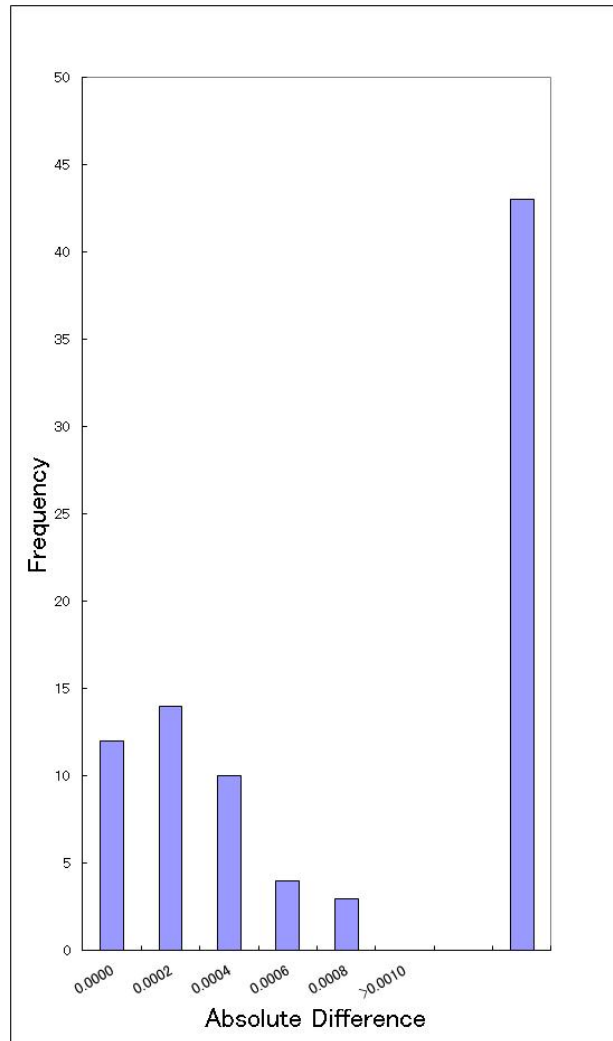


Fig.6.3.2 The histogram of the double conductivity ratio for the absolute difference of replicate samples

#### 5) Data archive

These raw datasets will be submitted to JAMSTEC Data Management Office (DMO).

#### (6) Reference

- Aoyama, M. T. Joyce, T. Kawano and Y. Takatsuki : Standard seawater comparison up to P129.  
Deep-Sea Research, I, Vol. 49, 1103~1114, 2002
- UNESCO : Tenth report of the Joint Panel on Oceanographic Tables and Standards.  
UNESCO Tech. Papers in Mar. Sci., 36, 25 pp., 1981

## 6.4 Continuous monitoring of surface seawater

### 6.4.1 Temperature, salinity, dissolved oxygen

#### 1. Personnel

Yuji Kashino (JAMSTEC): Principal Investigator

Shoko Tatamisashi (MWJ)

#### 2. Objective

Our purpose is to obtain salinity, temperature and dissolved oxygen data continuously in near-sea surface water.

#### 3. Instruments and Methods

The Continuous Sea Surface Water Monitoring System (Marine Works Japan Co. Ltd.) has four sensors and automatically measures salinity, temperature and dissolved oxygen in near-sea surface water every one minute. This system is located in the “*sea surface monitoring laboratory*” and connected to shipboard LAN-system. Measured data, time, and location of the ship were stored in a data management PC. The near-surface water was continuously pumped up to the laboratory from about 5 m water depth and flowed into the system through a vinyl-chloride pipe. The flow rate of the surface seawater was adjusted to be  $3 \text{ dm}^3 \text{ min}^{-1}$ . Specifications of the each sensor in this system are listed below.

##### a. Instruments

###### Software

Seamoni-kun Ver.1.20

###### Sensors

Specifications of the each sensor in this system are listed below.

###### Temperature and Conductivity sensor

Model:	SBE-45, SEA-BIRD ELECTRONICS, INC.
Serial number:	4552788-0264
Measurement range:	Temperature -5 to +35 °C Conductivity 0 to 7 S m <sup>-1</sup>
Initial accuracy:	Temperature 0.002 °C Conductivity 0.0003 S m <sup>-1</sup>

Typical stability (per month): Temperature 0.0002 °C  
 Conductivity 0.0003 S m<sup>-1</sup>  
 Resolution: Temperatures 0.0001 °C  
 Conductivity 0.00001 S m<sup>-1</sup>

Bottom of ship thermometer

Model: SBE 38, SEA-BIRD ELECTRONICS, INC.  
 Serial number: 3852788-0457  
 Measurement range: -5 to +35 °C  
 Initial accuracy: ±0.001 °C  
 Typical stability (per 6 month): 0.001 °C  
 Resolution: 0.00025 °C

Dissolved oxygen sensor

Model: OPTODE 3835, AANDERAA Instruments.  
 Serial number: 1233  
 Measuring range: 0 - 500 µmol dm<sup>-3</sup>  
 Resolution: <1 µmol dm<sup>-3</sup>  
 Accuracy: <8 µmol dm<sup>-3</sup> or 5% whichever is greater  
 Settling time: <25 s

4. Measurements

Periods of measurement, maintenance, and problems during MR12-03 are listed in Table 6.4.1-1.

Table 6.4.1-1 Events list of the surface seawater monitoring during MR12-03

System Date [UTC]	System Time [UTC]	Events	Remarks
2012/07/17	2:35	Start up a system. Check the logging data.	
2012/07/17	3:00	All of the measurements started and data was available.	
2012/08/28	04:00	All the measurements stopped.	

## 5. Preliminary Result

We took the surface water samples to compare sensor data with bottle data of salinity. The results are shown in Fig.6.4.1-1. All the salinity samples were analyzed by the Guideline 8400B “AUTOSAL”. Preliminary data of temperature, salinity, and dissolved oxygen at sea surface are shown in Fig.6.4.1-2.

## 6. Data archive

These data obtained in this cruise will be submitted to the Data Management Office (DMO) of JAMSTEC, and will be opened to the public via “R/V Mirai Data Web Page” in JAMSTEC home page.

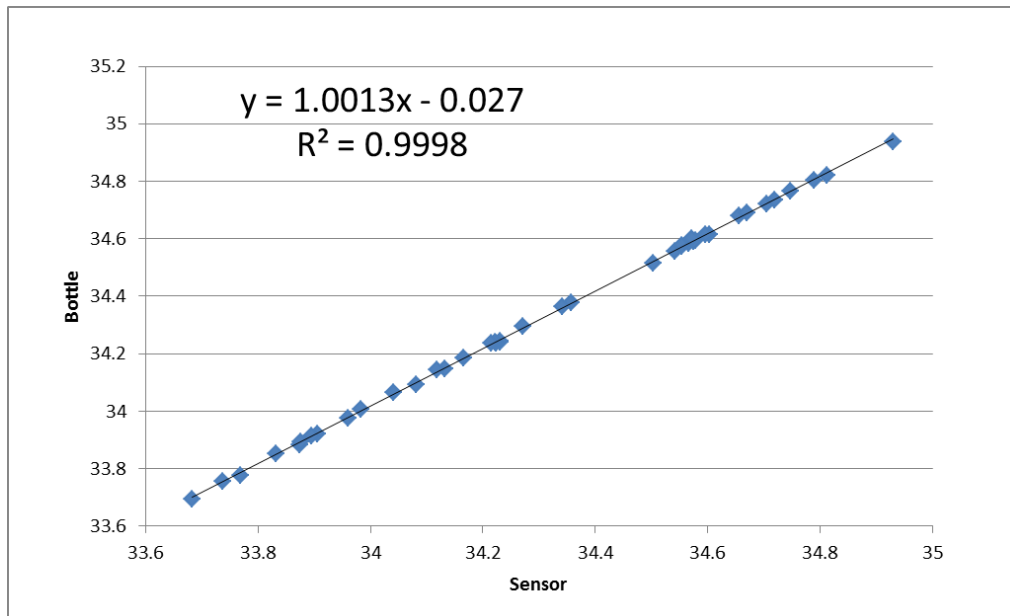
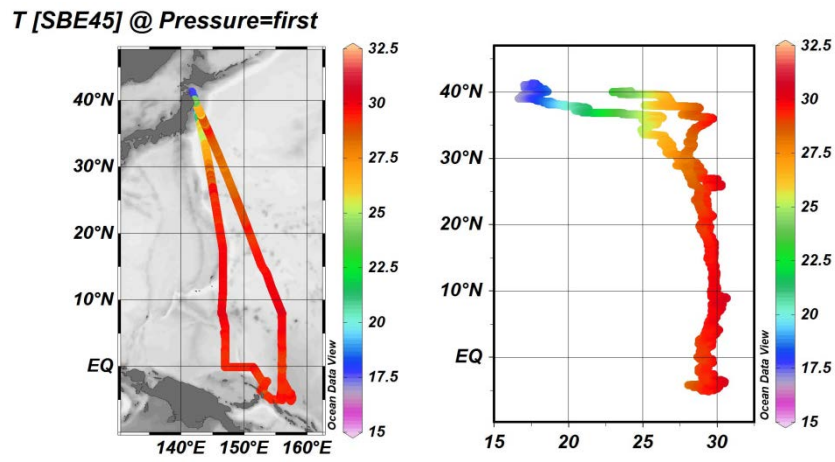
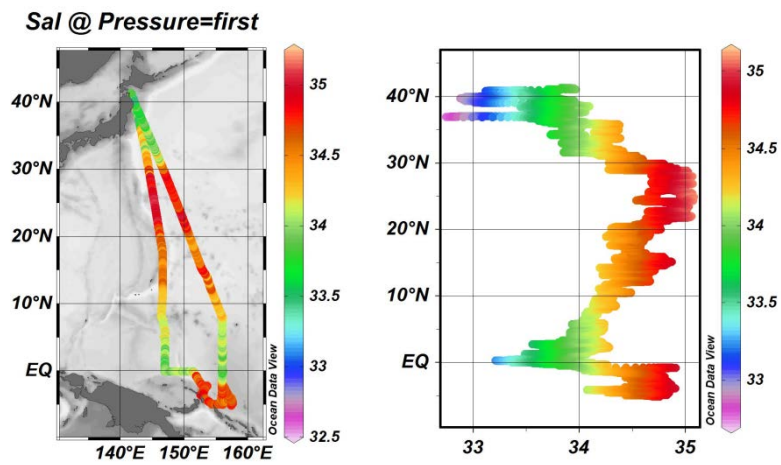


Fig.6.4.1-1 Correlation of salinity between sensor data and bottle data.

(a) Temperature



(b) Salinity



(c) Dissolved oxygen

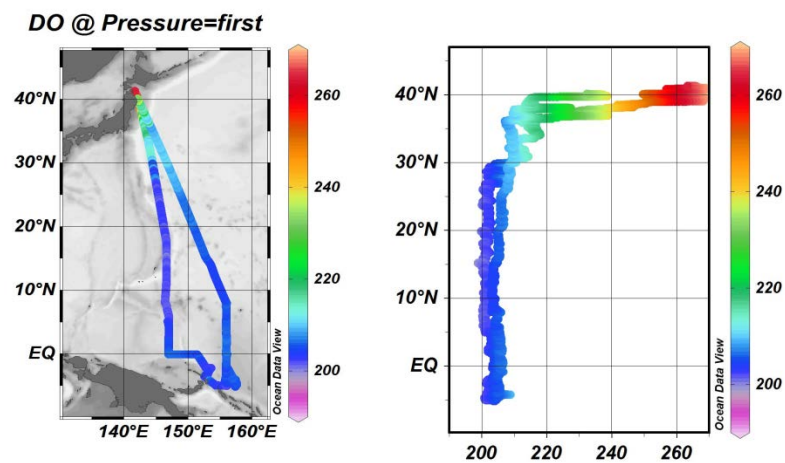


Fig.6.4.1-2 Spatial and temporal distribution of (a) temperature (b) salinity (c) dissolved oxygen in MR12-03 cruise.

## 6.5 Underway pCO<sub>2</sub>

**Shuji KAWAKAMI (JAXA): Principal Investigator**

**Yoshiyuki NAKANO (JAMSTEC MIO)**

**Hatsumi AOYAMA(MWJ): Operation Leader**

**Minoru KAMATA(MWJ)**

### (1) Objectives

Concentrations of CO<sub>2</sub> in the atmosphere are increasing at a rate of 1.5 ppmv yr<sup>-1</sup> owing to human activities such as burning of fossil fuels, deforestation, and cement production. Oceanic CO<sub>2</sub> concentration is also considered to be increased with the atmospheric CO<sub>2</sub> increase, however, its variation is widely different by time and locations. Underway pCO<sub>2</sub> observation is indispensable to know the pCO<sub>2</sub> distribution, and it leads to elucidate the mechanism of oceanic pCO<sub>2</sub> variation. We here report the underway pCO<sub>2</sub> measurements performed during MR12-03 cruise.

### (2) Methods, Apparatus and Performance

Oceanic and atmospheric CO<sub>2</sub> concentrations were measured during the cruise using an automated system equipped with a non-dispersive infrared gas analyzer (NDIR; LI-7000, Li-Cor). Measurements were done every about one and a half hour, and 4 standard gases, atmospheric air, and the CO<sub>2</sub> equilibrated air with sea surface water were analyzed subsequently in this hour. The concentrations of the CO<sub>2</sub> standard gases were 300.08, 349.96, 399.98 and 450.23 ppmv. Atmospheric air taken from the bow of the ship (approx.30 m above the sea level) was introduced into the NDIR by passing through a electrical cooling unit, a mass flow controller which controls the air flow rate of 0.5 L min<sup>-1</sup>, a membrane dryer (MD-110-72P, perma pure llc.) and chemical desiccant (Mg(ClO<sub>4</sub>)<sub>2</sub>). The CO<sub>2</sub> equilibrated air was the air with its CO<sub>2</sub> concentration was equivalent to the sea surface water. Seawater was taken from an intake placed at the approximately 4.5 m below the sea surface and introduced into the equilibrator at the flow rate of 4 - 5 L min<sup>-1</sup> by a pump. The equilibrated air was circulated in a closed loop by a pump at flow rate of 0.6 - 0.8 L min<sup>-1</sup> through two cooling units, a membrane dryer, the chemical desiccant, and the NDIR.

### (3) Preliminary results

Cruise track during pCO<sub>2</sub> observation is shown in Figure 6.5-1. Temporal variations of both oceanic and atmospheric CO<sub>2</sub> concentration (xCO<sub>2</sub>) are shown in Fig. 6.5-2.

### (4) Data Archive

Data obtained in this cruise will be submitted to the Data Management Office (DMO) of JAMSTEC, and will be opened to the public via "R/V Mirai Data Web Page" in JAMSTEC home page.

### (5) Reference

Dickson, A. G., Sabine, C. L. & Christian, J. R. (2007), Guide to best practices for ocean CO<sub>2</sub> measurements; PICES Special Publication 3, 199pp.

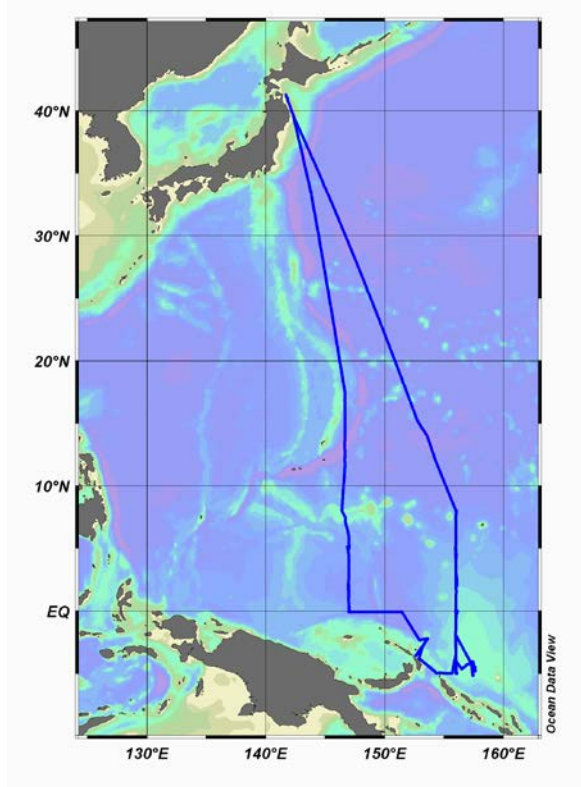


Figure 6.5-1 Observation map

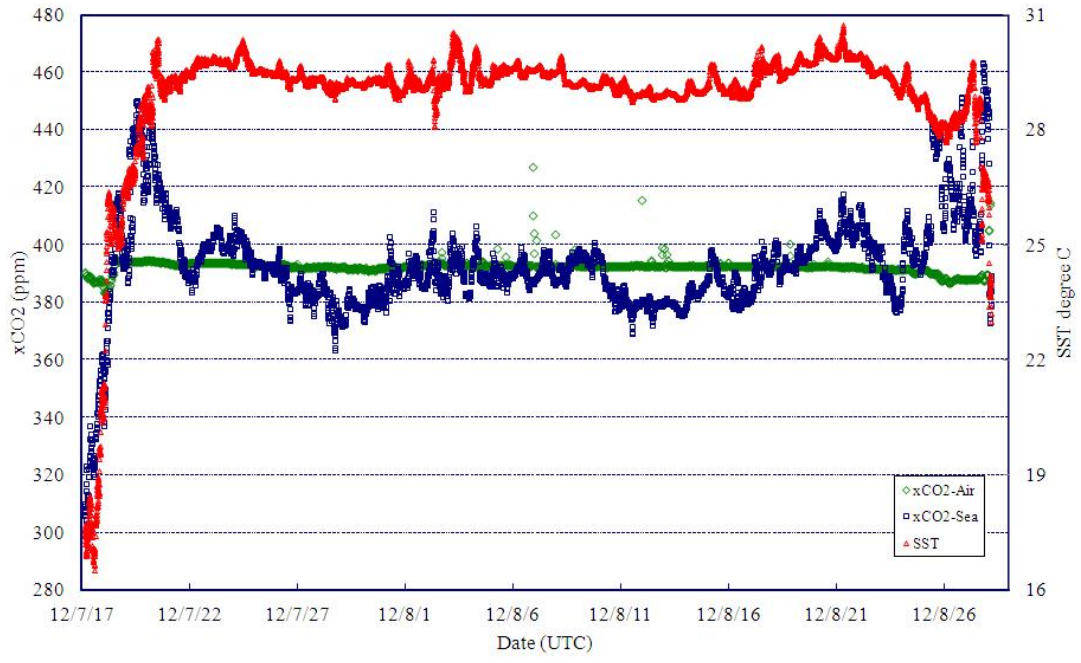


Figure 6.5-1 Temporal variations of oceanic and atmospheric CO<sub>2</sub> concentration (xCO<sub>2</sub>). Blue dots represent oceanic xCO<sub>2</sub> variation and green atmospheric xCO<sub>2</sub>. SST variation (red) is also shown.

## 6.6 Shipboard ADCP

### (1) Personnel

Yuji Kashino	(JAMSTEC): Principal Investigator
Wataru Tokunaga	(Global Ocean Development Inc., GODI)
Harumi Ota	(GODI)
Koichi Inagaki	(GODI)
Ryo Ohyama	(MIRAI Crew)

### (2) Objective

To obtain continuous measurement of the current profile along the ship's track.

### (3) Methods

Upper ocean current measurements were made in MR12-03 cruise, using the hull-mounted Acoustic Doppler Current Profiler (ADCP) system. For most of its operation the instrument was configured for water-tracking mode. Bottom-tracking mode, interleaved bottom-ping with water-ping, was made to get the calibration data for evaluating transducer misalignment angle. The system consists of following components;

- 1) R/V MIRAI has installed the Ocean Surveyor for vessel-mount (acoustic frequency 76.8 kHz; Teledyne RD Instruments). It has a phased-array transducer with single ceramic assembly and creates 4 acoustic beams electronically. We mounted the transducer head rotated to a ship-relative angle of 45 degrees azimuth from the keel
- 2) For heading source, we use ship's gyro compass (Tokimec, Japan), continuously providing heading to the ADCP system directory. Additionally, we have Inertial Navigation System (INS) which provide high-precision heading, attitude information, pitch and roll, are stored in ".N2R" data files with a time stamp.
- 3) DGPS system (Trimble SPS751 & StarFixXP) providing position fixes.
- 4) We used VmDas version 1.4.6 (TRD Instruments) for data acquisition.
- 5) To synchronize time stamp of ping with GPS time, the clock of the logging computer is adjusted to GPS time every 1 minute
- 6) We have placed ethylene glycol into the fresh water to prevent freezing in the sea chest.
- 7) The sound speed at the transducer does affect the vertical bin mapping and vertical velocity measurement, is calculated from temperature, salinity (constant value; 35.0 psu) and depth (6.5 m; transducer depth) by equation in Medwin (1975).

Data was configured for 16 m intervals starting 16 m below the surface. Every ping was recorded as raw ensemble data (.ENR). Also, 60 seconds and 300 seconds averaged data were recorded as short term average (.STA) and long term average (.LTA) data, respectively. Major parameters for the measurement (Direct Command) are shown in Table 6.6-1.

(4) Preliminary results

Fig.6.6-1 shows the surface current vector along the ship's track.

(5) Data archive

These data obtained in this cruise will be submitted to the Data Management Group (DMG) of JAMSTEC, and will be opened to the public via JAMSTEC home page.

Table 6.6-1 Major parameters

---

***Bottom-Track Commands***

BP = 001                      Pings per Ensemble (almost less than 1300m depth)  
23:32UTC 16 July to 18:06UTC 17 July, 2012  
18:56UTC 27 August to 00:11UTC 29 August, 2012

***Environmental Sensor Commands***

EA = +04500                  Heading Alignment (1/100 deg)  
EB = +00000                  Heading Bias (1/100 deg)  
ED = 00065                   Transducer Depth (0 - 65535 dm)  
EF = +001                      Pitch/Roll Divisor/Multiplier (pos/neg) [1/99 - 99]  
EH = 00000                   Heading (1/100 deg)  
ES = 35                          Salinity (0-40 pp thousand)  
EX = 00000                   Coord Transform (Xform:Type; Tilts; 3Bm; Map)  
EZ = 10200010                Sensor Source (C; D; H; P; R; S; T; U)  
C (1): Sound velocity calculates using ED, ES, ET (temp.)  
D (0): Manual ED  
H (2): External synchro  
P (0), R (0): Manual EP, ER (0 degree)  
S (0): Manual ES  
T (1): Internal transducer sensor  
U (0): Manual EU

***Timing Commands***

TE = 00:00:02.00              Time per Ensemble (hrs:min:sec.sec/100)  
TP = 00:02.00                   Time per Ping (min:sec.sec/100)

***Water-Track Commands***

WA = 255                        False Target Threshold (Max) (0-255 count)  
WB = 1                           Mode 1 Bandwidth Control (0=Wid, 1=Med, 2=Nar)  
WC = 120                        Low Correlation Threshold (0-255)  
WD = 111 100 000              Data Out (V; C; A; PG; St; Vsum; Vsum^2;#G;P0)  
WE = 1000                       Error Velocity Threshold (0-5000 mm/s)

WF = 0800	Blank After Transmit (cm)
WG = 001	Percent Good Minimum (0-100%)
WI = 0	Clip Data Past Bottom (0 = OFF, 1 = ON)
WJ = 1	Rcvr Gain Select (0 = Low, 1 = High)
WM = 1	Profiling Mode (1-8)
WN = 40	Number of depth cells (1-128)
WP = 00001	Pings per Ensemble (0-16384)
WS = 1600	Depth Cell Size (cm)
WT = 000	Transmit Length (cm) [0 = Bin Length]
WV = 0390	Mode 1 Ambiguity Velocity (cm/s radial)

---

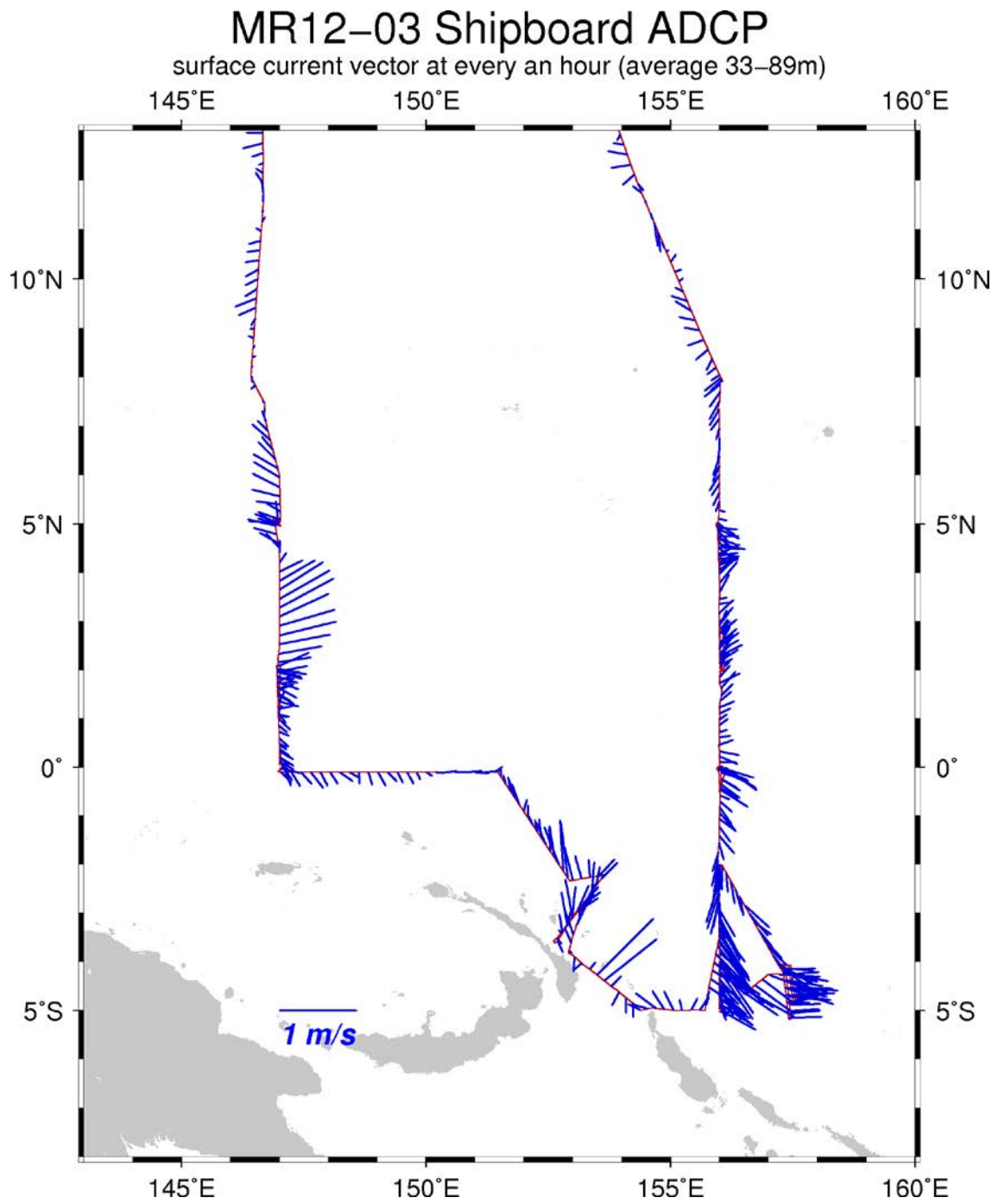


Fig 6.6-1. Surface current vector along the ship's track. (TRITON area)

## 6.7 Underway geophysics

### Personnel

Takeshi Hanyu	(JAMSTEC)	: Principal Investigator
Takeshi Matsumoto	(University of the Ryukyus)	: Principal Investigator (Not on-board)
Masao Nakanishi	(Chiba University)	: Principal Investigator (Not on-board)
Wataru Tokunaga	(Global Ocean Development Inc., GODI)	
Harumi Ota	(GODI)	
Koichi Inagaki	(GODI)	
Ryo Ohyama	(MIRAI Crew)	

### 6.7.1. Sea surface gravity

#### (1) Introduction

The local gravity is an important parameter in geophysics and geodesy. We collected gravity data at the sea surface.

#### (2) Parameters

Relative Gravity [CU: Counter Unit]  
[mGal] = (coef1: 0.9946) \* [CU]

#### (3) Data Acquisition

We measured relative gravity using LaCoste and Romberg air-sea gravity meter S-116 (Micro-g LaCoste, LLC) during the MR12-03 cruise from 17th July 2012 to 29th August 2012.

To convert the relative gravity to absolute one, we measured gravity, using portable gravity meter (Scintrex gravity meter CG-5), at Sekinehama as the reference point.

#### (4) Preliminary Results

Absolute gravity shown in Tabel 6.7.1-1

#### (5) Data Archives

Surface gravity data obtained during this cruise will be submitted to the Data Management Group (DMG) in JAMSTEC, and will be archived there.

Table 6.7.1-1

No	Date	UTC	Port	Absolute Gravity [mGal]	Sea Level [cm]	Draft [cm]	Gravity at Sensor * <sup>1</sup> [mGal]	L&R* <sup>2</sup> Gravity [mGal]
#1	July/16	21:50	Sekinehama	980,371.93	316	669	980,372.21	12,614.68
#2	Aug/12	03:33	Sekinehama	980,371.94	243	633	980,372.91	12,610.65

\*1: Gravity at Sensor = Absolute Gravity + Sea Level\*0.3086/100 + (Draft-530)/100\*0.2222

\*2: LaCoste and Romberg air-sea gravity meter S-116

## 6.7.2 Sea surface magnetic field

### 1) Three-component magnetometer

#### (1) Introduction

Measurement of magnetic force on the sea is required for the geophysical investigations of marine magnetic anomaly caused by magnetization in upper crustal structure. We measured geomagnetic field using a three-component magnetometer during the MR12-03 cruise from 17th July 2012 to 29th August 2012.

#### (2) Principle of ship-board geomagnetic vector measurement

The relation between a magnetic-field vector observed on-board,  $\mathbf{H}_{ob}$ , (in the ship's fixed coordinate system) and the geomagnetic field vector,  $\mathbf{F}$ , (in the Earth's fixed coordinate system) is expressed as:

$$\mathbf{H}_{ob} = \tilde{\mathbf{A}} \tilde{\mathbf{R}} \tilde{\mathbf{P}} \tilde{\mathbf{Y}} \mathbf{F} + \mathbf{H}_p \quad (a)$$

where  $\tilde{\mathbf{R}}$ ,  $\tilde{\mathbf{P}}$  and  $\tilde{\mathbf{Y}}$  are the matrices of rotation due to roll, pitch and heading of a ship, respectively.  $\tilde{\mathbf{A}}$  is a 3 x 3 matrix which represents magnetic susceptibility of the ship, and  $\mathbf{H}_p$  is a magnetic field vector produced by a permanent magnetic moment of the ship's body. Rearrangement of Eq. (a) makes

$$\tilde{\mathbf{R}} \mathbf{H}_{ob} + \mathbf{H}_{bp} = \tilde{\mathbf{R}} \tilde{\mathbf{P}} \tilde{\mathbf{Y}} \mathbf{F} \quad (b)$$

where  $\tilde{\mathbf{R}} = \tilde{\mathbf{A}}^{-1}$ , and  $\mathbf{H}_{bp} = -\tilde{\mathbf{R}} \mathbf{H}_p$ . The magnetic field,  $\mathbf{F}$ , can be obtained by measuring  $\tilde{\mathbf{R}}$ ,  $\tilde{\mathbf{P}}$ ,  $\tilde{\mathbf{Y}}$  and  $\mathbf{H}_{ob}$ , if  $\tilde{\mathbf{R}}$  and  $\mathbf{H}_{bp}$  are known. Twelve constants in  $\tilde{\mathbf{R}}$  and  $\mathbf{H}_{bp}$  can be determined by measuring variation of  $\mathbf{H}_{ob}$  with  $\tilde{\mathbf{R}}$ ,  $\tilde{\mathbf{P}}$  and  $\tilde{\mathbf{Y}}$  at a place where the geomagnetic field,  $\mathbf{F}$ , is known.

#### (3) Instruments on R/V MIRAI

A shipboard three-component magnetometer system (Tierra Tecnica SFG1214) is equipped on-board R/V MIRAI. Three-axes flux-gate sensors with ring-cored coils are fixed on the fore mast. Outputs from the sensors are digitized by a 20-bit A/D converter (1 nT/LSB), and sampled at 8 times per second. Ship's heading, pitch, and roll are measured by the Inertial Navigation System (INS) for controlling attitude of a Doppler radar. Ship's position (GPS) and speed data are taken from LAN every second.

#### (4) Data Archives

These data obtained in this cruise will be submitted to the Data Management Group (DMG) of JAMSTEC.

#### (5) Remarks

- 1) For calibration of the ship's magnetic effect, we made a "figure-eight" turn (a pair of clockwise and anti-clockwise rotation). This calibration was carried out as below.

27th Jul. 2012, 19:07 – 19:30UTC around at 02-05N, 146-57E  
 03rd Aug. 2012, 18:28 – 18:53UTC around at 05-02S, 156-01E  
 07th Aug. 2012, 05:06 – 05:52UTC around at 04-16S, 157-26E  
 11th Aug. 2012, 06:58 – 07:24UTC around at 00-03S, 155-59E  
 20th Aug. 2012, 02:40 – 03:17UTC around at 07-57S, 156-00E

## 2) Cesium magnetometer

### (1) Introduction

Measurement of total magnetic force on the sea is required for the geophysical investigations of marine magnetic anomaly caused by magnetization in upper crustal structure.

### (2) Data Period and Sensor Rotation

30 Jul. 2012, 01:32 – 30 Jul. 2012, 03:02UTC	Rotation = 0 degrees
30 Jul. 2012, 03:44 – 31 Jul. 2012, 18:34UTC	Rotation = 45 degrees
06 Aug. 2012, 04:43 – 06 Aug. 2012, 19:29UTC	Rotation = 0 degrees
07 Aug. 2012, 04:48 – 07 Aug. 2012, 19:29UTC	Rotation = 0 degrees

### (3) Specification

We measured total geomagnetic field using a cesium marine magnetometer (Geometrics Inc., G-882) and recorded by G-882 data logger (Clovertech Co., Ver.1.0.0). The G-882 magnetometer uses an optically pumped Cesium-vapor atomic resonance system. The sensor fish towed 500 m behind the vessel to minimize the effects of the ship's magnetic field. Table 6.7.2-1 shows system configuration of MIRAI cesium magnetometer system.

Table 6.7.2-1 System configuration of MIRAI cesium magnetometer.

Dynamic operating range:	20,000 to 100,000 nT
Absolute accuracy:	<±2 nT throughout range
Setting: Cycle rate;	0.1 sec
Sensitivity;	0.001265 nT at a 0.1 second cycle rate
Sampling rate;	1 sec

### (4) Data Archive

Total magnetic force data obtained during this cruise was submitted to the Data Management Group (DMG) of JAMSTEC, and archived there.

### 6.7.3. Swath Bathymetry

#### 1) Multi beam echo sounding system

##### (1) Introduction

R/V MIRAI is equipped with a Multi narrow Beam Echo Sounding system (MBES), SEABEAM 3012 Upgrade Model (L3 Communications ELAC Nautik). The objective of MBES is collecting continuous bathymetric data along ship's track to make a contribution to geological and geophysical investigations and global datasets.

##### (2) Data Acquisition

The "SEABEAM 3012 Upgrade Model" on R/V MIRAI was used for bathymetry mapping during the MR12-03 cruise from 17th July 2012 to 29th August 2012.

To get accurate sound velocity of water column for ray-path correction of acoustic multibeam, we used Surface Sound Velocimeter (SSV) data to get the sea surface (6.62m) sound velocity, and the deeper depth sound velocity profiles were calculated by temperature and salinity profiles from CTD, XCTD and Argo float data by the equation in Del Grosso (1974) during the cruise.

Table 6.7.3-1 shows system configuration and performance of SEABEAM 3012 system.

Table 6.7.3-1 SEABEAM 3012 System configuration and performance

Frequency:	12 kHz
Transmit beam width:	1.6 degree
Transmit power:	20 kW
Transmit pulse length:	2 to 20 msec.
Receive beam width:	1.8 degree
Depth range:	100 to 11,000 m
Beam spacing:	0.5 degree athwart ship
Swath width:	150 degree (max) 120 degree to 4,500 m 100 degree to 6,000 m 90 degree to 11,000 m
Depth accuracy:	Within < 0.5% of depth or +/-1m, whichever is greater, over the entire swath. (Nadir beam has greater accuracy; typically within < 0.2% of depth or +/-1m, whichever is greater)

##### (3) Preliminary Results

The results will be published after primary processing. For the operations of dredge in this cruise, underway geophysical data were used to explore detailed bathymetry and structure of the seafloor near the dredge sites. Objectives and preliminary results for the underway geophysical survey related with dredges are referred to Section 7.12.

**(4) Data Archives**

Bathymetric data obtained during this cruise will be submitted to the Data Management Group (DMG) in JAMSTEC, and will be archived there.

**2) Sub-bottom profiler**

**(1) Introduction**

R/V MIRAI is equipped with a Sub-bottom Profiler (SBP), Bathy2010 (SyQwest). The objective of SBP is collecting sub-bottom data along ship's track.

**(2) Data Acquisition**

Bathy2010 on R/V MIRAI was used for sub-bottom mapping during the following periods.

29 Jul. 2012, 22:41UTC – 31 Jul. 2012, 19:34UTC

05 Aug. 2012, 06:28UTC – 08 Aug. 2012 18:30UTC

Table 6.6.3-2 shows system configuration and performance of Bathy2010 system.

Table 6.6.3-2 Bathy2010 System configuration and performance

---

Frequency:	3.5 kHz
Transmit beam width:	23 degree
Transmit pulse length:	0.5 to 50 msec
Strata resolution:	Up to 8 cm with 300+ Meters of bottom penetration; bottom type dependant
Depth resolution:	0.1 Feet, 0.1 Meters
Depth accuracy:	±10 cm to 100 m, ± .3% to 6,000 m

**(3) Data Archives**

Sub-bottom data obtained during this cruise will be submitted to the Data Management Group (DMG) in JAMSTEC, and will be archived there.

## 7 Special Observations

### 7.1 TRITON buoys

#### 7.1.1 Operation of TRITON buoys

##### (1) Personnel

Yuji Kashino	(JAMSTEC): Principal Investigator
Akira Watanabe	(MWJ): Operation Leader
Hiroshi Matsunaga	(MWJ): Technical Staff
Tomohide Noguchi	(MWJ): Technical Staff
Hiroki Ushiomura	(MWJ): Technical Staff
Shungo Oshitani	(MWJ): Technical Staff
Tamami Ueno	(MWJ): Technical Staff
Rei Ito	(MWJ): Technical Staff
Tetsuya Nagahama	(MWJ): Technical Staff
Masaki Yamada	(MWJ): Technical Staff
Tetsuharu Iino	(MWJ): Technical Staff
Yohei Taketomo	(MWJ): Technical Staff
Yuki Miyajima	(MWJ): Technical Staff
Minoru Kamata	(MWJ): Technical Staff
Shoko Tatamisashi	(MWJ): Technical Staff
Hatsumi Aoyama	(MWJ): Technical Staff
Kazuma Takahashi	(MWJ): Technical Staff
Shihomi Saito	(MWJ): Technical Staff

##### (2) Objectives

The large-scale air-sea interaction over the warmest sea surface temperature region in the western tropical Pacific Ocean called warm pool that affects the global atmosphere and causes El Nino phenomena. The formation mechanism of the warm pool and the air-sea interaction over the warm pool have not been well understood. Therefore, long term data sets of temperature, salinity, currents and meteorological elements have been required at fixed locations. The TRITON program aims to obtain the basic data to improve the predictions of El Nino and variations of Asia-Australian Monsoon system.

TRITON buoy array is integrated with the existing TAO(Tropical Atmosphere Ocean) array, which is presently operated by the Pacific Marine Environmental Laboratory/National Oceanic and Atmospheric Administration of the United States. TRITON is a component of international research program of CLIVAR (Climate Variability and Predictability), which is a major component of World Climate Research Program sponsored by the World Meteorological Organization, the International Council of Scientific Unions, and the Intergovernmental Oceanographic Commission of UNESCO. TRITON will also contribute to the development of GOOS (Global Ocean Observing System) and GCOS (Global Climate Observing System).

Nine TRITON buoys have been successfully recovered and deployed during this R/V MIRAI cruise (MR12-03).

##### (3) Measured parameters

Meteorological parameters: wind speed, direction, atmospheric pressure, air temperature, relative humidity, radiation, precipitation.

Oceanic parameters: water temperature and conductivity at 1.5m, 25m, 50m, 75m, 100m, 125m, 150m, 200m, 300m, 500m 750m, depth at 300m and 750m, currents at 10m.

(4) Instrument

1) CTD and CT

SBE-37 IM MicroCAT

A/D cycles to average : 4  
Sampling interval : 600sec  
Measurement range, Temperature : -5~+33 deg-C  
Measurement range, Conductivity : 0~+7 S/m  
Measurement range, Pressure : 0~full scale range

2) CRN(Current meter)

SonTek Argonaut ADCM

Sensor frequency : 1500kHz  
Sampling interval : 1200sec  
Average interval : 120sec

3) Meteorological sensors

Precipitation

R.M.YOUNG COMPANY MODEL50202/50203

Atmospheric pressure

PAROPSCIENTIFIC.Inc. DIGIQUARTZ FLOATING BAROMETER 6000SERIES

Relative humidity/air temperature,Shortwave radiation, Wind speed/direction

Woods Hole Institution ASIMET

Sampling interval : 60sec  
Data analysis : 600sec averaged

(5) Locations of TRITON buoys deployment

Nominal location	8N, 156E
ID number at JAMSTEC	01014
Number on surface float	T02
ARGOS PTT number	28154
ARGOS backup PTT number	11592
Deployed date	21 Aug. 2012
Exact location	07° 58.02N, 156° 01.91E
Depth	4,846 m
Nominal location	5N, 156E
ID number at JAMSTEC	02014
Number on surface float	T03
ARGOS PTT number	27275
ARGOS backup PTT number	24235
Deployed date	18 Aug. 2012
Exact location	05° 01.21N, 155° 58.01 E
Depth	3,605 m
Nominal location	2N, 156E

ID number at JAMSTEC 03015  
Number on surface float T09  
ARGOS PTT number 30841  
ARGOS backup PTT number 29698  
Deployed date 15 Aug. 2012  
Exact location 02° 02.26N, 156° 01.26 E  
Depth 2,573 m

Nominal location EQ, 156E  
ID number at JAMSTEC 04015  
Number on surface float T10  
ARGOS PTT number 29759  
ARGOS backup PTT number 24715  
Deployed date 10 Aug. 2012  
Exact location 00° 00.97N, 156° 02.50 E  
Depth 1,953 m

Nominal location 2S, 156E  
ID number at JAMSTEC 05013  
Number on surface float T11  
ARGOS PTT number 32293  
ARGOS backup PTT number 29708  
Deployed date 09 Aug. 2012  
Exact location 02° 01.03S, 155° 57.52 E  
Depth 1,749 m

Nominal location 5S, 156E  
ID number at JAMSTEC 06013  
Number on surface float T17  
ARGOS PTT number 29767  
ARGOS backup PTT number 29738  
Deployed date 03 Aug. 2012  
Exact location 05° 02.01S, 156° 01.54 E  
Depth 1,523m

Nominal location 5N, 147E  
ID number at JAMSTEC 07013  
Number on surface float T18  
ARGOS PTT number 29719  
ARGOS backup PTT number 24230  
Deployed date 25 Jul. 2012  
Exact location 04° 57.82N, 147° 01.62 E  
Depth 4,293 m

Nominal location 2N, 147E  
ID number at JAMSTEC 08012  
Number on surface float T19

ARGOS PTT number 28157  
ARGOS backup PTT number 24240  
Deployed date 28 Jul. 2012  
Exact location 02° 04.45N, 146° 57.12 E  
Depth 4,491m

Nominal location EQ, 147E  
ID number at JAMSTEC 09013  
Number on surface float T22  
ARGOS PTT number 28320  
ARGOS backup PTT number 24229  
Deployed date 29 Jul. 2012  
Exact location 00° 03.54N, 147° 00.68 E  
Depth 4,473 m

(6) TRITON recovered

Nominal location 8N, 156E  
ID number at JAMSTEC 01013  
Number on surface float T01  
ARGOS PTT number 29765  
ARGOS backup PTT number 24242  
Deployed date 04 Dec. 2010  
Recovered date 19 Aug. 2012  
Exact location 07° 57.95N, 156° 02.09E  
Depth 4,842 m

Nominal location 5N, 156E  
ID number at JAMSTEC 02013  
Number on surface float T04  
ARGOS PTT number 27388  
ARGOS backup PTT number 29692  
Deployed date 06 Dec. 2010  
Recovered date 17 Aug. 2012  
Exact location 05° 01.29N, 155° 57.77 E  
Depth 3,601 m

Nominal location 2N, 156E  
ID number at JAMSTEC 03014  
Number on surface float T07  
ARGOS PTT number 27389  
ARGOS backup PTT number 29694  
Deployed date 08 Dec. 2010  
Recovered date 16 Aug. 2012  
Exact location 01° 57.17N, 156° 00.00 E  
Depth 2,563 m

Nominal location EQ, 156E

ID number at JAMSTEC 04014  
Number on surface float T05  
ARGOS PTT number 27401  
ARGOS backup PTT number 29697  
Deployed date 10 Dec. 2010  
Recovered date 11 Aug. 2012  
Exact location 00° 01.02S, 155° 57.35 E  
Depth 1,940 m

Nominal location 2S, 156E  
ID number at JAMSTEC 05012  
Number on surface float T06  
ARGOS PTT number 27399  
ARGOS backup PTT number 29710  
Deployed date 14 Dec. 2010  
Recovered date 08 Aug. 2012  
Exact location 01° 58.97S, 156° 01.84 E  
Depth 1,752 m

Nominal location 5S, 156E  
ID number at JAMSTEC 06012  
Number on surface float T08  
ARGOS PTT number 27394  
ARGOS backup PTT number 24243  
Deployed date 16 Dec. 2010  
Recovered date 04 Aug. 2012  
Exact location 04° 58.03S, 156° 01.00 E  
Depth 1,508m

Nominal location 5N, 147E  
ID number at JAMSTEC 07012  
Number on surface float T15  
ARGOS PTT number 29638  
ARGOS backup PTT number 24244  
Deployed date 26 Dec. 2010  
Recovered date 25 Jul. 2012  
Exact location 05° 02.53N, 146° 56.82 E  
Depth 4,257 m

Nominal location 2N, 147E  
ID number at JAMSTEC 08011  
Number on surface float T16  
ARGOS PTT number 29855  
ARGOS backup PTT number 24245  
Deployed date 24 Dec. 2010  
Recovered date 26 Jul. 2012  
Exact location 02° 04.47N, 146° 57.02 E

Depth 4,491 m

Nominal location EQ, 147E

ID number at JAMSTEC 09012

Number on surface float T20

ARGOS PTT number 29639

ARGOS backup PTT number 29696

Deployed date 21 Dec. 2010

Recovered date 29 Jul. 2012

Exact location 00° 01.48S, 146° 59.98 E

Depth 4,550 m

\*: Dates are UTC and represent anchor drop times for deployments and release time for recoveries, respectively.

#### (6) Details of deployed

We had deployed nine TRITON buoys, described them details in the list.

##### Deployment TRITON buoys

Observation No.	Location	Details
01013	8N156E	Deploy with full spec and 1 optional unit. JES10-CTIM : 750m
02013	5N156E	Deploy with full spec.
03014	2N156E	Deploy with full spec and 1 optional unit. SBE37 (CT) : 175m
04014	EQ156E	Deploy with full spec and 2 optional sensors. Security camera : with TRITON top buoy SBE37 (CT) : 175m
05012	2S156E	Deploy with full spec.
06012	5S156E	Deploy with full spec.
07012	5N147E	Deploy with full spec.
08011	2N147E	Deploy with full spec and 1 optional unit. SBE37 (CT) : 175m
09012	EQ147E	Deploy with full spec.

#### (7) Data archive

Hourly averaged data are transmitted through ARGOS satellite data transmission system in almost real time. The real time data are provided to meteorological organizations via Global Telecommunication System and utilized for daily weather forecast. The data will be also distributed world wide through Internet from JAMSTEC and PMEL home pages. All data will be archived at JAMSTEC Mutsu Institute.

TRITON Homepage : <http://www.jamstec.go.jp/jamstec/triton>

## 7.1.2 Inter-comparison between shipboard CTD and TRITON transmitted data

### (1) Personnel

Yuji Kashino	(JAMSTEC): Principal Investigator
Akira Watanabe	(MWJ): Technical Staff
Shungo Oshitani	(MWJ): Technical Staff

### (2) Objectives

TRITON CTD data validation.

### (3) Measured parameters

- Temperature
- Conductivity
- Pressure

### (4) Methods

TRITON buoy underwater sensors are equipped along a wire cable of the buoy below sea surface. We used the same CTD (SBE 9/11Plus) system with general CTD observation (See section 6.2.1) on R/V MIRAI for this intercomparison. We conducted 1 CTD cast at each TRITON buoy site before recovery, conducted 1 XCTD cast at each TRITON buoy site after deployment. The cast was performed immediately after the deployment and before recovery. R/V MIRAI was kept the distance from the TRITON buoy within 2 nm.

TRITON buoy data was sampled every 1 hour except for transmission to the ship. We compared CTD observation by R/V MIRAI data with TRITON buoy data using the 1 hour averaged value.

As our temperature sensors are expected to be more stable than conductivity sensors, conductivity data and salinity data are selected at the same value of temperature data. Then, we calculate difference of salinity from conductivity between the shipboard CTD data on R/V MIRAI and the TRITON buoy data for each recovery of buoys.

Compared site			
Observation No.	Latitude	Longitude	Condition
01013	8N	156E	Before Recover
02013	5N	156E	Before Recover
03014	2N	156E	Before Recover
04014	EQ	156E	Before Recover
05012	2S	156E	Before Recover
06012	5S	156E	Before Recover
07012	5N	147E	Before Recover
08011	2N	147E	Before Recover
09012	EQ	147E	Before Recover

### (5) Results

Most of temperature, conductivity and salinity data from TRITON buoy showed good agreement with CTD cast data in T-S diagrams. See the Figures 7.1.2-1.

To evaluate the performance of the conductivity sensors on TRITON buoy, the data from had deployed buoy and shipboard CTD data at the same location were analyzed.

The estimation was calculated as recovered buoy data minus shipboard CTD (9Plus) data.

The salinity differences are from -0.8288 to 0.3072 for all depths. Below 300db, salinity differences are from -0.0664 to 0.0940 (See the Figures 7.1.2-2(a)). The average of salinity differences was 0.0316 with standard deviation of 0.1313.

The estimation of time-drift was calculated as recovered buoy data minus deployed buoy data. The salinity changes for 1 year are from -0.8227 to 0.3091, for all depths. Below 300db, salinity changes for 1 year are from -0.0659 to 0.1055 (See the figures 7.1.2-2(b)). The average of salinity differences was 0.0334 with standard deviation of 0.1313.

#### (6) Data archive

All raw and processed CTD data files were copied on 3.5 inch magnetic optical disks and submitted to JAMSTEC TOCS group of the Ocean Observation and Research Department. All original data will be stored at JAMSTEC Mutsu brunch. (See section 7.1)

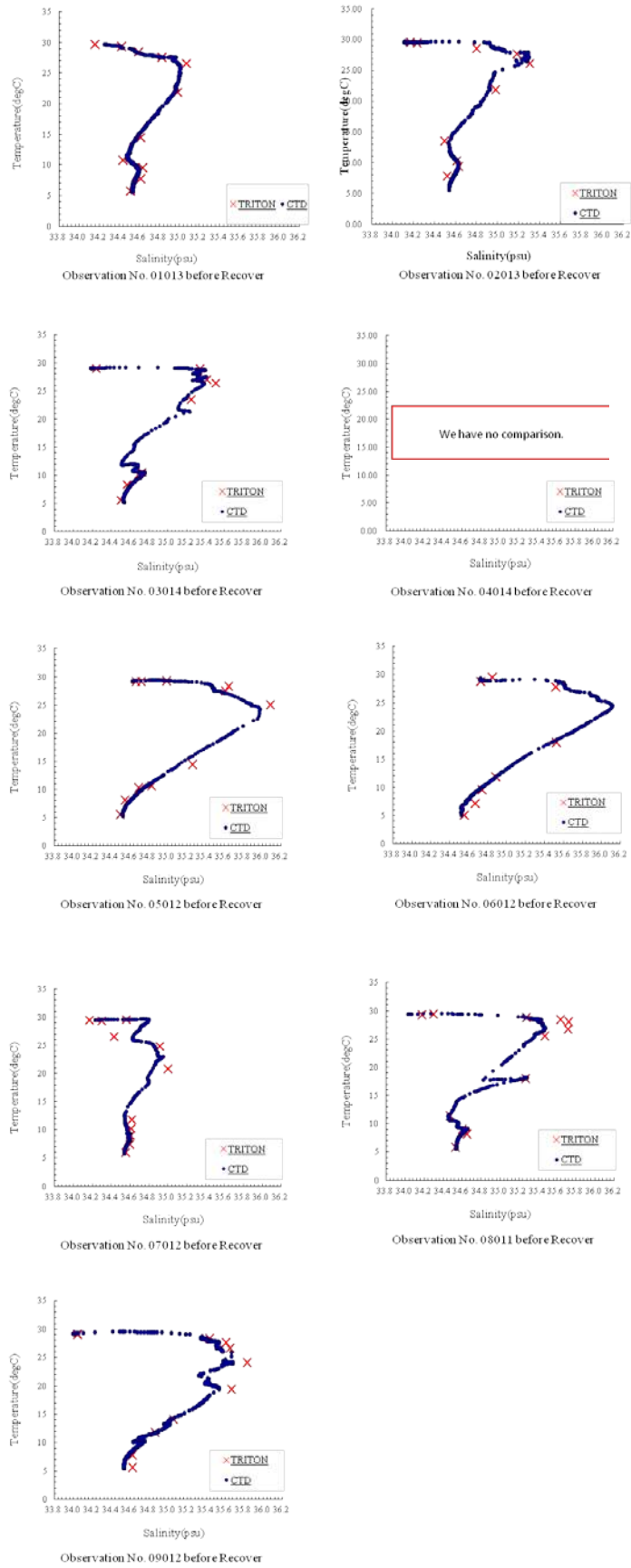


Fig. 7.1.2.-1 T-S diagram of TRITON buoys data and shipboard CTD data

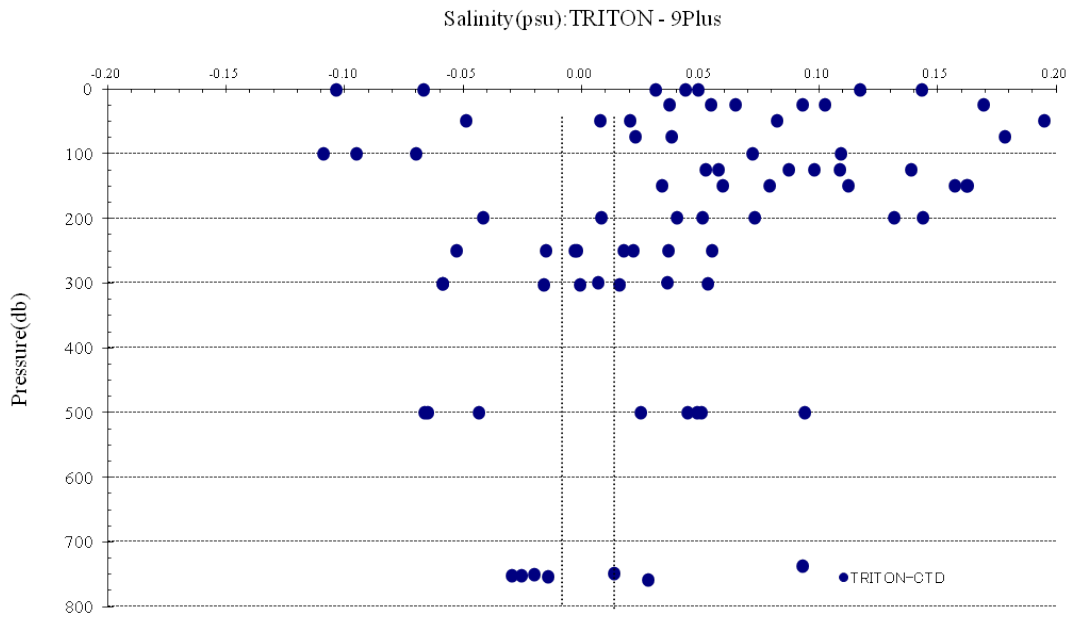


Fig.7.1.2.-2 (a) Salinity differences between TRITON buoys data and shipboard CTD data before recovery

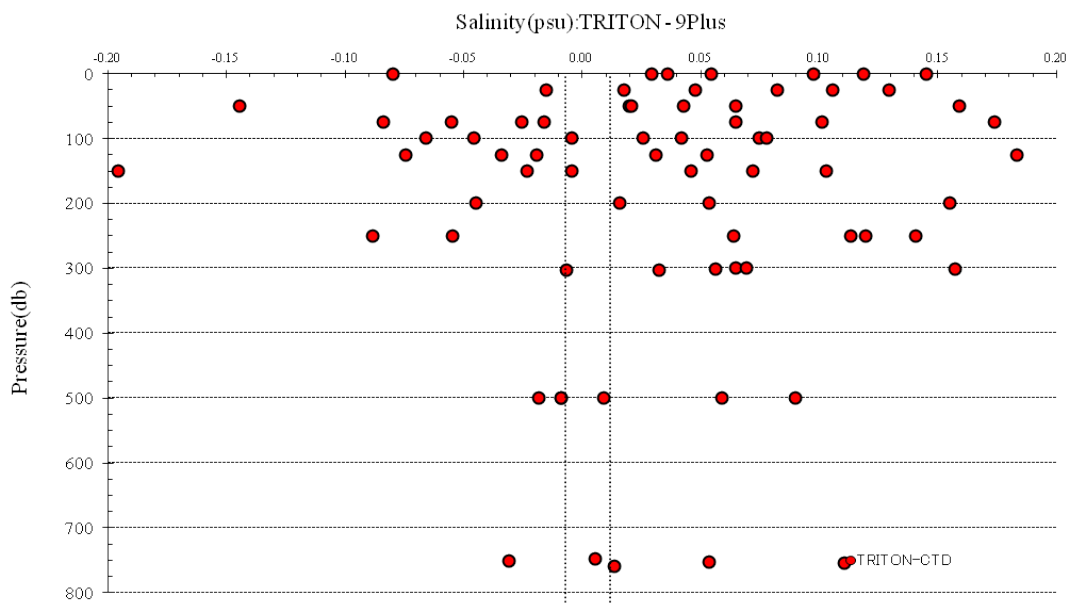


Fig.7.1.2.-2 (b) Salinity differences between deployment data and recovery data for 1 year

### 7.1.3 Performance test of pCO<sub>2</sub> sensor

**Shuichi Watanabe and Yoshiyuki Nakano (JAMSTEC)**

#### (1) Objective

A lot of observations to obtain the fate of CO<sub>2</sub> in the atmosphere which is related with long term climate change have been carried in the world. However, the sea surface pCO<sub>2</sub> observations on ships of opportunity and research vessels concentrated in the North Atlantic and North Pacific. To obtain the spatial and temporal variation of surface pCO<sub>2</sub> in the whole ocean, new simplified automated pCO<sub>2</sub> measurement system is needed.

We have been developing newly small and simple *in situ* system for pCO<sub>2</sub> measurement using spectrophotometric technique. In this cruise, we aim at testing the new pCO<sub>2</sub> sensor and recovering prototype pCO<sub>2</sub> sensor deployed by MR10-07 cruise in the open sea. The new pCO<sub>2</sub> sensor is attached with TRITON buoy and start mooring (2°N, 156°E) for about one year.

#### (2) Method

The pCO<sub>2</sub> sensor for the measurement of pCO<sub>2</sub> is based on the optical absorbance of the pH indicator solution. The CO<sub>2</sub> in the surrounding seawater equilibrates with the pH indicator solution across gas permeable membranes, and the resulting change in optical absorbance, representing the change of pH, is detected by the photo multiplier detector. We calculated the pH in the pH indicator solution from the absorbance ratios. In this cruise I decided to use AF Teflon tube (amorphous fluoropolymer, AF Teflon, AF-2400) as an equilibrium membrane because this material is well suited to pCO<sub>2</sub> measurements due to its high gas permeability. This measuring system was constructed from LED light source, optical fiber, CCD detector, micro pump, and downsized PC. The new simple system is attached in aluminum drifting buoy with satellite communication system, which size is about 300 mm diameter and 500 mm length and weight is about 15 kg (Fig. 7.1.3-1). A Li-ion battery is occupied about one third of the drifting buoy. This system also has a lead-acid battery with two 5W solar panels. The solar panel unit is attached with the middle of TRITON buoy tower and connected with pCO<sub>2</sub> sensor by cable. In the laboratory experiment, we obtained high response time (less than 10 minutes) and precision within 3 μatm.

#### (3) Preliminary results

We succeeded in recovering the pCO<sub>2</sub> sensor with TRITON buoy at 2°N, 156°E. We obtained long term (about one year) pCO<sub>2</sub> data from the prototype pCO<sub>2</sub> sensor every three days via satellite system. We are checking the obtained pCO<sub>2</sub> data from the sensor.

#### (4) Data Archive

All data will be submitted to JAMSTEC Data Management Office (DMO) and is currently under its control.

Reference

DOE (1994), Handbook of methods for the analysis of the various parameters of the carbon dioxide system in sea water; version 2, A. G. Dickson & C. Goyet, Eds., ORNS/CDIAC-74

Nakano, Y., H. Kimoto, S. Watanabe, K. Harada and Y. W. Watanabe (2006): Simultaneous Vertical Measurements of In situ pH and CO<sub>2</sub> in the Sea Using Spectrophotometric Profilers. *J. Oceanogra.*, 62, 71-81.

Yao, W. and R. H. Byrne (2001): Spectrophotometric determination of freshwater pH using bromocresol purple and phenol red, *Environ. Sci. Technol.*, 35, 1197-1201.

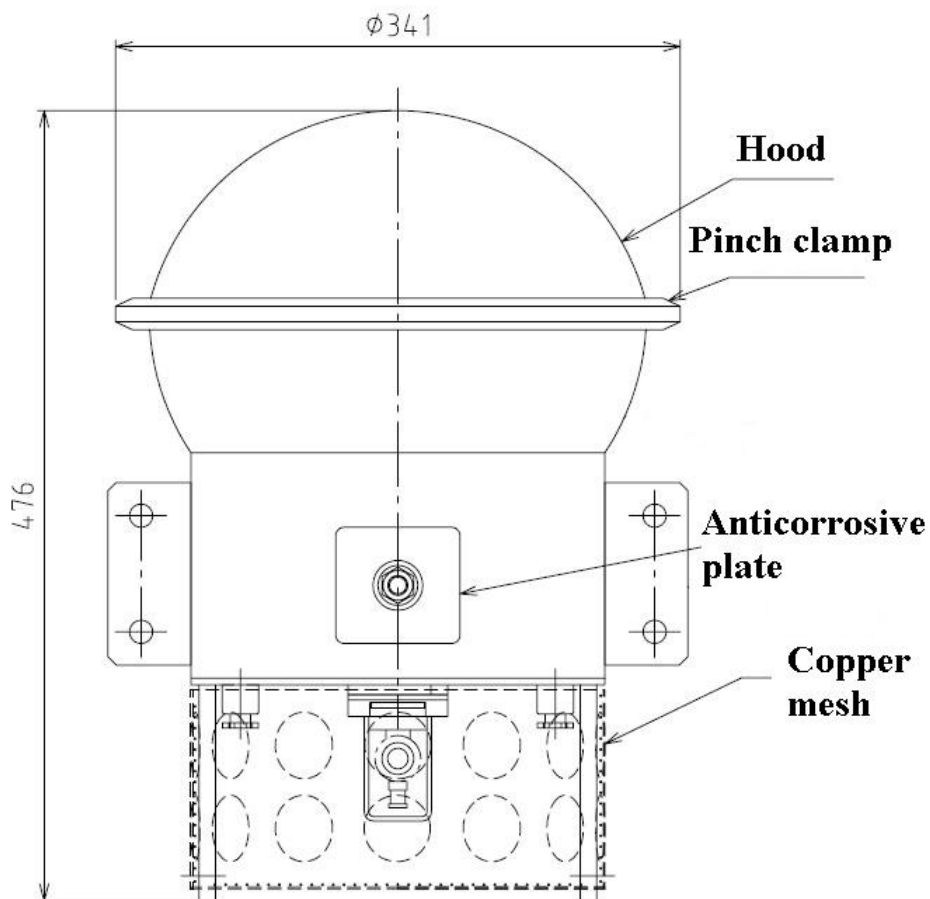


Fig. 7.1.3-1 Side view of pCO<sub>2</sub> sensor.

## 7.2 Subsurface ADCP moorings

### (1) Personnel

Yuji Kashino	(JAMSTEC): Principal Investigator
Takuya Hasegawa	(JAMSTEC): Scientist
Tomohide Noguchi	(MWJ): Operation leader
Tetsuharu Iino	(MWJ): Technical staff
Hiroki Ushiromura	(MWJ): Technical staff
Syoko Tatamisashi	(MWJ): Technical staff
Syungo Oshitani	(MWJ): Technical staff
Hatsumi Aoyama	(MWJ): Technical staff
Rei Ito	(MWJ): Technical staff

### (2) Objectives

The purpose of this ADCP observation is to get knowledge of physical process underlying the dynamics of oceanic circulation in the western equatorial Pacific Ocean. We have been observing subsurface currents using ADCP moorings along the equator. In this cruise (MR12-03), we recovered two subsurface ADCP moorings at Eq-147E and Eq-156E. And we deployed three subsurface ADCP moorings at Eq-147E, 2.6S-153E and 2.8S-153E.

Deployment of the ADCP mooring at 2.6S-153E and 2.8S-153E (off PNG) is new one. Components of this mooring are depicted in Figure 7.2-1 and Figure 7.2-2.

### (3) Parameters

- Current profiles
- Echo intensity
- Pressure, Temperature and Conductivity

### (4) Methods

Two instruments are mounted at the top float of the mooring. One is ADCP (Acoustic Doppler Current Profiler) to observe upper-ocean currents from subsurface down to around 300m depths. The second instrument mounted below the float is CTD, which observes pressure, temperature and salinity for correction of sound speed and depth variability. Additionally, there are ADCP and CTD at intermediate part mooring rope. Details of the instruments and their parameters are as follows:

#### 1) ADCP

Broadband ADCP 150 kHz (Teledyne RD Instruments, Inc.)

Distance to first bin : 8 m

Pings per ensemble : 16 (Only Eq-156E is 10 pings.)

Time per ping : 2.00 seconds

Number of depth cells : 40

Bin length : 8.00 m

Sampling Interval : 3600 seconds

Recovered ADCP

- Serial Number : 1220 (Mooring No.101222-00147E)
- Serial Number : 1221 (Mooring No.101212-00156E)

Deployed ADCP

- Serial Number : 1224 (Mooring No.120812-00156E)
- Serial Number : 1152 (Mooring No.120801-2.6S153E)

Work horse ADCP 75 kHz (Teledyne RD Instruments, Inc.)

Distance to first bin : 7.04 m

Pings per ensemble : 27

Time per ping : 6.66 seconds

Number of depth cells : 60

Bin length : 8.00 m

Sampling Interval : 3600 seconds

Deployed ADCP

- Serial Number : 3200 (Mooring No.120801-2.6S153E)
- Serial Number : 7176 (Mooring No.120801-2.8S153E)
- Serial Number : 2541 (Mooring No.120801-2.8S153E)

2) CTD

SBE-16 (Sea Bird Electronics Inc.)

Sampling Interval : 1800 seconds

Recovered CTD

- Serial Number : 1286 (Mooring No.101222-00147E)
- Serial Number : 1274 (Mooring No.101212-00156E)

Deployed CTD

- Serial Number : 1282 (Mooring No. 120812-00156E)
- Serial Number : 2611 (Mooring No.120801-2.6S153E)
- Serial Number : 1276 (Mooring No.120801-2.6S153E)

- Serial Number : 1283 (Mooring No.120801-2.8S153E)
- Serial Number : 1280 (Mooring No.120801-2.8S153E)

### 3) Other instrument

#### (a) Acoustic Releaser (BENTHOS,Inc.)

##### Recovered Acoustic Releaser

- Serial Number : 954 (Mooring No.101222-00147E)
- Serial Number : 636 (Mooring No.101222-00147E)
- Serial Number : 963 (Mooring No.101212-00156E)
- Serial Number : 961 (Mooring No.101212-00156E)

##### Deployed Acoustic Releaser

- Serial Number : 719 (Mooring No.101212-00156E)
- Serial Number : 634 (Mooring No.101212-00156E)
- Serial Number : 956 (Mooring No.120801-2.6S153E)
- Serial Number : 716 (Mooring No.120801-2.6S153E)
- Serial Number : 694 (Mooring No.120801-2.8S153E)
- Serial Number : 632 (Mooring No.120801-2.8S153E)

#### (b) Transponder (BENTHOS,Inc.)

##### Recovered Transponder

- Serial Number : 57069 (Mooring No.101222-00147E)
- Serial Number : 67491 (Mooring No.101212-00156E)

##### Deployed Transponder

- Serial Number : 46472 (Mooring No.120801-2.6S153E)
- Serial Number : 56413 (Mooring No.120801-2.8S153E)

### (5) Deployment

Deployments of the ADCP mooring at Eq-156E and 2.8S-153E were planned to mount the ADCP at about 340m depths. Deployment of the ADCP mooring at 2.6S-153E was planned to mount the ADCP at about 260m depths. During the deployment, we monitored the depth of the acoustic releaser after dropped the anchor.

The position of the mooring No. 101212-00156E

Date: 12 Aug. 2012    Lat: 00-02.21S    Long: 156-07.95E    Depth: 1,949m

The position of the mooring No. 120801-2.6S153E

Date: 1 Aug. 2012    Lat: 02-38.17S    Long: 153-21.04E    Depth: 3,218m

The position of the mooring No. 120801-2.8S153E

Date: 1 Aug. 2012    Lat: 02-48.35S    Long: 153-13.18E    Depth: 3,473m

#### (6) Recovery

We recovered two ADCP moorings. One was deployed on 22 Dec.2010 and the other was deployed on 12 Dec. 2010 (MR10-07cruise). After the recovery, we uploaded CTD data into a computer, and then raw data were converted into ASCII code. However, since the battery was exhausted, ADCP recovered at Eq-147E and Eq-156E was not able to collect data. When we returned to JAMSTEC, we tried to download data from these ADCPs, however, it was failed.

The time series of moored CTDs is shown in Figure 7.2-3 and Figure 7.2-4.

#### (7) Data archive

All data will be opened at the following web page:.

[http://www.jamstec.go.jp/rigc/j/tcvrp/ipocvrt/adcp\\_data.html](http://www.jamstec.go.jp/rigc/j/tcvrp/ipocvrt/adcp_data.html)

**2.635S-153.350E Deployment [MR12-03]**

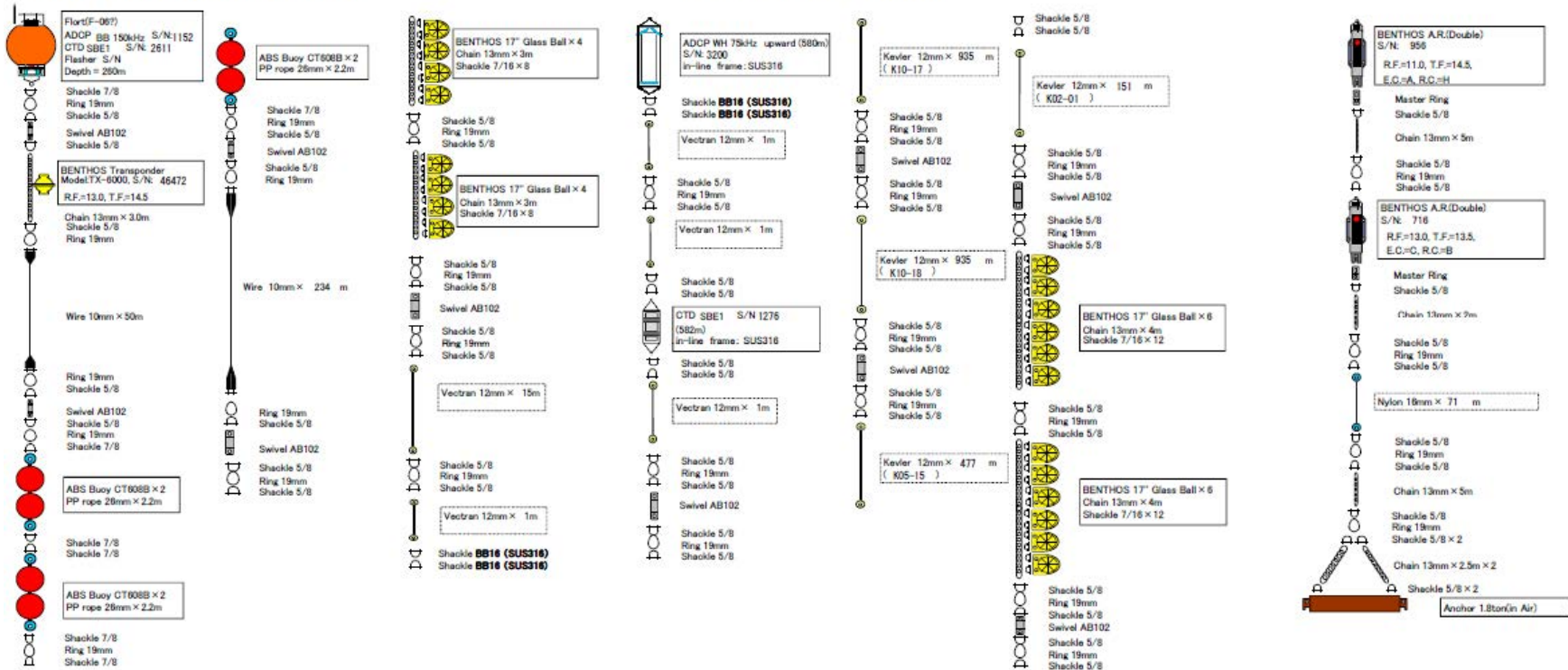


Fig.7.2-1 Mooring diagram of Deploy mooring (2.6S-153E)

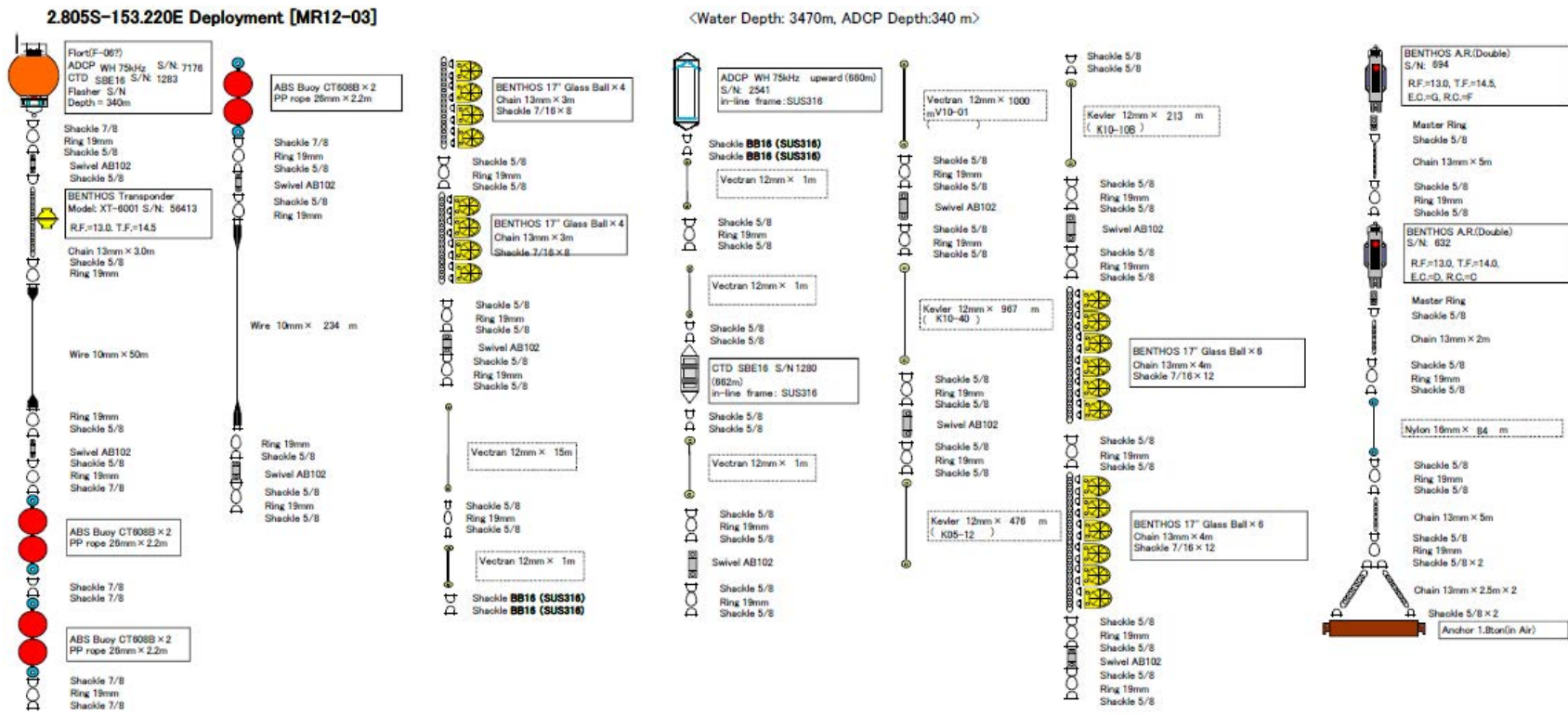


Fig.7.2-2 Mooring diagram of Deploy mooring (2.8S-153E)

### EQ147E CTD

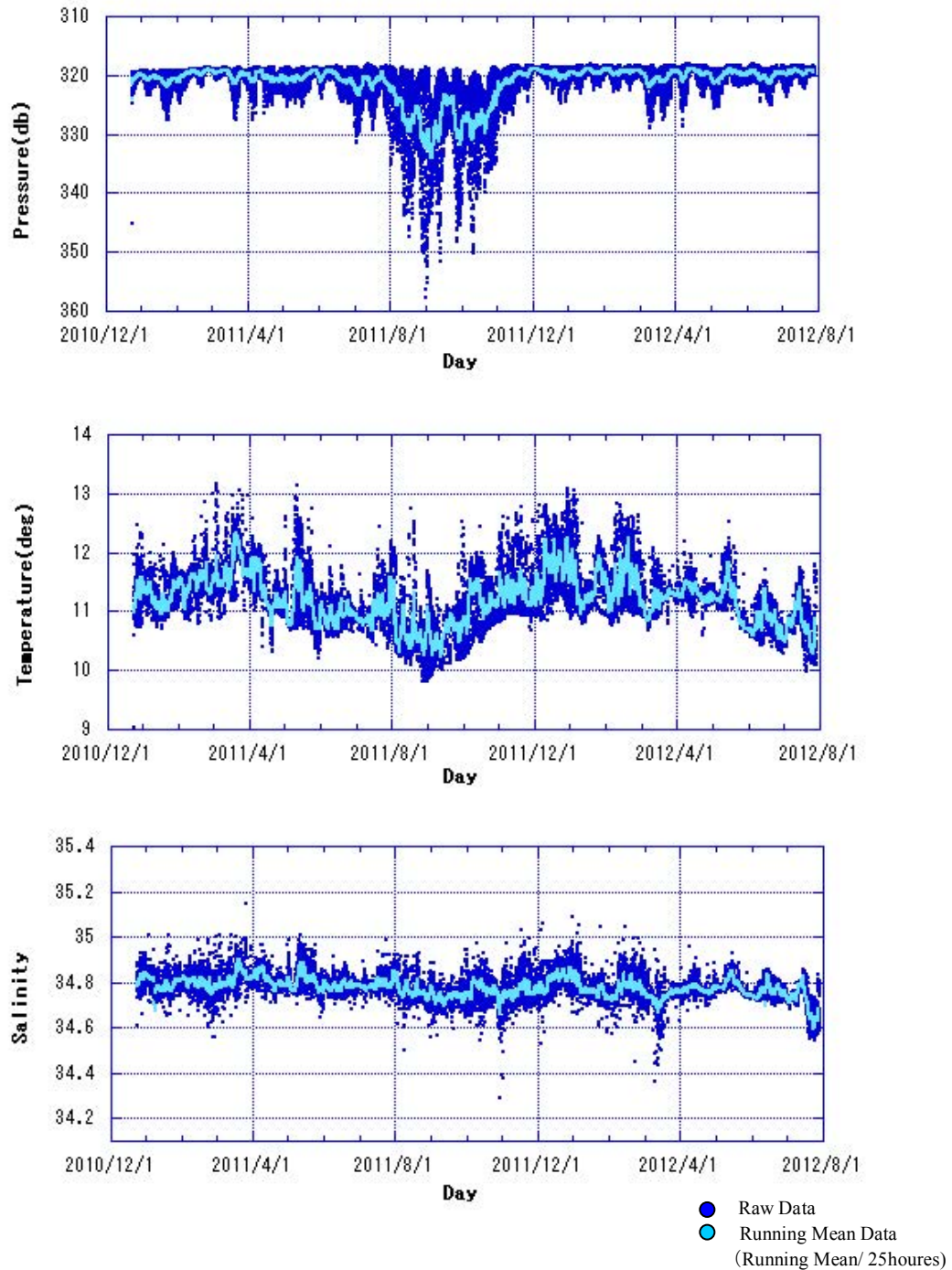


Fig.7.2-3 Time-series of the observed pressure (*top panel*), temperature (*middle panel*) and salinity (*bottom panel*) obtained from CTD at Eq-147E. The *dark-blue* curve indicates the raw data, while the *light-blue* curve shows the filtered data from 25 hours running-mean. (2010/12/23-2012/07/29)

### EQ156E CTD

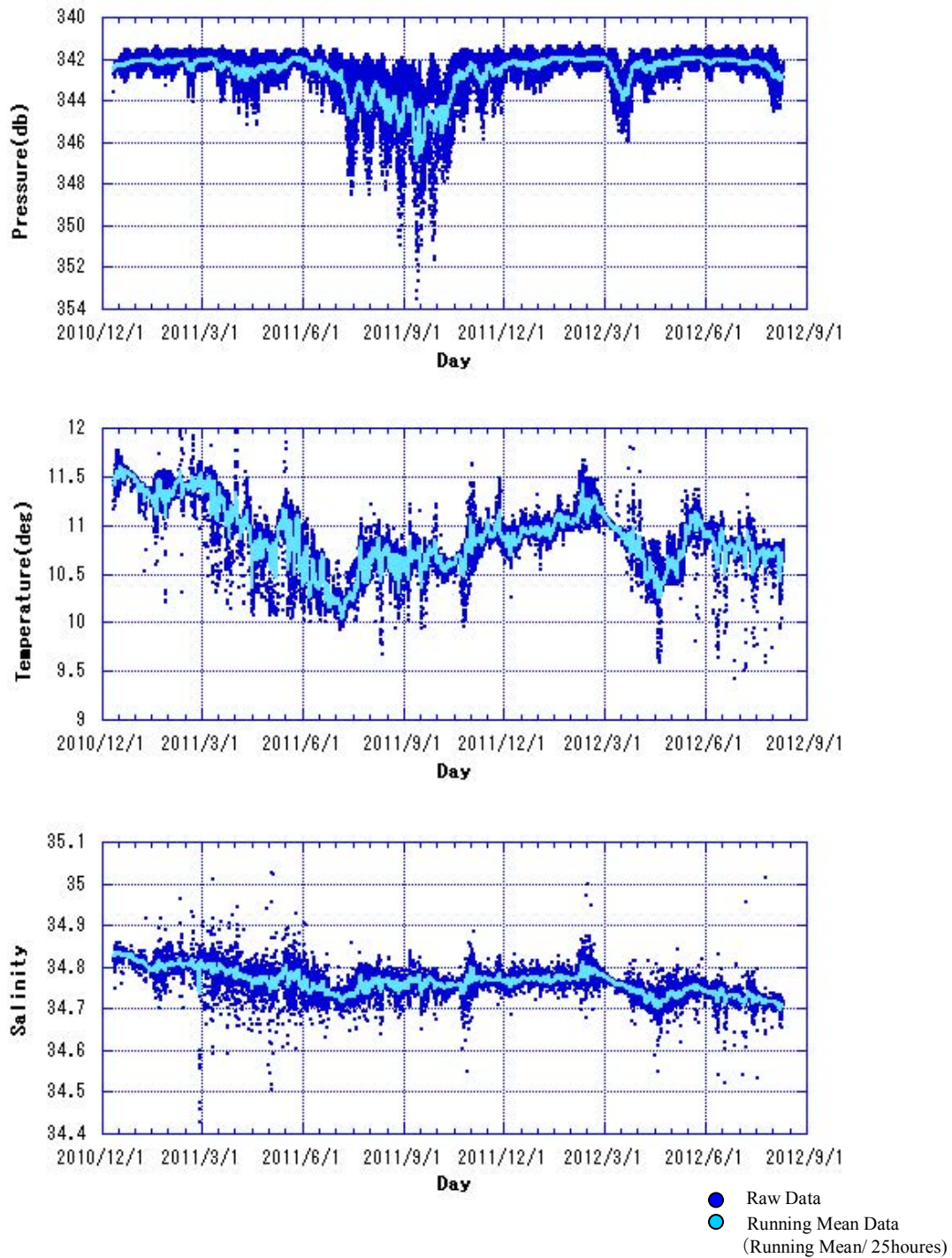


Fig.7.2-4 Time-series of the observed pressure (*top panel*), temperature (*middle panel*) and salinity (*bottom panel*) obtained from CTD at Eq-156E. The *dark-blue* curve indicates the raw data, while the *light-blue* curve shows the filtered data from 25 hours running-mean. (2010/12/12-2010/08/11)

### 7.3 Current profile observations using a high frequency lowered acoustic Doppler current profiler

Personnel      Miho Ishizu (University of Hawaii/International Pacific Center)  
                    Takuya Hasegawa (JAMSTEC)

#### (1) Objective

To measure the small vertical scale (SVS) velocity structure in the tropics.

#### (2) Overview of instrument and operation

In order to measure the velocity structure at fine vertical scales a high frequency ADCP was used in lowered mode (LADCP). The instrument was a Teledyne RDI Workhorse Sentinel 600kHz ADCP rated for 1000m depth. The instrument was attached to the frame of the CTD system using a steel collar sealed around the instrument by three bolts on each side, with the collar attached to the rosette frame by two u-bolts on two mounting points. A rope was tied to the top end of the instrument to minimize vertical slippage and for added safety (see Figure 7.4-1). The instrument was deployed on CTD stations C01-C34 in the tropics, performing well throughout its use.



Fig 7.4-1 Mounting of LADCP on CTD System (photo: Y. Kashino)

The instrument is self-contained with an internal battery pack. The health of the battery is monitored by the recorded voltage count. The relationship between the actual battery voltage and the recorded voltage count is obscure and appears to vary with the instrument and environmental conditions. Taking a direct measurement of the state of the battery

requires opening up the instrument. Direct measurements of the battery voltage were taken before and after the deployment and compared to the recorded voltage count:

	Battery Voltage (V)	Voltage Count (VC)	ratio (V/VC)
Before	44.82	153	0.29
After	40.60	141	0.29

implying an almost constant relationship of  $V \sim 0.29VC$ . RDI recommends the battery be changed when V gets below 30V.

### (3) Setup and Parameter settings

At all stations the LADCP was controlled at deploy and recover stages by a Linux PC using the python script **ladcp600\_mr1203.py** (written by Eric Firing, University of Hawai'i). The commands sent to the instrument at setup were contained in **ladcp600.cmd**. The instrument was set up to have a relatively small bin depth (2m) and a fast ping rate (every 0.25 sec). The full list of commands sent to the instrument were:

```

CR1          # Retrieve parameter (default)
TC2          # Ensemble per burst
WP1          # Pings per ensemble
TE 00:00:00.00 # Time per ensemble (time between data collection cycles)
TP 00:00.25  # Time between pings in mm:ss
WN25        # Number of Depth cells
WS0200      # Depth cell size (in cms)
WF0088      # Blank after transit (recommended setting for 600kHz)
WB0         # Mode 1 bandwidth control (default - wide)
WV250       # Ambiguity velocity (in cm/s)
EZ0111101  # Sensor source (speed of sound excluded)
EX00000     # Beam coordinates
CF11101     # Data flow control parameters

```

(see the RDI Workhorse "Commands and Data Output Format" document for details.)

To add flexibility, the instrument could also be controlled at deploy and recover stages by the RDI software (**BBTalk**) installed on the JAMSTEC Windows PC with the same list of commands as above. In this cruise, we did not have the opportunity to use **BBTalk**.

### (4) Data processing

An initial sampling of the data was made using the following scripts to check that the instrument was performing correctly

```

make.plots.py    integrity check
                   plot pressure, temperature, voltage and current counts

```

## plot velocity from all 4 beams

The principal onboard data processing was performed using the Lamont Doherty Earth Observatory (LDEO, Columbia University) LADCP software package version IX\_6beta (available at <ftp://ftp/ldeo.columbia.edu/pub/ant/LADCP>). The package is based on a number of matlab scripts. The package performs an inverse of the LADCP data, incorporating CTD (for depth) and GPS data, to provide a vertical profile of the horizontal components of velocity, U and V (eastward and northward, respectively), that is a best fit to specified constraints. The down- and up-casts are solved separately, as well as the full cast inverse. The package also calculates U and V from the vertical shear of velocity.

The software is run using the matlab script **process\_cast\_mr1203.m** with the configuration file **set\_cast\_params.m**. Frequent CTD data are required. Files of 1 second averaged CTD data were prepared for each station. Accurate time keeping is also required, particularly between the CTD and GPS data. To ensure this, the CTD data records also included the GPS position. The LDEO software allows the ship's ADCP data (SADCP) to be included in the inverse calculation. The SADCP data were not included in this case so as to provide an independent check on the functioning of the LADCP.

On-station SADCP velocity profiles were produced by averaging the five-minute averaged profiles (mr1203002\_000000.LTA and mr1203003\_000000.LTA produced using VmDAS) over the period of the CTD/LADCP cast. Care was taken to ensure the average did not contain any spurious data from periods when the ship was maneuvering.

### (5) Preliminary results

An example of the on-board processed data is presented in Figure 7.3-2 and 7.3-3 compares the full cast inverse, up- and down-cast inverse, and the shear solutions for the zonal (U) and meridional (V) components of the velocity vector with the corresponding SADCP profile for Station C02M01. The LADCP velocity has been fitted to the mean and linear shear of the SADCP velocity. There is a very good correspondence between the general structure of all velocity profiles. While the large vertical scale flow is in a good agreement with the SADCP data (gray line), the LADCP solutions show a lot of smaller scale structure, not resolved by the SADCP. Especially noticeable in Figure 7.3-2 are features in V between 50-300m that are barely resolved by the SADCP.

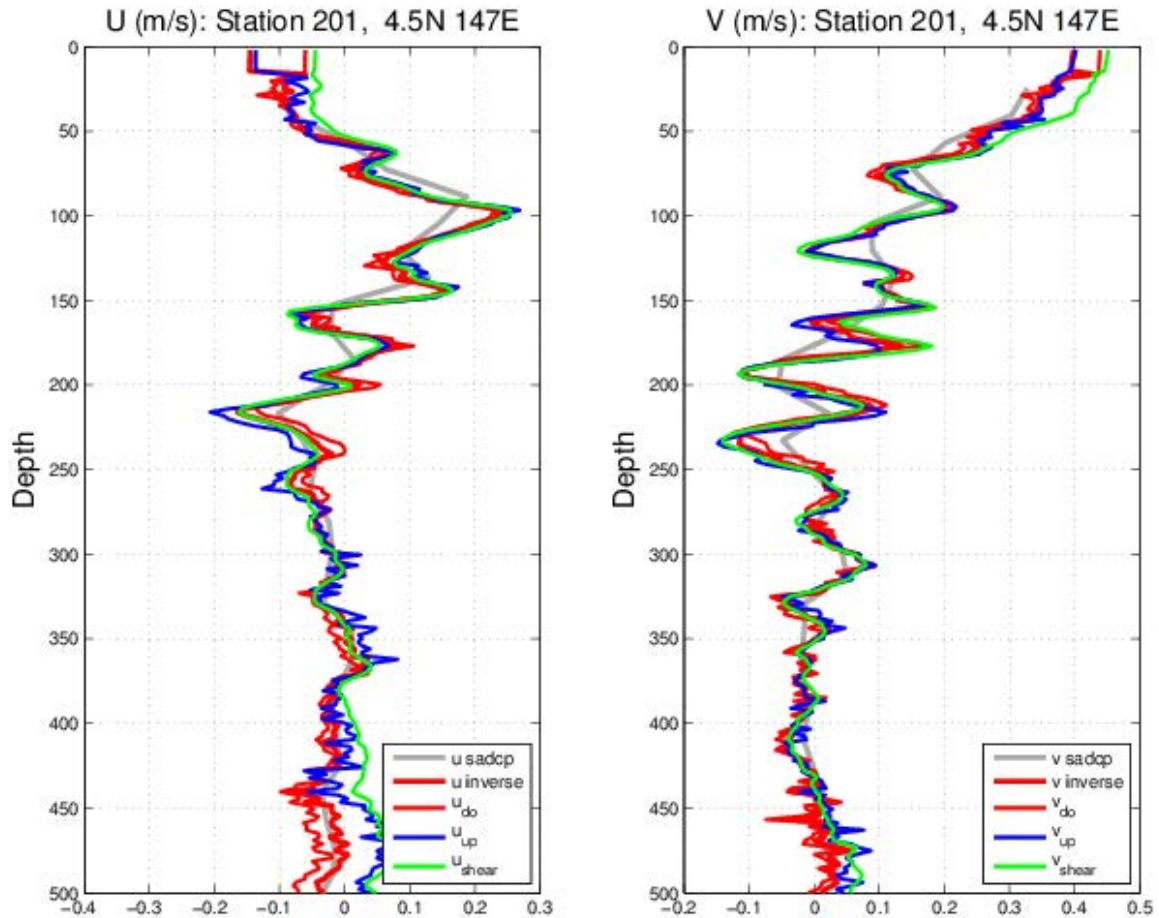


Figure 7.3-2 CTD Station C02M01: Vertical profiles of U and V calculated by a number of methods using LADCP data. Full cast inverse (u inverse), downcast only inverse (u\_do), up-cast only inverse (u\_up) and shear solution (u\_shear). Also shown are the profiles using SADCP data (u\_sadcp).

These small vertical scale structures are often associated with small vertical scale anomalies in salinity profiles. As an example, the down- and up-cast inverse solutions for U and V are compared with salinity over a portion of the CTD Station C02\_01 profile in Figure 7.3-3. The fact that a number of the same small scale features are evident in both the down- and up-cast profiles of both U and V, confirms the ability of the instrument to measure small vertical scale features in velocity. There is a strong correspondence between the small-scale features in V and salinity and to a smaller extent between U and salinity as well (e.g., slightly above and below the 200 m depth), although the exact relationship will depend on the time evolution of the fields.

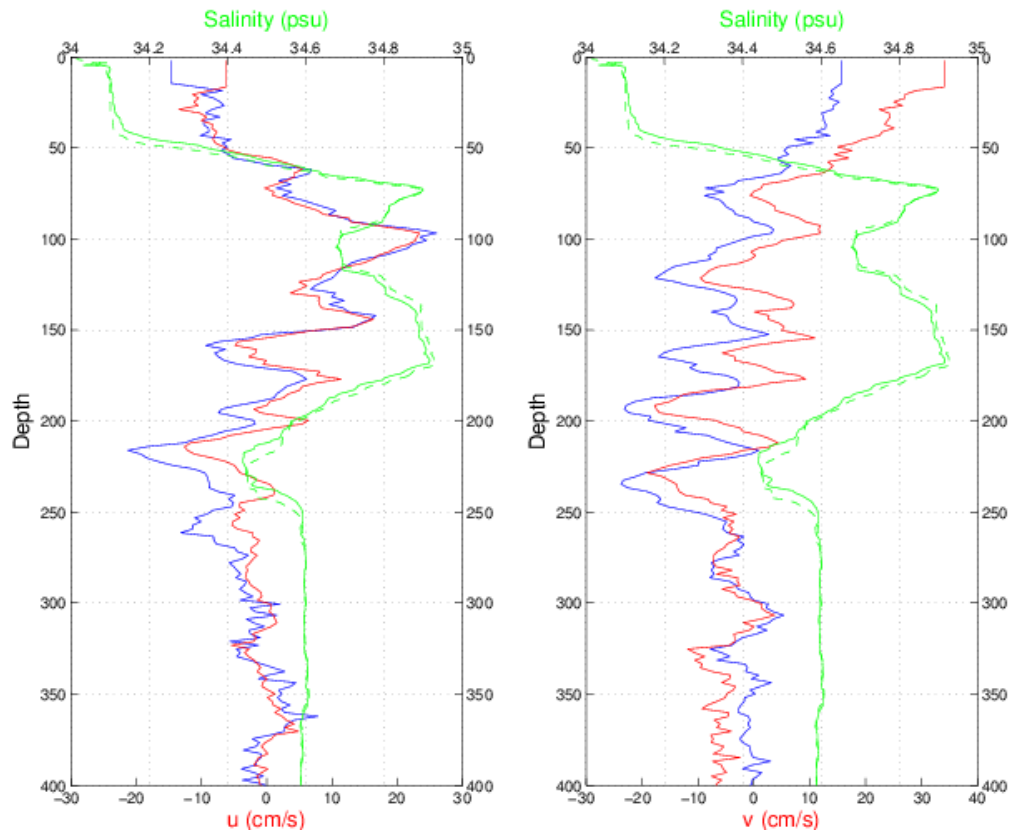


Figure 7.3-3 CTD Station C02M01: Vertical profile of the downcast (green full line) and up-cast (green dashed line) salinity overlain with downcast (red) and up-cast (blue) horizontal velocity components (zonal left panel; meridional right panel). Note the correspondence of salinity with the small vertical scale meridional velocity features.

The measurements at individual stations are combined to produce latitudinal and longitudinal sections of the velocity fields. Figures 7.3-4, 7.3-5, 7.3-6 and 7.3-7 show the zonal and meridional components of the velocity vector as a function of latitude and depth at 147E and 156E correspondingly. All plots show the abundance of features with vertical scales 30 – 60 m. Smaller scale features, not evident in the plots shown, are present and resolved by the LADCP. The intensity of such features seems to be independent of latitude. Many SVS features clearly extend over several stations and/or show remarkable spatial correlation. This is particularly evident in contour plots of meridional velocity along latitudinal sections of 147E and 156E. The origin of these features is the subject of an ongoing observational and theoretical investigation. A comparison with the turbulence energy dissipation rate profiles obtained on this cruise using a microstructure profiles (MSP) suggests that these features may account for a significant fraction of the overall dissipation in the thermocline, but further analysis is necessary to quantify their role.

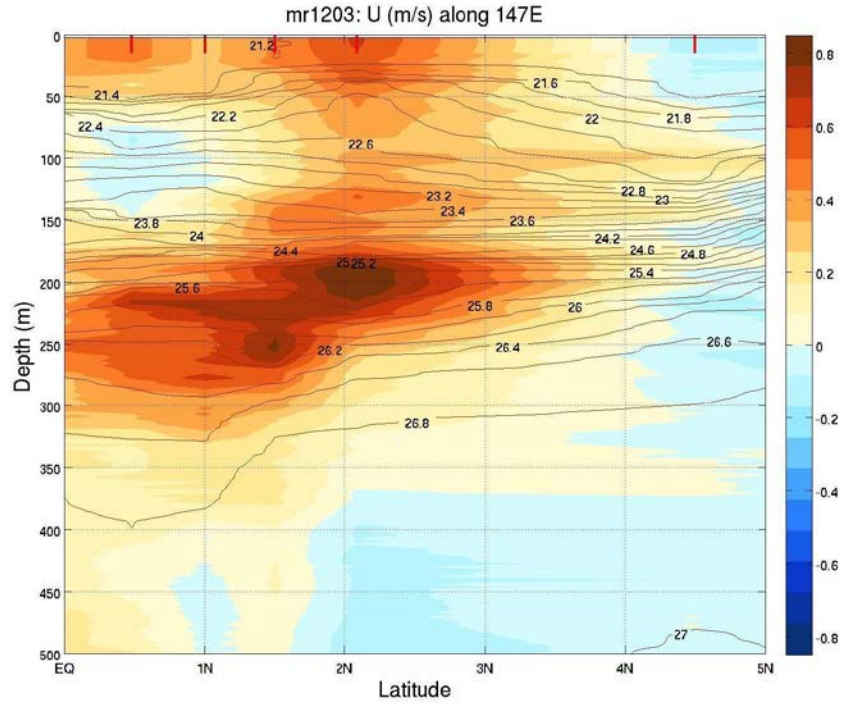


Figure 7.3-4. Latitudinal section of the zonal component of velocity and potential density at 147E.

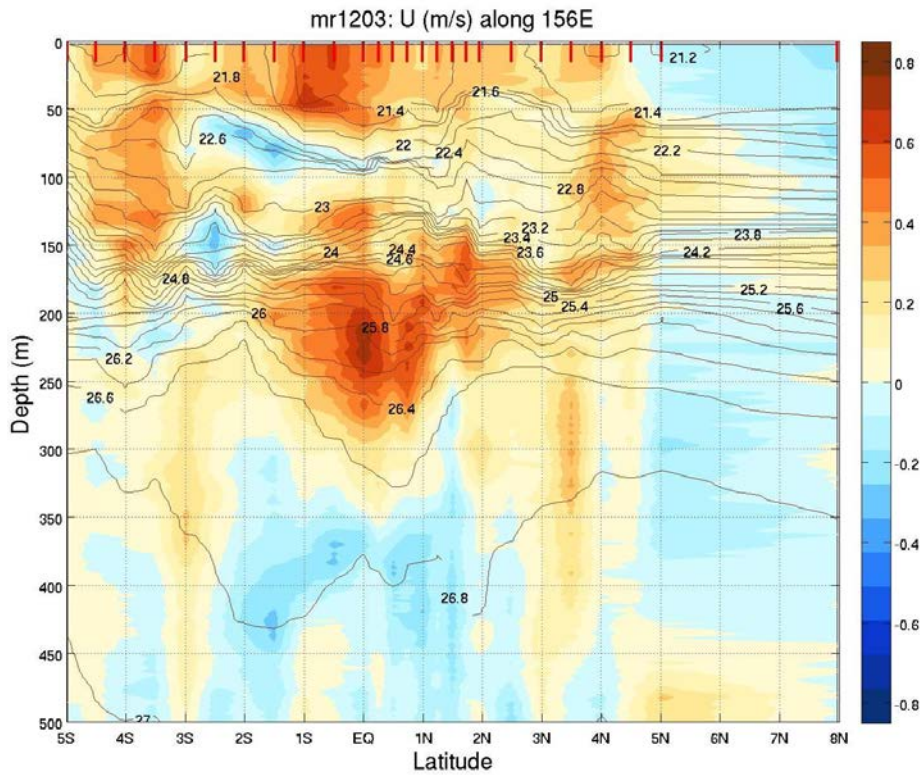


Figure 7.3-5. Latitudinal section of the zonal component of velocity and potential density at 156E.

## 7.4 Observation of ocean turbulence

Personnel Yuji Kashino (RIGC, JAMSTEC)  
 Wataru Tokunaga (Global Ocean Development Inc.)  
 Harumi Ota (Global Ocean Development Inc.)  
 Koichi Inagaki (Global Ocean Development Inc.)  
 Ryo Ohyama (Mirai crew, Global Ocean Development Inc.)

### (1) Introduction

The western equatorial Pacific is called “Water Mass Crossroad” (Fine et al., 1994) because of complicated ocean structure due to various water masses from the northern and southern Pacific oceans. Small structure associated with ocean mixing such as interleaving was sometimes observed. Because this mixing effect is not fully implemented in the ocean general circulation model presently, it should be evaluated by in-situ observation. Considering this background, JAMSTEC started collaboration research with International Pacific Research Center (IPRC) of Univ. of Hawaii since 2007, and observations using lowered acoustic Doppler current profiler (LADCP) with high frequency were carried out since MR07-07 Leg 1. These observations revealed interesting fine structures with vertical scale of order 10m and horizontal scale of order 100km. For better understanding of ocean fine structures involving this phenomenon, we observe ocean turbulence using a Turbulence Ocean Microstructure Acquisition Profiles, Turbo Map-L, developed by JFE Advantech Co Ltd. during this cruise.

### (2) Measurement parameters

Using the Turbo Map-L, we measured following parameters:

Parameter	Type	Range	Accuracy	Sample Rate
$\partial u/\partial z$	Shear probe	0~10 /s	5%	512Hz
$T+\partial T/\partial z$	EPO-7 thermistor	-5~45°C	±0.01°C	512Hz
T	Platinum wire thermometer	-5~45°C	±0.01°C	64Hz
Conductivity	Inductive Cell	0~70mS	±0.01mS	64Hz
Depth	Semiconductor strain gauge	0~1000m	±0.2%	64Hz
x acceleration	Solid-state fixed mass	±2G	±1%	256Hz
y acceleration	Solid-state fixed mass	±2G	±1%	256Hz
z acceleration	Solid-state fixed mass	±2G	±1%	64Hz
Chlorophyll	Fluorescence	0~100 μg/Lm	0.5 μg/L or ±1%	256Hz
Turbidity	Backscatter	0~100ppm	1ppm or ±2%	256Hz
$\partial u/\partial z$	Shear probe	0~10 /s	5%	512Hz

We use following sensor and twin shear probes:

FP07 sensor

Cast No. 1- 15 SN:219

Cast No. 16-78 SN:220

Shear Ch1 sensor

All casts: SN:718

Shear Ch2 sensor

Cast No. 1- 2 SN:797

Cast No. 3- 8 SN:875

Cast No. 9-78 SN:876

(3) Observation stations.

No.	Date	Longitude	Latitude	Logging Time		Observation Depth[m]	File name (.BIN)	Note
				Start	Stop			
01	2012/07/25	146-55.55E	05-03.83N	8:44	9:03	634	MR1203-1	*1
02	2012/07/25	146-55.52E	05-04.12N	9:17	9:34	581	MR1203-2	
03	2012/07/26	146-59.91E	04-30.33N	5:17	5:39	725	MR1203-3	
04	2012/07/26	146-59.92E	02-05.30N	20:16	20:34	541	MR1203-4	
05	2012/07/27	147-00.36E	01-29.84N	5:18	5:39	565	MR1203-5	
06	2012/07/27	147-00.20E	00-59.90N	9:15	9:32	545	MR1203-6	
07	2012/07/29	147-00.38E	00-29.84N	9:10	9:28	524	MR1203-7	
08	2012/07/29	147-02.12E	00-01.53N	20:03	20:22	613	MR1203-8	
09	2012/08/03	156-00.12E	03-30.27S	7:56	8:14	574	MR1203-9	
10	2012/08/04	156-02.38E	04-58.78S	2:48	3:06	628	MR1203-10	
11	2012/08/04	156-00.17E	04-30.20S	7:10	7:27	556	MR1203-11	
12	2012/08/05	156-00.20E	04-00.35S	5:49	6:04	528	MR1203-12	
13	2012/08/08	156-00.51E	02-00.92S	19:21	19:41	632	MR1203-13	
14	2012/08/09	156-00.06E	02-30.06S	3:02	3:19	585	MR1203-14	
15	2012/08/09	156-00.07E	03-00.06S	6:58	7:16	581	MR1203-15	*2
16	2012/08/09	156-00.26E	03-00.15S	7:49	8:06	578	MR1203-16	
17	2012/08/10	156-00.05E	01-30.28S	5:01	5:17	555	MR1203-17	
18	2012/08/10	156-00.14E	01-00.18S	9:05	9:22	569	MR1203-18	
19	2012/08/12	156-00.36E	00-30.28S	6:57	7:15	597	MR1203-19	
20	2012/08/12	156-00.18E	00-00.03N	19:33	19:52	535	MR1203-20	
21	2012/08/12	156-00.69E	00-00.21N	20:09	20:28	543	MR1203-21	
22	2012/08/12	156-00.94E	00-00.42N	20:45	21:04	588	MR1203-22	
23	2012/08/12	156-00.84E	00-00.09N	22:31	22:50	568	MR1203-23	

24	2012/08/12	156-01.13E	00-00.22N	23:06	23:23	568	MR1203-24	
25	2012/08/12	156-01.45E	00-00.34N	23:39	23:57	606	MR1203-25	
26	2012/08/13	155-59.76E	00-00.09N	1:27	1:46	523	MR1203-26	
27	2012/08/13	155-59.98E	00-00.24N	2:04	2:22	575	MR1203-27	
28	2012/08/13	156-00.09E	00-00.39N	2:39	2:56	535	MR1203-28	
29	2012/08/13	156-00.14E	00-00.28N	4:27	4:46	552	MR1203-29	
30	2012/08/13	156-00.21E	00-00.55N	5:06	5:24	560	MR1203-30	
31	2012/08/13	156-00.32E	00-00.63N	5:41	6:00	573	MR1203-31	
32	2012/08/13	156-00.14E	00-00.00N	7:30	7:48	544	MR1203-32	
33	2012/08/13	156-00.25E	00-00.03N	8:03	8:20	567	MR1203-33	
34	2012/08/13	156-00.43E	00-00.12N	8:34	8:52	574	MR1203-34	
35	2012/08/13	156-00.05E	00-00.12S	10:29	10:46	527	MR1203-35	
36	2012/08/13	156-00.62E	00-00.06S	11:04	11:22	558	MR1203-36	
37	2012/08/13	156-01.20E	00-00.02S	11:38	11:54	529	MR1203-37	
38	2012/08/13	155-59.62E	00-00.17N	13:27	13:45	511	MR1203-38	
39	2012/08/13	156-00.13E	00-00.26N	14:00	14:17	532	MR1203-39	
40	2012/08/13	156-00.56E	00-00.32N	14:32	14:50	563	MR1203-40	
41	2012/08/13	155-59.42E	00-00.21S	16:27	16:45	552	MR1203-41	
42	2012/08/13	155-59.79E	00-00.11S	16:58	17:16	551	MR1203-42	
43	2012/08/13	156-00.13E	00-00.02N	17:29	17:49	594	MR1203-43	
44	2012/08/13	155-59.68E	00-00.18S	19:29	19:49	593	MR1203-44	
45	2012/08/13	155-59.93E	00-00.06S	20:06	20:24	572	MR1203-45	
46	2012/08/13	156-00.15E	00-00.07N	20:40	20:59	584	MR1203-46	
47	2012/08/13	156-00.16E	00-15.07N	23:23	23:42	551	MR1203-47	
48	2012/08/13	156-00.25E	00-15.13N	23:57	0:14	568	MR1203-48	
49	2012/08/14	156-00.32E	00-15.18N	0:31	0:48	552	MR1203-49	
50	2012/08/14	156-00.13E	00-30.12N	3:11	3:27	519	MR1203-50	
51	2012/08/14	156-00.19E	00-30.28N	3:43	3:58	525	MR1203-51	
52	2012/08/14	156-00.24E	00-30.39N	4:13	4:30	521	MR1203-52	*3
53	2012/08/14	156-00.29E	00-30.47N	4:46	5:03	536	MR1203-53	
54	2012/08/14	156-00.22E	00-45.27N	7:19	7:36	533	MR1203-54	
55	2012/08/14	156-00.22E	00-45.35N	7:49	8:05	529	MR1203-55	
56	2012/08/14	156-00.23E	00-45.44N	8:18	8:36	541	MR1203-56	
57	2012/08/14	156-00.24E	01-00.34N	10:49	11:05	544	MR1203-57	
58	2012/08/14	156-00.47E	01-00.65N	11:19	11:35	544	MR1203-58	
59	2012/08/14	156-00.70E	01-00.98N	11:51	12:05	528	MR1203-59	
60	2012/08/14	156-00.13E	01-15.09N	14:10	14:27	535	MR1203-60	

61	2012/08/14	156-00.32E	01-15.37N	14:40	14:57	550	MR1203-61	
62	2012/08/14	156-00.55E	01-15.65N	15:09	15:25	538	MR1203-62	
63	2012/08/14	156-02.80E	01-30.41N	17:43	17:59	516	MR1203-63	
64	2012/08/14	156-03.00E	01-30.84N	18:14	18:30	527	MR1203-64	
65	2012/08/14	156-03.17E	01-31.21N	18:44	18:59	524	MR1203-65	
66	2012/08/14	156-00.35E	01-45.41N	21:10	21:29	628	MR1203-66	
67	2012/08/14	156-00.44E	01-45.55N	21:45	22:03	613	MR1203-67	
68	2012/08/14	156-00.52E	01-45.74N	22:22	22:41	596	MR1203-68	
69	2012/08/15	156-01.67E	01-57.68N	0:47	1:07	602	MR1203-69	
70	2012/08/15	156-01.70E	01-57.90N	1:20	1:37	583	MR1203-70	
71	2012/08/15	156-01.74E	01-58.14N	1:50	2:07	578	MR1203-71	
72	2012/08/15	156-00.23E	02-30.21N	5:44	6:01	606	MR1203-72	
73	2012/08/16	156-00.16E	03-00.07N	7:00	7:17	595	MR1203-73	
74	2012/08/17	156-00.15E	03-30.14N	8:17	8:36	660	MR1203-74	
75	2012/08/17	155-59.33E	05-01.02N	19:09	19:27	645	MR1203-75	
76	2012/08/18	156-02.79E	04-29.92N	4:19	4:37	585	MR1203-76	
77	2012/08/18	156-00.09E	03-59.97N	8:19	8:36	562	MR1203-77	
78	2012/08/19	156-00.71E	07-58.63N	19:13	19:31	600	MR1203-78	

\*1) Because we found spike noise in vertical acceleration in this cast, we carried out the second cast.

\*2) Because data from FP07 sensor was bad in this cast, we carried out the second cast after FP07 sensor was exchanged.

\*3) Because we found large shear around the depths of 410m and 460m in this cast, we conducted an additional cast.

During this cruise, we conducted following special observations for better understanding the fine structure and its daily variability:

a) 24-hours observation at the equator, 156E (every 3 hours)

b) Observations with meridional interval of 15 nautical miles between 2N and equator along 156E

During both observations, 3 cast were carried out at each time.

#### (4) Operation and data processing

We operated the Turbo Map-L by a crane which is usually used for foods supply and installed in the middle of ship. We lowered it at the starboard of R/V Mirai (Photo 7-4-1).

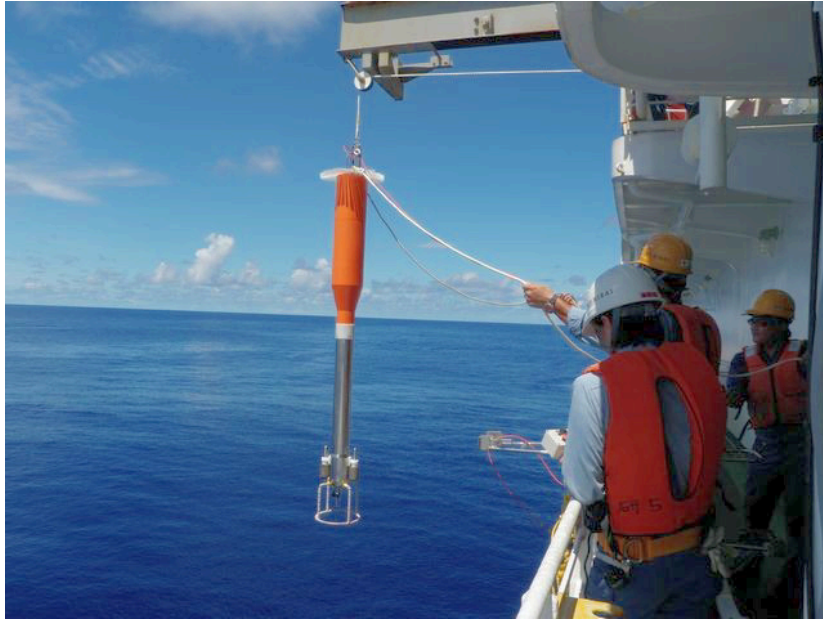


Photo 7-4-1. Observation using Turbo Map-L.

Measurement depth was 500m because our interest is ocean turbulence around thermocline. Descent rate of the Turbo Map-L was  $0.5 - 0.7 \text{ m s}^{-1}$ .

Data acquisition and processing were carried out using a PC in the Atmospheric Gas Observation Room of R/V Mirai (Photo 7-4-2). Data processing software was TM-Tool ver 3.04D provided by JFE Advantech Co Ltd.



Photo 7-4-2. Data acquisition and processing in the Atmospheric Gas Observation Room.

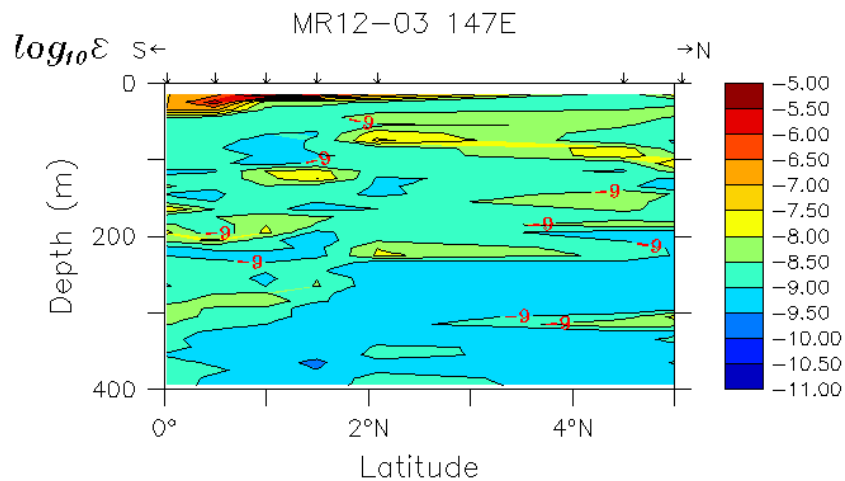
## 5) Results

Figure 7-4-1 shows the sections of logarithm of energy dissipation rate (epsilon) along 147E, and 156E. Compared with salinity section (Figure 2-2), there are following tendencies:

- High epsilon was generally seen in the high salinity water exceeding 35 PSU (100-200m).
- There is minimum layer of epsilon below 200m depth.

These results suggest that ocean mixing is active around high salinity water exceeding 35 PSU (South Pacific Tropical Water).

a)



b)

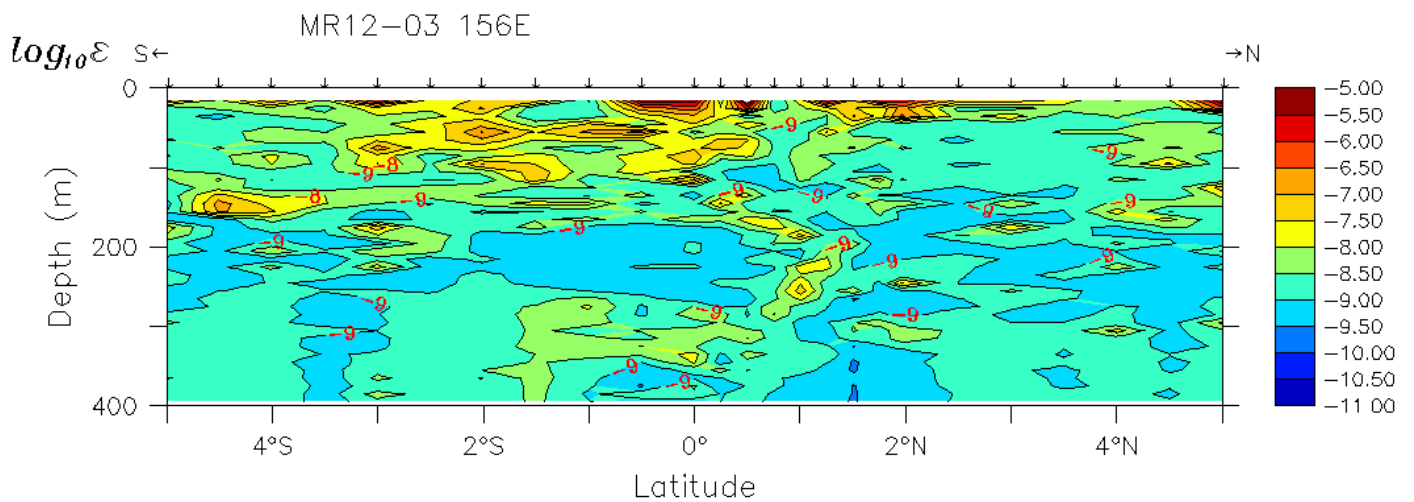


Figure 7-4-1. Vertical section of logarithm of energy dissipation rate along a) and b) 156E during MR12-03 cruise.

## 7.5 Argo floats

### 7.5.1 Profiling floats for JAMSTEC Argo Project

#### (1) Personnel

<i>Toshio Suga</i>	<i>(JAMSTEC/RIGC): Principal Investigator (not on board)</i>
<i>Shigeki Hosoda</i>	<i>(JAMSTEC/RIGC): not on board</i>
<i>Kanako Sato</i>	<i>(JAMSTEC/RIGC): not on board</i>
<i>Mizue Hirano</i>	<i>(JAMSTEC/RIGC): not on board</i>
<i>Hiroki Ushiomura</i>	<i>(MWJ): Technical Staff (Operation Leader)</i>

#### (2) Objectives

The objective of deployment is to clarify the structure and temporal/spatial variability of water masses in the North Pacific such as North Pacific Tropical Water in the subtropical North Pacific.

The profiling floats launched in this cruise measure vertical profiles of temperature and salinity automatically every ten days. As the vertical resolution of the profiles is very fine, the structure and variability of the water mass can be displayed well. Therefore, the profile data from the floats will enable us to understand the variability and the formation mechanism of the water mass.

#### (3) Parameters

- water temperature, salinity, and pressure

#### (4) Methods

##### i. Profiling float deployment

We launched an Arvor float manufactured by nke. These floats equip an SBE41cp CTD sensor manufactured by Sea-Bird Electronics Inc.

The floats usually drift at a depth of 1000 dbar (called the parking depth), diving to a depth of 2000 dbar and rising up to the sea surface by decreasing and increasing their volume and thus changing the buoyancy in ten-day cycles. During the ascent, they measure temperature, salinity, and pressure. They stay at the sea surface for approximately nine hours, transmitting the CTD data to the land via the ARGOS system, and then return to the parking depth by decreasing volume. The status of floats and their launches are shown in Table 7.5.1-1.

**Table 7.5.1-1 Status of floats and their launches**

**Float(2000dbar)**

<b>Float Type</b>	<b>Arvor float manufactured by nke.</b>
<b>CTD sensor</b>	<b>SBE41cp manufactured by Sea-Bird Electronics Inc.</b>
<b>Cycle</b>	<b>10 days (approximately 9 hours at the sea surface)</b>
<b>ARGOS transmit interval</b>	<b>30 sec</b>
<b>Target Parking Pressure</b>	<b>1000 dbar</b>
<b>Sampling layers</b>	<b>115 (2000,1950,1900,1850,1800,1750,1700,1650,1600,1550,1500, 1450, 1400, 1350, 1300, 1250, 1200, 1150, 1100, 1050, 1000, 980, 960, 940, 920, 900, 880, 860, 840, 820, 800, 780, 760, 740, 720, 700, 680, 660, 640, 620, 600, 580, 560, 540, 520, 500, 490, 480, 470, 460, 450, 440, 430, 420, 410, 400, 390, 380, 370, 360, 350, 340, 330, 320, 310, 300, 290, 280, 270, 260, 250, 240, 230, 220,210, 200, 195, 190, 185, 180, 175, 170, 165, 160, 155, 150, 145, 140, 135, 130, 125, 120, 115, 110, 105, 100, 95, 90, 85, 80, 75, 70, 65, 60, 55, 50, 45, 40, 35, 30, 25, 20, 15, 10, 4 or surface dbar)</b>

**Launches**

<b>Float S/N</b>	<b>ARGOS ID</b>	<b>Date and Time of Reset (UTC)</b>	<b>Date and Time of Launch(UTC)</b>	<b>Location of Launch</b>	<b>CTD St. No.</b>
<b>11009</b>	<b>112238</b>	<b>2012/08/21 22:50</b>	<b>2012/08/21 23:56</b>	<b>12-00.29N 154-18.12E</b>	<b>C35</b>

**(5) Data archive**

The real-time data are provided to meteorological organizations, research institutes, and universities via Global Data Assembly Center (GDAC: <http://www.usgoda.gov/argo/argo.html>, <http://www.coriolis.eu.org/>) and Global Telecommunication System (GTS), and utilized for analysis and forecasts of sea conditions.

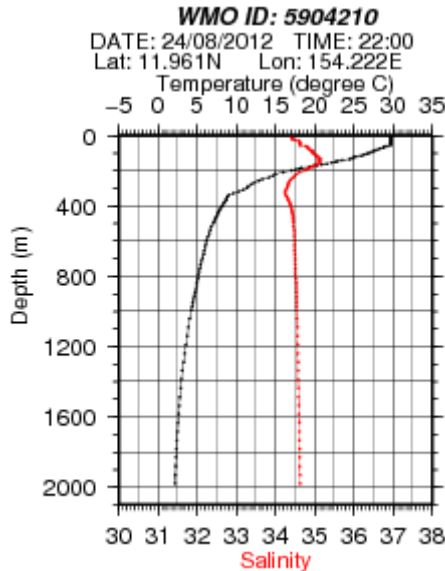


**Fig. 7.5.1-1. The profile of the float launched during MR12-03.**

## 7.5.2 ARGO float mission off Papua New Guinea

### (1) Personal

#### (a) On board

Takuya Hasegawa (JAMSTEC/RIGC: Principal Investigator for this mission)

Hiroki Ushiomura (MWJ: Chief technical staff of MR12-03 for this mission)

Rei Ito (MWJ)

Kazuma Takahashi (MWJ)

#### (b) Not on board

Toshio Suga (JAMSTEC/RIGC)

Shigeki Hosoda (JAMSTEC/RIGC)

Kanako Sato (JAMSTEC/RIGC)

Mizue Hirano (JAMSTEC/RIGC)

Hiroyuki Nakajima (MWJ)

Kentaro Ando (JAMSTEC/RIGC)

Takanori Horii (JAMSTEC/RIGC)

Yoshimu Kusumoto (Hydro System development Inc)

### (2) Outline and objectives

One Argo float (Navigation European Marine Observer: NEMO: Fig.7.5.2-1) was launched off Papua New Guinea (2.72S-153.27E, near subsurface-ADCP moorings deployment points; see Fig.7.5.2-2) on 1st August 2012 (UTC) as a part of CLIVAR-SPICE related observations during MR12-03.

The purpose of this NEMO float mission is to obtain one temperature and salinity profile per one day in order to merge the data with current velocity observed by two subsurface-ADCP moorings deployed at around 2.7S-153E to explore temperature and salinity transport of the New Ireland Coastal Undercurrent (NICU), which is suggested to be important for Pacific warm water pool changes by recent studies.

For this purpose, mission parameters of this NEMO float were highly tuned to make the float stay near the ADCP moorings deployment points (see subsection (4)). In addition, MTMs (Mobile Terminated Messages), which can change the mission parameters of

NEMO float after its launch via Iridium communication, can be automatically made using mission-control-programs that were specially made for this mission at Argo float. The MTMs to the NEMO float are automatically sent via Iridium communication server from Argo-float data server at Yokosuka HQ of JAMSTEC using these programs at 06:00 (UTC) everyday. The contents of MTMs (e.g., parking depth) are decided by the programs by use of information of MOMs (Mobile Originated Messages; those are emitted from the NEMO float using Iridium communication and include information concerning position of NEMO float, observed temperature and other data, and technical information of the NEMO float). The MTMs can be made and sent by manual operation in addition to the automatic operation using the mission-control-programs.

As described above, this NEMO-float mission focuses on water properties of NICU off Papua New Guinea. After the NEMO float will go out from the NICU area, its mission will be changed to that of standard Argo floats with 10-day observation cycle by using MTMs.

### **(3) Parameters**

Water temperature, salinity and pressure

### **(4) Methods and float information**

- (a) Type of the float: NEMO float, manufactured by Optimare Ltd.
- (b) Serial number of the NEMO float: 222
- (c) Iridium communication number (IMED): 300234011420390
- (d) Date and time of launch (UTC): 2012/08/01 05:29
- (e) Location of launch: 2.72S-153.27E
- (f) Main sensor: SBE41CP CTD sensor, manufactured by Sea-Bird Electronics Inc.
- (g) Transmission system: Iridium communication (SBD type)
- (h) Mission cycle time: 1440 minutes (nearly 30 minutes at the sea surface)
- (i) Startup delay: 1380 minutes (23:00 UTC)
- (j) Startup time: 480 minutes
- (k) Maximum transmission time at sea surface: 60 minutes
- (l) Observing layer: from surface to 650 dbar with continuous mode (1 Hz sampling)
- (m) CTD pressure sample interval during descent: 10 seconds

- (n) Target parking pressure: 550 dbar near launching point
- (o) Ascent speed and mode: 0.10 m/s with controlled mode
- (p) Descent speed and mode: 0.08 m/s with controlled mode
- (q) Seg speed: 0.08 m/s
- (r) CTD sample interval at parking pressure: 1440 minutes
- Mission parameters related to parking depth, mission cycle time, ascent speeds, observation layer etc. can be changed after launch by MTMs using Iridium communication.

### (5) Data archive

The real-time data are provided to meteorological organizations, research institutes, and universities via Global Data Assembly Center (GDAC: <http://www.usgodae.org/argo/argo.html>, <http://www.coriolis.eu.org/>) and Global Telecommunication System (GTS), and utilized for analysis and forecasts of sea conditions.



Fig

Figure 7.5.2-1: NEMO float just after and before its launch (left and right, respectively).

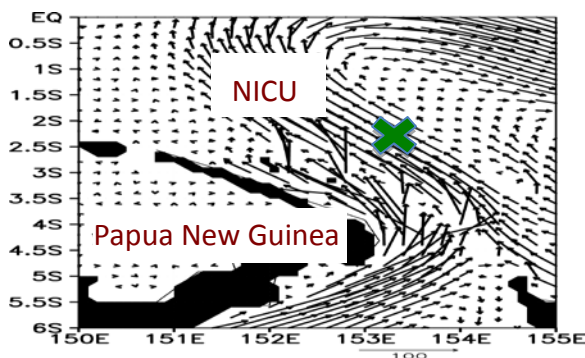


Figure 7.5.2-2: Location of launch of the NEMO float (2.72S-153.27E: shown by a green cross mark). Current velocities for NICU layer from high-resolution ocean general circulation model (OFES) simulation are also shown by black arrows (unit in cm/s).

## **7.6 Global Drifter Program – SVP Drifting Buoys**

### **(1) Personnel**

*Rick Lumpkin (National Oceanographic Atmospheric Administration /  
Global Drifter Program): Principal Investigator of GDP (not on board)*  
*Shaun Dolk (National Oceanographic Atmospheric Administration /  
Global Drifter Program): (not on board)*

### **(2) Objectives**

The objective of deploying the 20 drifting buoys is to compliment the current global array of drifting buoys. The western equatorial region is of great value, as there are few deployment opportunities in this region. As a result, the data collected from these instruments will significantly affect the current dataset of historical drifters in the area.

### **(3) Parameters**

Sea surface temperature and ocean current velocities.

### **(4) Methods**

#### **i. Profiling float deployment**

We launched ten (10) drifting buoys manufactured by Clearwater Instruments and ten (10) drifters manufactured by Data Buoy instrumentation. These drifters are equipped with thermistor sensors to measure the temperature at the surface of the ocean. The drifters float at the surface, following upper ocean surface currents. The measured temperature and location data are sent to the Drifter Data Assembly Center via the ARGOS transmitting system for data processing and quality control procedures. The drifters are expected to transmit for 450 days, while maintaining a drogue presence for 300 days. The status of drifters and their launches are shown in Table 7.6.1.

**Table 7.6.1 Status of drifters and their launches**

<b>Drifter Type</b>	<b>Surface Velocity Profiler (SVP) Type drifter Manufactured by Clearwater and DBi.</b>
---------------------	---

**Launches**

<b>Drifter S/N</b>	<b>Date</b>	<b>Time (UTC)</b>	<b>Latitude</b>	<b>Longitude</b>
107631	4-Aug-12	23:33	04 57.54 S	155 59.65 E
107632	5-Aug-12	6:28	04 01.00 S	156 00.73 E
101849	9-Aug-12	8:25	03 00.28 S	156 00.45 E
101851	10-Aug-12	1:25	02 01.09 S	155 57.95 E
107633	10-Aug-12	9:51	01 00.49 S	156 00.64 E
107634	13-Aug-12	21:22	00 00.35 N	156 00.50 E
107635	14-Aug-12	12:26	01 01.47 N	156 00.93 E
101930	16-Aug-12	7:37	03 00.23 N	156 00.49 E
101943	16-Aug-12	23:50	02 00.64 N	156 02.86 E
101927	18-Aug-12	8:55	03 59.98 N	156 00.05 E
107644	19-Aug-12	1:22	05 00.96 N	155 58.54 E
107641	19-Aug-12	6:55	06 00.01 N	155 59.99 E
101760	19-Aug-12	12:08	07 00.00 N	156 00.00 E
107645	21-Aug-12	1:38	07 57.82 N	156 02.65 E
107642	21-Aug-12	7:30	09 00.00 N	155 34.50 E
107643	21-Aug-12	12:32	09 59.99 N	155 08.99 E
101757	21-Aug-12	17:35	11 00.02 N	154 43.49 E
101853	21-Aug-12	23:57	12 00.31 N	154 18.13 E
101951	22-Aug-12	4:58	13 00.02 N	153 56.41 E
101933	22-Aug-12	10:00	14 00.01 N	153 34.84 E

**(5) Data archive**

The real time data are provided via DAC Data Products, which you can access at (<http://www.aoml.noaa.gov/phod/dac/meds.html>). The quality controlled data are provided to oceanographic organizations, research institutes, and universities via Drifter Data Assembly Center (<http://www.aoml.noaa.gov/phod/dac/dirall.html>) and Global Telecommunication System (GTS), and utilized for analysis and forecasts of the ocean conditions and the climates.

## 7.7 Radiosonde observation for the validation of GOSAT and ship-borne sky radiometer products

<b>Shuji KAWAKAMI</b>	<b>(JAXA EORC, PI)</b>
<b>Kazuma AOKI</b>	<b>(Toyama University, PI/not on board)</b>
<b>Tadahiro HAYASAKA</b>	<b>(Tohoku University, not on board)</b>
<b>Yoshimi KAWAI</b>	<b>(JAMSTEC RIGC, not on board)</b>
<b>Wataru TOKUNAGA</b>	<b>(GODI)</b>
<b>Harumi OHTA</b>	<b>(GODI)</b>
<b>Kouichi INAGAKI</b>	<b>(GODI)</b>

### (1) Objective

We performed the radiosonde observations to obtain vertical profiles of temperature and water vapor for the validation of GOSAT and ship-borne sky radiometer products, and to investigate atmospheric and cloud structure responding to the ocean temperature front of the Kuroshio Extension.

### (2) Parameters

According to the manufacturer, the range and accuracy of parameters measured by the radiosonde sensor (RS92-SGP) are as follows;

Parameter	Range	Accuracy
Pressure	3~1080 hPa	+/- 1 hPa (1080-100 hPa), +/- 0.6 hPa (100-3 hPa)
Temperature	-90~60 °C	+/- 0.5 °C
Humidity	0~100 %	5 %

### (3) Method

Atmospheric soundings by radiosondes were performed in the western Pacific Ocean. In total, 45 soundings were carried out, but note that one sounding (RS37) stopped at only 6569 m height (Table 7.7-1, Figure 7.7-1). The main system consisted of processor (Vaisala, DigiCORA III MW31), GPS antenna (GA20), UHF antenna (RB21), ground check kit (GC25), balloon launcher (ASAP), and GPS radiosonde sensor (RS92-SGP).

### (4) Preliminary results

Precipitable water calculated from the sounding data is shown in Figures 7.7-2. Note that it was derived from the surface to the middle troposphere for RS37. The Kuroshio Extension region became quite humid after the Baiu season, and the precipitable water in this region was close to that in the tropics.

### (5) Data archive

Raw data were recorded in ASCII format every 2 seconds during ascent. These raw data were submitted to the Data Management Group of JAMSTEC just after the cruise.

Table 7.7-1. Radiosonde launch log.

Sounding No.	Launching			Maximum		Duration (sec)
	Date (UT)	Lon	Lat	Altitude	hPa	
RS01	2012/07/17 20:34:43	37.846	142.758	20287	55.3	5224
RS02	2012/07/18 02:34:34	36.729	143.036	22700	37.9	6424
RS03	2012/07/18 08:31:16	35.748	143.257	21902	42.8	4542
RS04	2012/07/18 14:30:34	34.707	143.517	23008	35.7	5484
RS05	2012/07/18 20:30:27	33.603	143.765	22953	35.9	5352
RS06	2012/07/20 03:01:03	27.621	144.896	23035	35.1	5208
RS07	2012/07/21 14:10:15	20.871	146.088	21777	42.3	5492
RS08	2012/07/23 03:10:24	13.640	146.665	24690	26.3	5942
RS09	2012/07/24 14:25:36	6.791	146.794	23021	34.1	5646
RS10	2012/07/25 02:41:49	4.972	146.971	22927	34.6	5068
RS11	2012/07/27 14:25:21	1.535	146.974	20365	52.3	6474
RS12	2012/07/28 02:40:44	2.084	146.964	23337	32.3	5244
RS13	2012/07/30 14:24:47	-0.100	149.160	17370	86.8	2916
RS14	2012/07/31 02:40:06	-0.209	150.538	21303	44.8	5392
RS15	2012/08/02 02:11:17	-3.273	153.069	24271	27.9	6380
RS16	2012/08/02 14:25:24	-4.868	154.249	22476	37.0	5712
RS17	2012/08/05 02:12:18	-4.584	156.001	23578	31.2	6312
RS18	2012/08/05 14:25:09	-4.265	157.004	20772	49.0	6284
RS19	2012/08/07 15:10:10	-4.784	157.589	22198	38.9	5384
RS20	2012/08/08 02:10:05	-4.275	157.394	24896	25.2	6310
RS21	2012/08/08 14:25:22	-2.716	156.444	23409	31.9	6012
RS22	2012/08/10 03:09:46	-1.786	155.979	23495	31.4	5950
RS23	2012/08/10 13:50:17	-0.593	156.017	22632	36.1	6082
RS24	2012/08/11 00:10:13	-0.019	156.095	22934	34.5	5372
RS25	2012/08/11 02:09:43	-0.040	156.141	23132	33.3	5538
RS26	2012/08/11 04:11:15	-0.046	156.063	19712	58.4	4626
RS27	2012/08/12 03:10:13	-0.037	156.133	20040	55.1	5432
RS28	2012/08/12 15:30:49	-0.001	155.976	21245	45.2	5108
RS29	2012/08/13 13:50:04	0.003	155.992	22607	36.3	5514
RS30	2012/08/14 02:09:59	0.361	156.003	24429	27.1	6360
RS31	2012/08/14 14:26:35	1.250	156.001	22148	38.9	5128
RS32	2012/08/16 13:51:17	2.410	156.083	23308	32.5	6092
RS33	2012/08/17 02:11:42	2.379	156.018	23909	29.5	5512
RS34	2012/08/19 03:10:14	5.254	155.992	24060	29.0	6026
RS35	2012/08/19 13:55:14	7.262	155.999	22979	34.3	5814
RS36	2012/08/20 02:10:51	7.970	156.022	21334	44.7	5228
RS37	2012/08/22 13:57:27	14.583	153.183	6569	457.2	1308
RS38	2012/08/23 14:31:27	18.185	151.593	23319	32.9	5910
RS39	2012/08/24 02:35:24	20.524	150.663	22418	38.0	5486

RS40	2012/08/25 03:04:56	25.431	148.658	20283	54.2	5288
RS41	2012/08/26 14:31:01	32.652	145.552	22658	37.5	5696
RS42	2012/08/26 20:29:51	33.812	145.029	23827	31.4	6184
RS43	2012/08/27 02:30:09	34.914	144.525	23758	31.7	5920
RS44	2012/08/27 08:30:08	36.080	143.994	24003	30.8	6298
RS45	2012/08/27 14:30:17	37.251	143.437	22434	39.3	5546

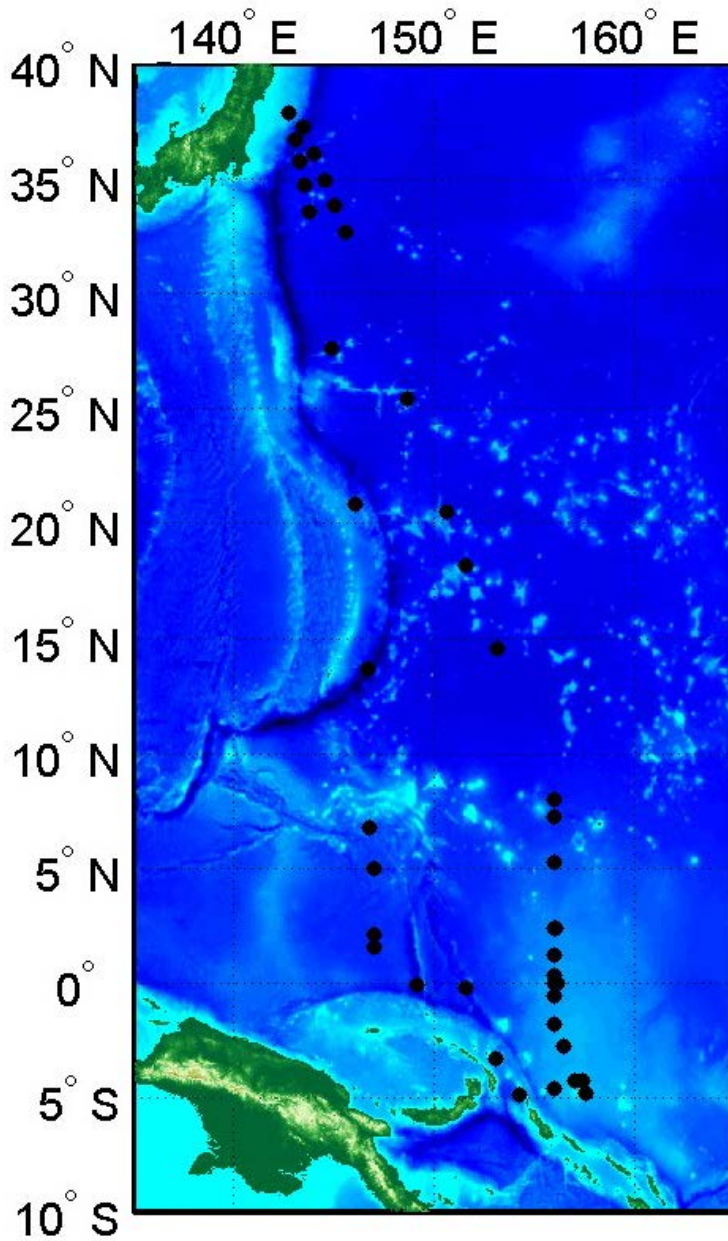


Figure 7.7-1. Positions of the GPS radiosonde (dots).

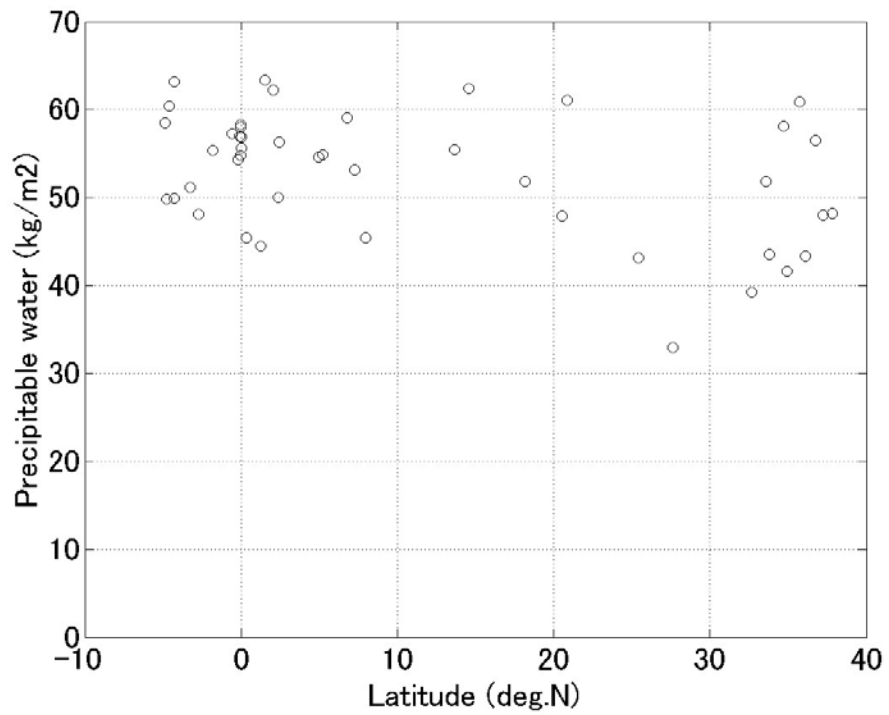
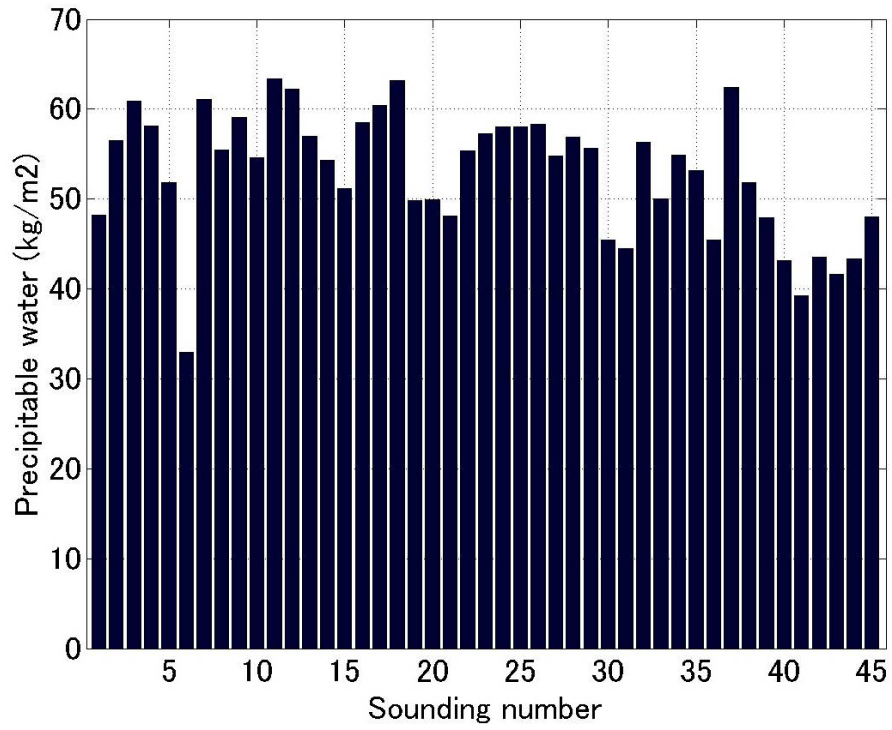


Figure 7.7-2. Precipitable water for (upper) each sounding number and (lower) latitude.

## 7.8 Validation of GOSAT products over sea using a ship-borne compact system for measuring atmospheric trace gas column densities

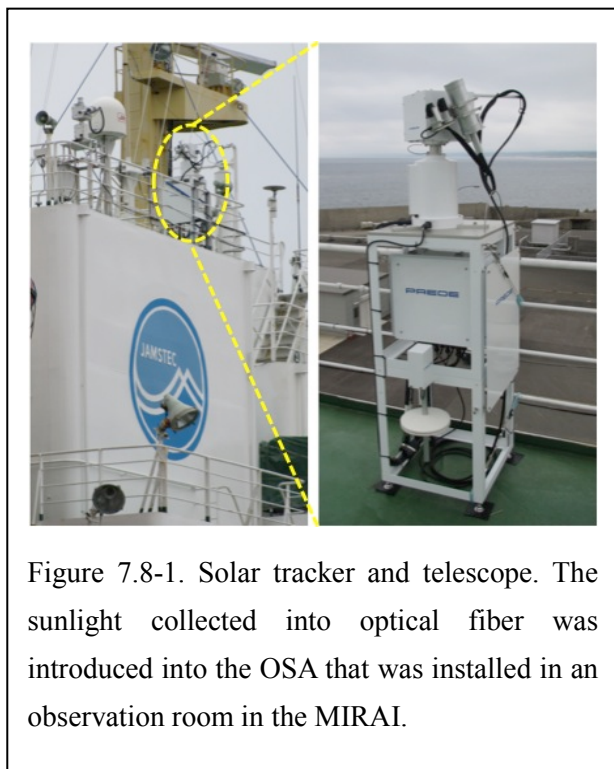
**Shuji KAWAKAMI (JAXA EORC)**  
**Hirofumi OHYAMA (JAXA SAPC)**

### (1) Objective

Greenhouse gases Observing SATellite (GOSAT) was launched on 23 January 2009 in order to monitor the global distributions of atmospheric greenhouse gas concentrations: column-averaged dry-air mole fractions of carbon dioxide (CO<sub>2</sub>) and methane (CH<sub>4</sub>). A network of ground-based high-resolution Fourier transform spectrometers provides essential validation data for GOSAT. Vertical CO<sub>2</sub> profiles obtained during ascents and descents of commercial airliners equipped with the in-situ CO<sub>2</sub> measuring instrument are also used for the GOSAT validation. Because such validation data are obtained mainly over land, there are very few data available for the validation of the over-sea GOSAT products. The objectives of our research are to acquire the validation data over sea using an automated compact instrument and to compare the acquired data with the over-sea GOSAT products.

### (2) Description of instruments deployed

The column-averaged dry-air mole fractions of CO<sub>2</sub> and CH<sub>4</sub> can be estimated from absorption by atmospheric CO<sub>2</sub> and CH<sub>4</sub> that is observed in a solar spectrum. An optical spectrum analyzer (OSA, Yokogawa M&I co., AQ6370) was used for measuring the solar absorption spectra in the near-infrared spectral region. A solar tracker (PREDE co., ltd.) and a small telescope (Figure 7.8-1) collected the sunlight into the optical fiber that was connected to the OSA. The solar tracker searches the sun every one minute until the sunlight with a defined intensity is detected. The measurements of the solar spectra were performed during solar zenith angles of <80°. In addition, radiosonde observations, which were collocated with the GOSAT overpass time (both daytime and nighttime), were made to obtain vertical profiles of atmospheric temperature and humidity.



### (3) Analysis method

The CO<sub>2</sub> absorption spectrum at the 1.6 μm band measured with the OSA is shown in Figure 2. The absorption spectrum can be simulated based on radiative transfer theory using assumed atmospheric profiles of pressure, temperature, and trace gas concentrations. The column abundance of CO<sub>2</sub> (CH<sub>4</sub>) was retrieved by adjusting the assumed CO<sub>2</sub> (CH<sub>4</sub>) profile to

minimize the differences between the measured and simulated spectra. Figure 3 shows an example of spectral fit performed for the spectral region with the CO<sub>2</sub> absorption lines. The column-averaged dry-air mole fraction of CO<sub>2</sub> (CH<sub>4</sub>) was obtained by taking the ratio of the CO<sub>2</sub> (CH<sub>4</sub>) column to the dry-air column.

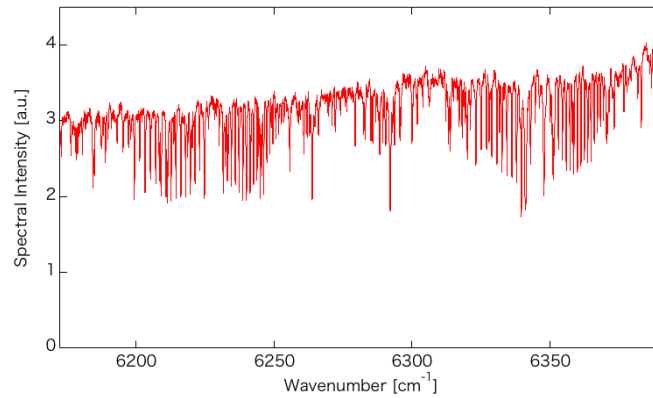


Figure 7.8-2. 1.6 μm CO<sub>2</sub> absorption spectrum measured with the OSA.

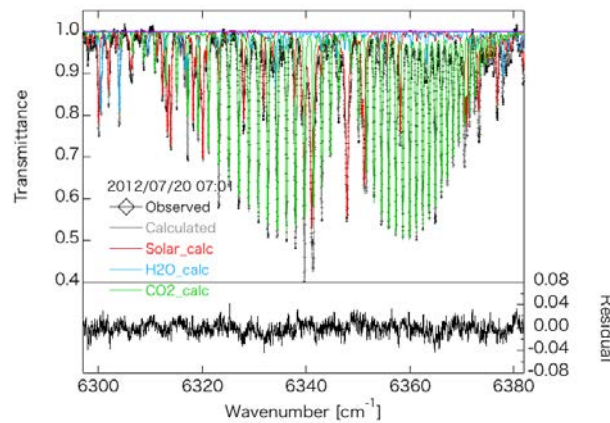


Figure 7.8-3. Spectral fit performed for the 6297–6382 cm<sup>-1</sup> region using an OSA spectrum. Open diamonds denote the measured spectrum, and the solid line denotes the spectrum calculated from the retrieval result. The residual between the measured and calculated spectra is also shown.

#### (4) Preliminary results

The observations were made from July 17 to August 29 continuously in daytime including while the ship was at the Sekinehama sea-port (Table 7.8-1 and Figure 7.8-1). Radiosonde data were obtained at the GOSAT overpass in daytime (Table 7.8-1).

CO <sub>2</sub> observations		Radiosonde at the GOSAT overpass in daytime		
Date	Time(JST)	Time (JST)	Latitude (degN)	Longitude(degE)
2012/07/17	7:25-18:00			
2012/07/18	7:02-10:15			
2012/07/19	7:24-17:52			
2012/07/20	6:34-18:00	12:00	27.621	144.896
2012/07/21	5:02-17:09			
2012/07/22	5:42-10:03			
2012/07/23	7:02-16:34	12:10	13.640	146.665
2012/07/24	5:44-17:00			
2012/07/25	10:36-15:24	11:55	4.972	146.971
2012/07/26	6:13-11:29			
2012/07/27	5:51-13:02			
2012/07/28	--	11:40	2.084	146.964
2012/07/29	--			
2012/07/30	9:55-17:58			
2012/07/31	8:03-16:29	11:40	-3.273	153.069
2012/08/01	5:45-16:51			
2012/08/02	5:18-16:55	11:10	-3.273	153.069
2012/08/03	6:14-16:30			
2012/08/04	5:18-16:41			
2012/08/05	5:22-12:52	11:10	-4.584	156.001
2012/08/06	5:22-13:53			
2012/08/07	5:24-16:51			
2012/08/08	5:23-16:05	11:10	-4.275	157.394
2012/08/09	6:56-16:11			
2012/08/10	5:12-12:52			
2012/08/11	5:06-16:00	11:10	-0.040	156.141
2012/08/12	6:05-13:48			
2012/08/13	5:41-11:48			
2012/08/14	5:24-16:01	11:10	0.361	156.003
2012/08/15	5:26-15:48			
2012/08/16	--			
2012/08/17	5:27-16:05	11:10	2.379	156.018
2012/08/18	5:08-16:04			
2012/08/19	5:18-16:02			
2012/08/20	5:21-16:41	11:10	5.254	155.992
2012/08/21	6:31-15:51			
2012/08/22	5:19-12:00			
2012/08/23	6:49-14:31			
2012/08/24	5:25-16:34	11:35	20.524	150.663
2012/08/25	5:25-16:59	12:05	25.431	148.658
2012/08/26	5:34-16:59			
2012/08/27	5:34-15:24			
2012/08/28	5:57-17:41			
2012/08/29	6:17-10:19			

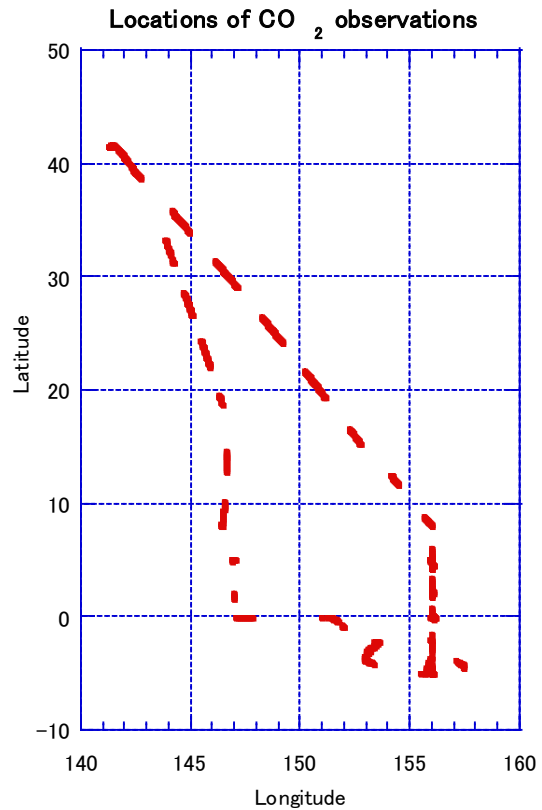


Table 7.8-1. Period of CO<sub>2</sub> observations and Radiosonde      Figure 7.8-1. Locations of CO<sub>2</sub> observations

(5) Data archive

The column-averaged dry-air mole fractions of CO<sub>2</sub> and CH<sub>4</sub> retrieved from the OSA spectra will be submitted to JAMSTEC Data Integration and Analyses Group (DIAG).

## **7.9 Lidar observations of clouds and aerosols**

**Nobuo SUGIMOTO (NIES)**

**Ichiro MATSUI (NIES)**

**Atsushi SHIMIZU (NIES)**

**Tomoaki NISHIZAWA (NIES)**

**Hajime OKAMOTO (Kyusyu university)**

(Lidar operation was supported by Global Ocean Development Inc. (GODI).)

### (1) Objectives

Objectives of the observations in this cruise is to study distribution and optical characteristics of ice/water clouds and marine aerosols using a two-wavelength polarization Mie lidar.

### (2) Description of instruments deployed

Vertical profiles of aerosols and clouds are measured with a two-wavelength polarization Mie lidar. The lidar employs a Nd:YAG laser as a light source which generates the fundamental output at 1064nm and the second harmonic at 532nm. Transmitted laser energy is typically 30mJ per pulse at both of 1064 and 532nm. The pulse repetition rate is 10Hz. The receiver telescope has a diameter of 20 cm. The receiver has three detection channels to receive the lidar signals at 1064 nm and the parallel and perpendicular polarization components at 532nm. An analog-mode avalanche photo diode (APD) is used as a detector for 1064nm, and photomultiplier tubes (PMTs) are used for 532 nm. The detected signals are recorded with a transient recorder and stored on a hard disk with a computer. The lidar system was installed in a container which has a glass window on the roof, and the lidar was operated continuously regardless of weather. Every 10 minutes vertical profiles of four channels (532 parallel, 532 perpendicular, 1064, 532 near range) are recorded.

### (3) Preliminary results

The two wavelength polarization Mie lidar worked well and succeeded in getting the lidar data during the observation period from July 17 to Aug. 29, 2012.

Examples of the measured data are depicted in Fig. 7.9-1. The figures indicates that the lidar can detect aerosols in the planetary boundary layer (PBL) formed below 1km, water clouds formed at the top of the PBL, ice clouds in the upper layer. It should be noted that the lidar could detect ice clouds (cirrus) up to very high altitude of 16km since optical and microphysical properties and distributions of cirrus are key parameters for evaluating climate change. The figure also depicts that the lidar signals in the PBL are larger on Aug. 7 than on Aug. 6 and Aug. 8, implying that the aerosol concentration and/or their optical properties changes. The measured depolarization ratios in the three days are low, indicating that the spherical aerosols (e.g., sulfate, nitrate, organic carbon, and sea-salt particles) are rich. Combined analysis of the spectral ratio of lidar signals, surface wind speed, relative humidity and observation area data are effective in order to understand this phenomena better.

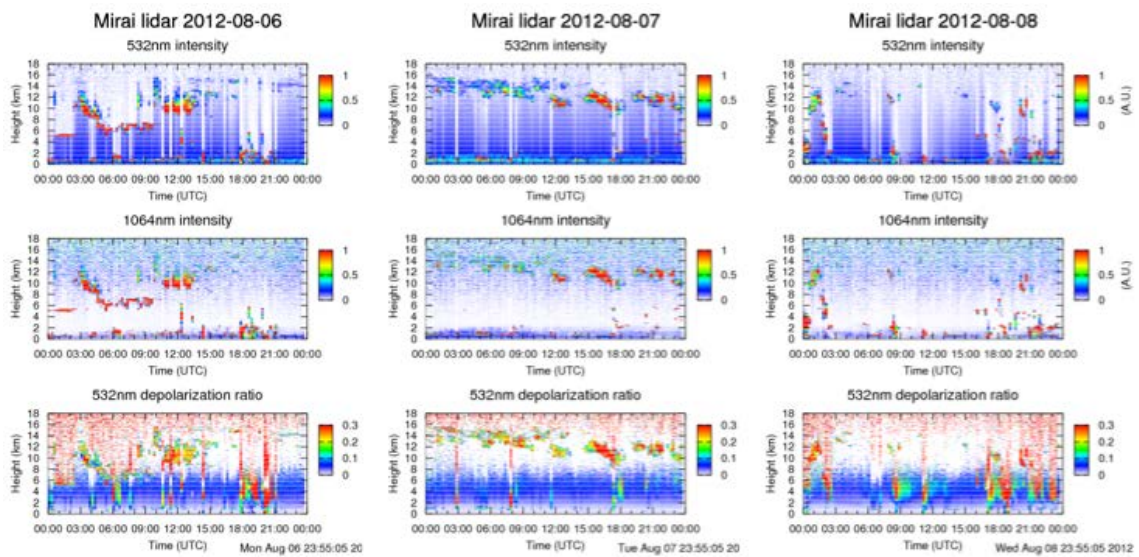


Figure 7.9-1: Time-height sections of backscatter intensities at 532nm and 1064nm and total depolarization ratios at 532nm measured from Aug. 6 to Aug. 8, 2012.

#### (4) Data archive

- Raw data

temporal resolution 10min / vertical resolution 6 m

data period (UTC): July. 17, 2012 – Aug. 29, 2012

lidar signal at 532 nm, lidar signal at 1064 nm, depolarization ratio at 532 nm

- Processed data (plan)

cloud base height, apparent cloud top height, phase of clouds (ice/water), cloud fraction

boundary layer height (aerosol layer upper boundary height),

backscatter coefficient of aerosols, particle depolarization ratio of aerosols

\* Data policy and Citation

Contact NIES lidar team ([nsugimot/i-matsui/shimizua/nisizawa@nies.go.jp](mailto:nsugimot/i-matsui/shimizua/nisizawa@nies.go.jp)) to utilize lidar data for productive use.

## 7.10 Aerosol optical characteristics measured by Shipborne Sky radiometer

**Kazuma Aoki (University of Toyama) Principal Investigator / not onboard**  
**Tadahiro Hayasaka (Tohoku University) Co-worker / not onboard**

### (1) Objective

Objective of the observations in this aerosol is to study distribution and optical characteristics of marine aerosols by using a ship-borne sky radiometer (POM-01 MKII: PREDE Co. Ltd., Japan). Furthermore, collections of the data for calibration and validation to the remote sensing data were performed simultaneously.

### (2) Methods and Instruments

Sky radiometer is measuring the direct solar irradiance and the solar aureole radiance distribution, has seven interference filters (0.34, 0.4, 0.5, 0.675, 0.87, 0.94, and 1.02  $\mu\text{m}$ ). Analysis of these data is performed by SKYRAD.pack version 4.2 developed by Nakajima *et al.* 1996.

#### @ Measured parameters

- Aerosol optical thickness at five wavelengths (400, 500, 675, 870 and 1020 nm)
- Ångström exponent
- Single scattering albedo at five wavelengths
- Size distribution of volume (0.01  $\mu\text{m}$  – 20  $\mu\text{m}$ )

# GPS provides the position with longitude and latitude and heading direction of the vessel, and azimuth and elevation angle of sun. Horizon sensor provides rolling and pitching angles.

### (3) Preliminary results

This study is not onboard. Data obtained in this cruise will be analyzed at University of Toyama.

### (4) Data archives

Measurements of aerosol optical data are not archived so soon and developed, examined, arranged and finally provided as available data after certain duration. All data will archived at University of Toyama (K.Aoki, SKYNET/SKY: <http://skyrad.sci.u-toyama.ac.jp/>) after the quality check and submitted to JAMSTEC.

## 7.11 Continuous measurement of the water stable isotopes over the Ocean

### (1) Personnel

**Yasushi Fujiyoshi** (Hokkaido Univ./JAMSTEC) *Principal Investigator (not on-board)*  
**Naoyuki Kurita** (JAMSTEC)

#### Operator

**Wataru Tokunaga, Harumi Ota, Kouichi Inagaki** (*Global Ocean Development Inc.: GODI*)  
**Ryo Ohyama** (*MIRAI Crew*)

### (2) Objective

It is well known that the variability of stable water isotopes (HDO and H<sub>2</sub><sup>18</sup>O) reflects the integrated history of water mass exchange that occurs during transportation from the upstream region. Thus, water isotope tracer is recognized as the powerful tool to study of the hydrological cycles in the marine atmosphere. However, oceanic region is one of sparse region of the isotope data, it is necessary to fill the data to identify the moisture sources by using the isotope tracer. In this study, to fill this sparse observation area, intense water isotopes observation was conducted along the cruise track of MR12-03.

### (3) Method

Following observation was carried out throughout this cruise.

#### - Atmospheric moisture sampling:

Water vapor isotopes in ambient air was continuously measured using the laser instrument based on off-axis integrated cavity output spectroscopy, manufactured by Los Gatos Research, Inc. (LGR) (Water Vapor Iso- tope Analyzer, WVIA) coupled with an accessory device for the vaporization of a liquid water standard (Water Vapor Isotope Standard Source, WVISS). The WVISS is programmable from the WVIA and thus this coupled system is capable of automatically conducting a calibration routine at specific intervals.

Air intake was attached at the middle level (20m above the sea level) of the mast at the compass deck and a sampling tube (20 m length of Nylon tubing (Junron A), 8mm O.D.) was connected from air intake to a 3-way valve attached to the WVISS. A 1.0 μm filter with PTFE membrane was placed where the tube enters the air intake. Air was drawn via the pump at a flow rate of 3 l min<sup>-1</sup> to the laboratory and then a part of air was sacked via the WVIA external pump at a flow rate of 0.5 l min<sup>-1</sup>. Every 25 min, the 3-way valve automatically switched from ambient/outdoor inlet to WVISS standard air, whereupon standard air with a H<sub>2</sub>O concentration of 12 000 ppm was introduced to the WVIA for 5 min. After finishing the reference gas measurement, the valve switches back and ambient air sampling is resumed. Raw data from the analyzer is stored on the internal hard disk, and is transferred via ethernet cable. Calibration is undertaken as a post-processing step using the external computer system.

#### - Rainwater sampling

Rainwater samples gathered in rain/snow collector were collected just after precipitation events have ended. The collected sample was then transferred into glass bottle (6ml) immediately after the measurement of precipitation amount.

#### - Surface seawater sampling

Seawater sample taken by the pump from 4m depths were collected in glass bottle (6ml) around the noon at the local time.

**(4) Water samples for isotope analysis**

Sampling of rainfall for isotope analysis is summarized in Table 7.11-1 (38 samples). Described rainfall amount is calculated from the collected amount of precipitation. Sampling of surface seawater taken by pump from 4m depths is summarized in Table 7.11-2 (43 samples).

**(5) Data archive**

The isotopic data of water vapor can obtain from the laser based water vapor isotope analyzer on board. The archived raw observed data (see Figure 7.11-1) was submitted to JAMSTEC Data Integration and Analysis Group (DIAG) after the cruise immediately. As for collected water samples, isotopes (HDO, H<sub>2</sub><sup>18</sup>O) analysis will be done at RIGC/JAMSTEC, and then analyzed isotopes data will be submitted to JAMSTEC DIAG.

**Table 7.11-1 Summary of precipitation sampling for isotope analysis.**

	Date	Time (UT)	Lon	Lat	Date	Time (UT)	Lon	Lat	Rain (mm)	R/S
R-01	7.16	23:50	141-14.37E	41-21.97N	7.18	05:09	143-08.39E	36-15.48E	21.6	R
R-02	7.18	05:09	143-08.39E	36-15.48E	7.21	16:29	146-10.94E	20-18.28N	62.0	R
R-03	7.21	16:29	146-10.94E	20-18.28N	7.22	00:54	146-28.63E	18-38.10N	32.0	R
R-04	7.22	01:02	146-28.83E	18-36.53N	7.22	08:03	146-39.87E	17-15.40N	36.0	R
R-05	7.22	08:09	146-39.90E	17-14.50N	7.24	21:12	147-00.86E	05-25.78N	41.0	R
R-06	7.24	21:12	147-00.86E	05-25.78N	7.26	10:37	147-00.00E	03-38.00N	168.0	R
R-07	7.26	10:37	147-00.00E	03-38.00N	7.27	12:02	146-59.35E	01-16.60N	32.0	R
R-08	7.27	12:02	146-59.35E	01-16.60N	7.27	23:51	146-57.75E	02-04.41N	60.0	R
R-09	7.27	23:53	146-57.71E	02-04.41N	7.28	10:55	146-58.69E	01-08.83N	91.5	R
R-10	7.28	10:55	146-58.69E	01-08.83N	7.29	07:23	147-00.90E	00-17.80N	82.8	R
R-11	7.29	07:25	147-00.86E	00-18.20N	7.30	21:27	150-39.42E	00-06.00S	50.0	R
R-12	7.30	21:27	150-39.42E	00-06.00S	7.31	00:08	151-11.48E	00-06.01S	28.0	R
R-13	7.31	00:08	151-11.48E	00-06.01S	7.31	03:15	151-38.03E	00-21.28S	9.0	R
R-14	7.31	03:15	151-38.03E	00-21.28S	8.2	21:51	155-34.42E	04-59.93S	20.3	R
R-15	8.2	21:51	155-34.42E	04-59.93S	8.3	14:28	156-01.45E	04-33.20S	44.0	R
R-16	8.3	14:28	156-01.45E	04-33.20S	8.5	03:03	156-00.00E	04-17.84S	15.8	R
R-17	8.5	03:25	155-59.98E	04-17.18S	8.5	20:03	157-24.68E	04-16.60S	158.0	R
R-18	8.5	20:03	157-24.68E	04-16.60S	8.6	21:37	157-23.65E	04-15.48S	32.0	R
R-19	8.6	21:37	157-23.65E	04-15.48S	8.8	21:32	155-59.36E	02-00.90S	71.0	R
R-20	8.8	08:32	155-59.36E	02-00.90S	8.9	15:51	155-58.54E	02-37.74S	92.5	R
R-21	8.9	15:51	155-58.54E	02-37.74S	8.9	21:23	155-58.19E	02-01.79S	5.8	R
R-22	8.9	21:23	155-58.19E	02-01.79S	8.10	03:42	155-59.30E	01-36.84S	10.0	R
R-23	8.10	03:42	155-59.30E	01-36.84S	8.10	19:55	156-03.78E	00-00.70N	13.8	R
R-24	8.10	19:55	156-03.78E	00-00.70N	8.11	19:38	155-57.98E	00-01.21S	105.0	R
R-25	8.11	19:38	155-57.98E	00-01.21S	8.12	02:12	156-08.49E	00-02.00S	18.9	R

R-26	8.21	02:16	156-08.36E	00-02.06S	8.12	22:07	156-00.55E	00-00.13N	100.3	R
R-27	8.12	22:13	156-00.60E	00-00.12N	8.13	06:47	155-59.81E	00-00.03N	81.8	R
R-28	8.13	06:50	155-59.83E	00-00.02N	8.16	05:02	156-00.15E	02-44.74N	55.2	R
R-29	8.16	05:02	156-00.15E	02-44.74N	8.17	20:48	155-58.18E	05-01.19N	7.7	R
R-30	8.17	20:48	155-58.18E	05-01.19N	8.18	20:02	155-56.53E	04-56.96N	10.8	R
R-31	8.18	20:06	155-56.43E	04-57.10N	8.19	00:46	155-57.53E	05-00.32N	8.3	R
R-32	8.19	00:46	155-57.53E	05-00.32N	8.19	02:40	155-59.50E	05-14.60N	22.7	R
R-33	8.19	02:47	155-59.54E	05-15.88N	8.19	08:20	156-00.04E	06-16.10N	40.5	R
R-34	8.19	08:22	156-00.04E	06-16.46N	8.19	20:50	156-01.60E	07-58.05N	115.0	R
R-35	8.19	20:50	156-01.60E	07-58.05N	8.22	19:11	152-45.96E	15-12.15N	170.0	R
R-36	8.22	19:11	152-45.96E	15-12.15N	8.23	19:35	151-11.15E	19-13.06N	18.0	R
R-37	8.23	19:35	151-11.15E	19-13.06N	8.26	08:50	146-01.90E	31-34.29N	2.5	R
R-38	8.26	08:50	146-01.90E	31-34.29N	8.28	00:22	142-25.51E	39-22.09N	0.8	R

**Table 7.11-2 Summary of sea surface water sampling for isotope analysis**

	Sampling No.	Date	Time (UTC)	Position	
				LON	LAT
O-	1	7.17	03:05	141-42.11E	41-15.96N
O-	2	7.18	03:01	143-03.51E	36-37.16N
O-	3	7.19	03:47	144-03.70E	32-06.77N
O-	4	7.20	03:34	144-54.24E	27-30.44N
O-	5	7.21	03:02	145-42.31E	23-02.44N
O-	6	7.22	03:02	146-32.71E	18-21.81N
O-	7	7.23	03:00	146-39.85E	13-36.17N
O-	8	7.24	03:04	146-28.74E	08-51.58N
O-	9	7.25	02:00	146-57.48E	04-58.24N
O-	10	7.26	02:06	146-55.30E	04-56.42N
O-	11	7.27	02:01	147-00.97E	02-00.18N
O-	12	7.28	02:03	146-57.86E	02-04.97N
O-	13	7.29	02:01	147-04.86E	00-00.02N
O-	14	7.30	02:00	146-58.79E	00-05.74S
O-	15	7.31	02:01	151-31.00E	00-10.72S
O-	16	8.1	01:01	153-21.05E	02-36.35S
O-	17	8.2	01:01	153-06.94E	03-08.81S
O-	18	8.3	01:03	155-47.00E	04-32.04S
O-	19	8.4	01:00	156-02.25E	05-00.16S
O-	20	8.5	01:02	155-59.89E	04-42.23S
O-	21	8.6	01:03	157-24.03E	04-16.20S
O-	22	8.7	01:00	157-22.58E	04-16.06S
O-	23	8.8	01:00	157-23.68E	04-16.58S

O-	24	8.9	01:02	155-59.90E	02-15.16S
O-	25	8.10	01:01	155-57.84E	02-01.50S
O-	26	8.11	01:00	156-08.27E	00-02.49S
O-	27	8.12	01:00	156-08.92E	00-01.34S
O-	28	8.13	01:01	155-59.56E	00-00.06N
O-	29	8.14	00:59	156-00.37E	00-15.21N
O-	30	8.15	00:53	156-01.68E	01-57.73N
O-	31	8.16	00:06	156-00.94E	02-02.46N
O-	32	8.17	01:00	156-02.09E	02-13.87N
O-	33	8.18	01:02	155-56.58E	04-58.16N
O-	34	8.19	01:00	155-58.08E	05-00.52N
O-	35	8.20	01:02	156-00.23E	07-58.71N
O-	36	8.21	01:01	156-02.25E	07-57.05N
O-	37	8.22	01:03	154-13.30E	12-13.00N
O-	38	8.23	01:00	152-35.52E	15-38.99N
O-	39	8.24	01:00	150-44.89E	20-18.64N
O-	40	8.25	02:02	148-42.01E	25-19.86N
O-	41	8.26	02:02	146-38.75E	30-09.32N
O-	42	8.27	02:01	144-32.15E	34-53.32N
O-	43	8.28	03:00	142-12.20E	39-54.36N

---

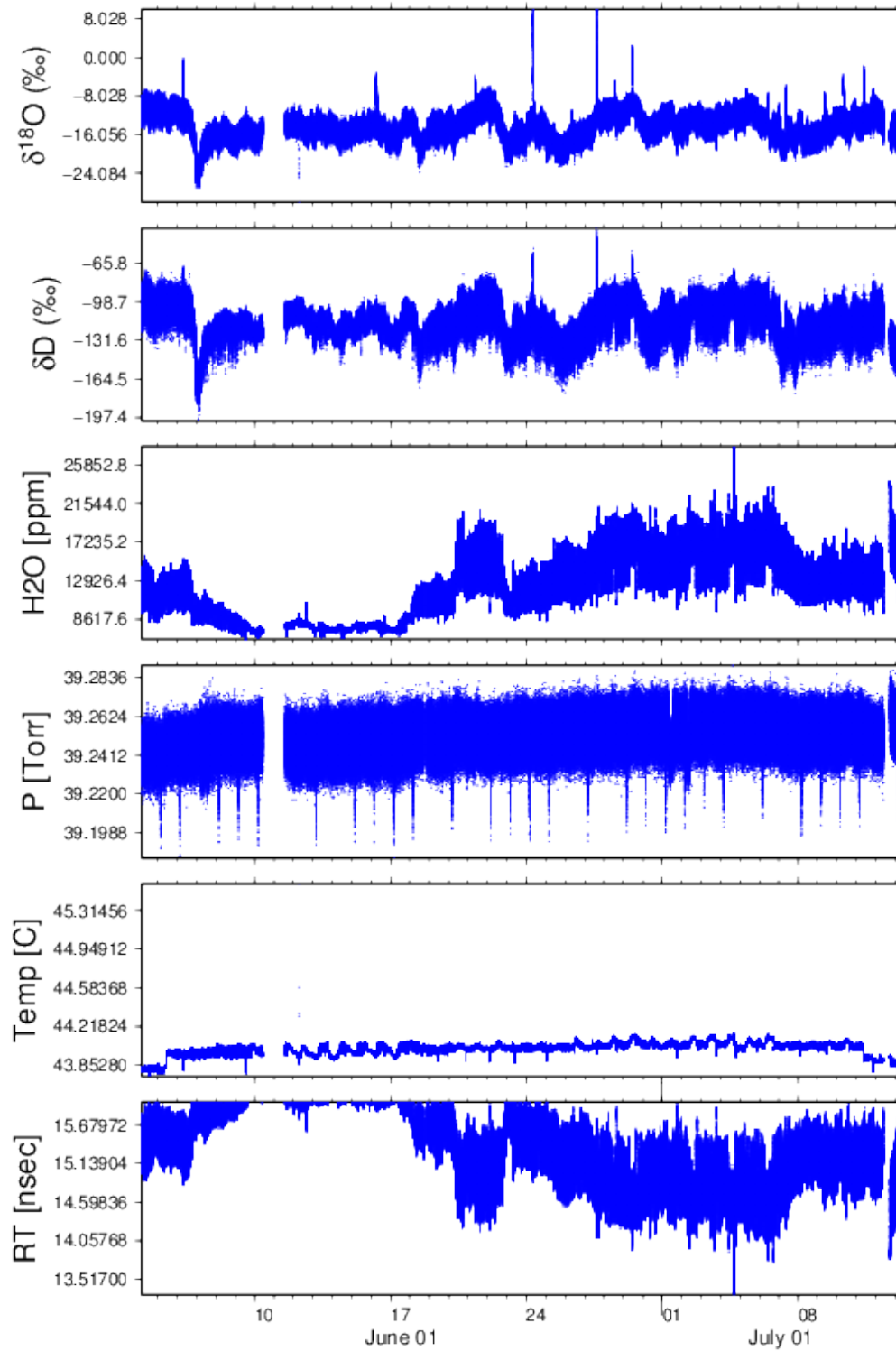


Figure 7.11-1

Continuous time-series of  $\delta^{18}\text{O}$ ,  $\delta\text{D}$ ,  $\text{H}_2\text{O}$  concentration, cavity pressure, cavity temperature, and residence time measured by the WVIA (raw data) during the MR12-02 cruise.

## 7.12 Rock sampling using a dredge

Personnel	Takeshi Hanyu (IFREE, JAMSTEC)
	Kenji Shimizu (IFREE, JAMSTEC)
	Maria L. G. Tejada (IFREE, JAMSTEC)
	Makoto Nakamura (Chiba University)
	Yohei Taketomo (Marine Works Japan Ltd.)
	Yuki Miyajima (Marine Works Japan Ltd.)
	Tetsuharu Iino (Marine Works Japan Ltd.)
	Wataru Tokunaga (Global Ocean Development Inc.)
	Harumi Ota (Global Ocean Development Inc.)
	Koichi Inagaki (Global Ocean Development Inc.)
	Ryo Ohyama (Mirai Crew)

### (1) Scientific Objectives

The Ontong Java Plateau (OJP) has been recognized to be one of the voluminous large igneous provinces (LIP) on Earth. Its volume is estimated to be at least  $6 \times 10^7 \text{ km}^3$  (e.g., Kerr and Mahoney, 2007), and the main body of OJP had been formed by magma formation and eruption in relatively short time ( $\sim 2\text{-}3 \text{ Ma}$ ). Therefore, the rate of magma emplacement at OJP exceeds any volcanisms that occur on the present Earth's surface (mid-ocean ridges, subduction zones and intra-plate volcanoes). It has been an issue of debate if such extensive and prodigious volcanism caused severe change of the oceanic environment (e.g., Tarduno et al., 1998; Larson and Erba, 1999; Tejada et al., 2009; Erba, 2010). These are the reasons why OJP is the privileged study area of many geochemists and geophysicists. There are several hypotheses proposed for the origin of OJP, including large-scale melting of upwelling lower mantle (Richards et al., 1989; Campbell, 2007; Tejada et al., 2004), mantle melting caused by meteorite impact (Rogers, 1982; Jones et al., 2002; Ingle and Coffin, 2004; Tejada et al., 2004), and shallow mantle melting facilitated by plate breakups (Anderson et al., 1992; Anderson, 2005), or mixed with recycled crustal materials (e.g., Korenaga, 2004; 2005; Lustrino, 2005).

Since OJP sits largely under the ocean, rock sampling has been thus far restricted. Malaita and Santa Isabel are the places where part of OJP crust is exposed on the surface due to its collision with the Solomon Islands (Figure 7.12-1). Ocean drilling was also attempted at several sites in the northern part of the plateau, and basement rocks have been successfully recovered by drilling through very thick sediment cover. The major findings from these studies are that (1) the first (and presumably the largest) lava emplacement took place in relatively short

time (~1 Ma) around 120 Ma ago, (2) it is followed by relatively minor emplacement around 90 Ma ago, (3) subordinate lava eruptions took place around 60 and 30 Ma ago, and (4) geochemical compositions are homogeneous compared to other LIP and hotspot volcanoes, but three types of rocks with slightly different geochemical characteristics have been recognized (Mahoney et al., 1993; Tejada et al., 2002; Fitton and Godard, 2004). Recent effort for rock sampling was to dredge the western side of OJP (Lyra Basin) with R/V Kairei in 2006 (Figure 7.12-1), which provides valuable geochemical data set to the research community (Shimizu et al., in preparation).

In this cruise (MR12-03), we try to sample rocks from a volcano (Nuugurigia) that stands in the heart of OJP (high plateau). This volcano has an atoll on the top. Its submarine flank is likely to be covered by thick sediments and marine deposits. However, some volcanic cones were discovered on the northeastern flank of the volcano during geophysical survey with R/V Kairei in 2010. These cones sit on a submarine ridge extending northeast from the central volcano. The surface of these cones shows strong acoustic reflection, documenting thin or nil sediment cover on them. It is expected that the rocks collected by dredges from these cones could provide new information on the eruption history, magma forming processes, and source compositions of OJP. We also conduct underway geophysical survey for bathymetry, gravity, and geomagnetics (c.f. Section 6.6) to study the structure of the submarine flank of the volcano.

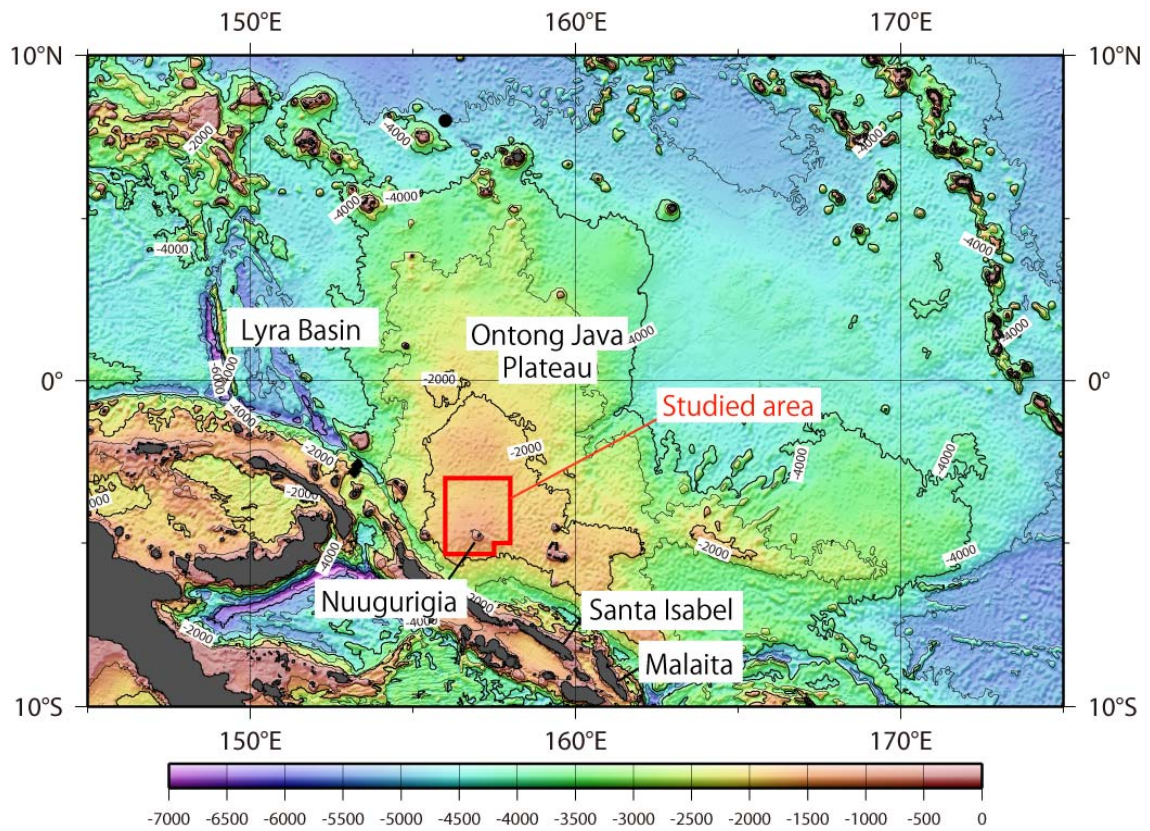


Figure 7.12-1 Bathymetric map of Ontong Java Plateau. Studied area is around the Nuugurigia atoll in the heart of the plateau (red square).

## (2) Dredge system

The dredge system during MR12-03 is illustrated in Figures 7.12-2 and 7.12-3. Chief components of the system are a transponder, a lead wire, a chain, weights, a pipe dredge, fuse wires, life wires, and a chain-bag dredge (box-type or cylinder-type). The dredge assemblages were connected with a ship-board winch wire (17mm in diameter; 24.2 ton for breaking force).

1. The transponder is used to estimate the position and depth of the dredge system. It is attached on the winch wire 50 m above its end.
2. The lead wire is 200 m long and 12 mm in diameter. The breaking force is 7.24 ton. It is connected with the winch wire by shackles (3.15 ton) and a swivel (5 ton).
3. The chain is used to stabilize the dredge on the sea floor during operation. It is 5 m long and 19 mm in diameter. It is connected with the lead wire by shackles (3.25 ton) and a swivel (5 ton).
4. The weights keep the dredge on the sea floor during operation. A weight is 50 kg. Four weights are assembled and are connected with the chain by a fuse wire (0.25 m long and 8 mm in diameter; 3.22 ton for breaking force), a life wire covered with a hose (1.7 m long and 10 mm in diameter; 5.03 ton for breaking force), shackles (2 ton), and a swivel (1 ton).
5. The pipe dredge is connected with the chain by a fuse wire (0.25 m long and 8 mm in diameter; 3.22 ton for breaking force), a life wire covered with a hose (1.0 m long and 10 mm in diameter; 5.03 ton for breaking force), shackles (0.6 ton; 1.2 ton), and a swivel (1 ton).
6. A dredge is connected with the chain by a fuse wire (0.25 m long and 8 mm in diameter; 3.22 ton for breaking force), a life wire covered with a hose (5 m long and 10 mm in diameter; 5.03 ton for breaking force), shackles (0.6 ton; 2 ton; 3.25 ton), a swivel (3 ton), and a master ring (3.2 ton). Either box-type or cylinder-type dredges were used at each dredge site. The box-type dredge has a square jaw (60 × 45 cm) with a chain-bag and a box-type bucket. The cylinder-type dredge has a round jaw (65 cm in diameter) with tied chains behind it.

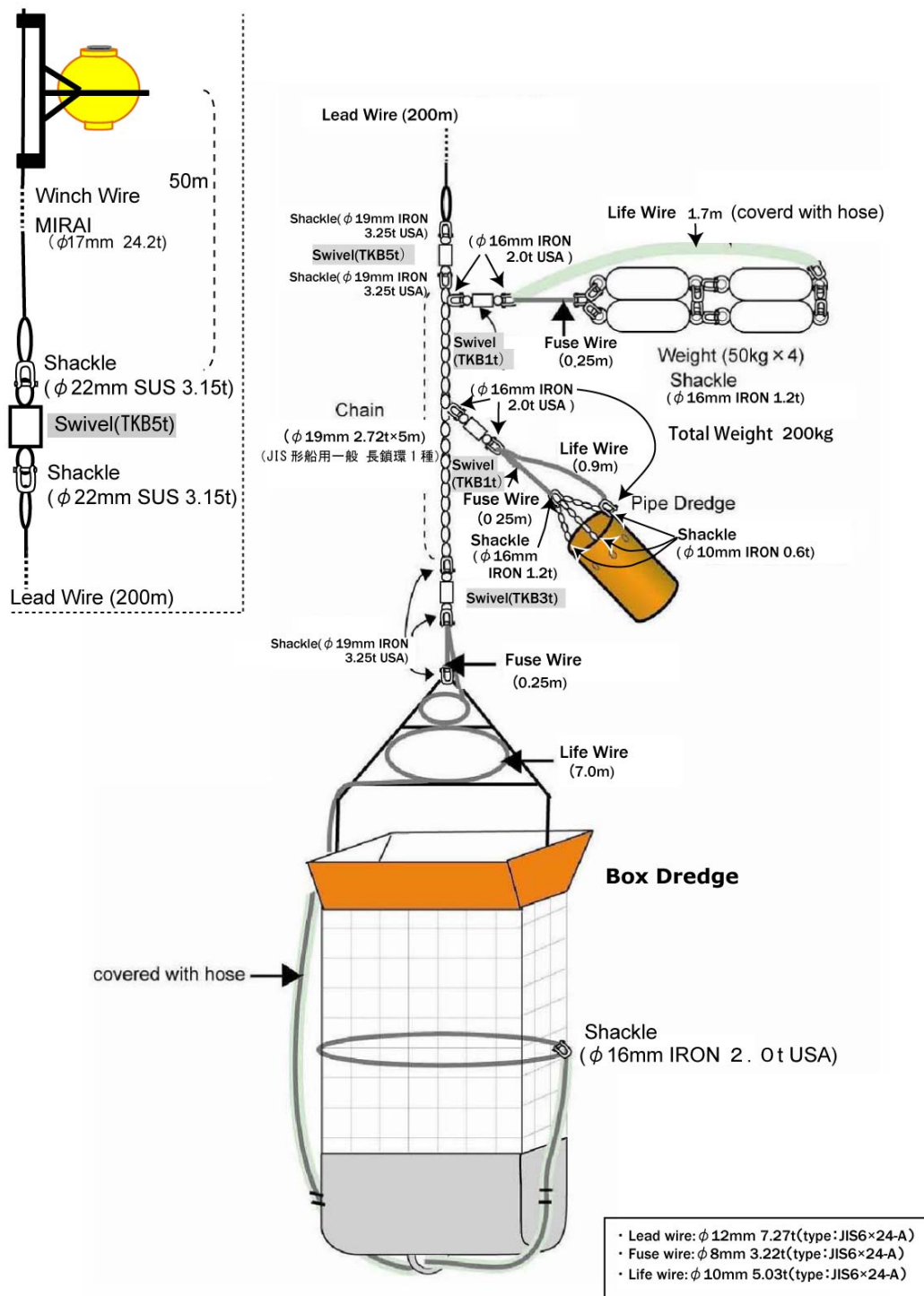
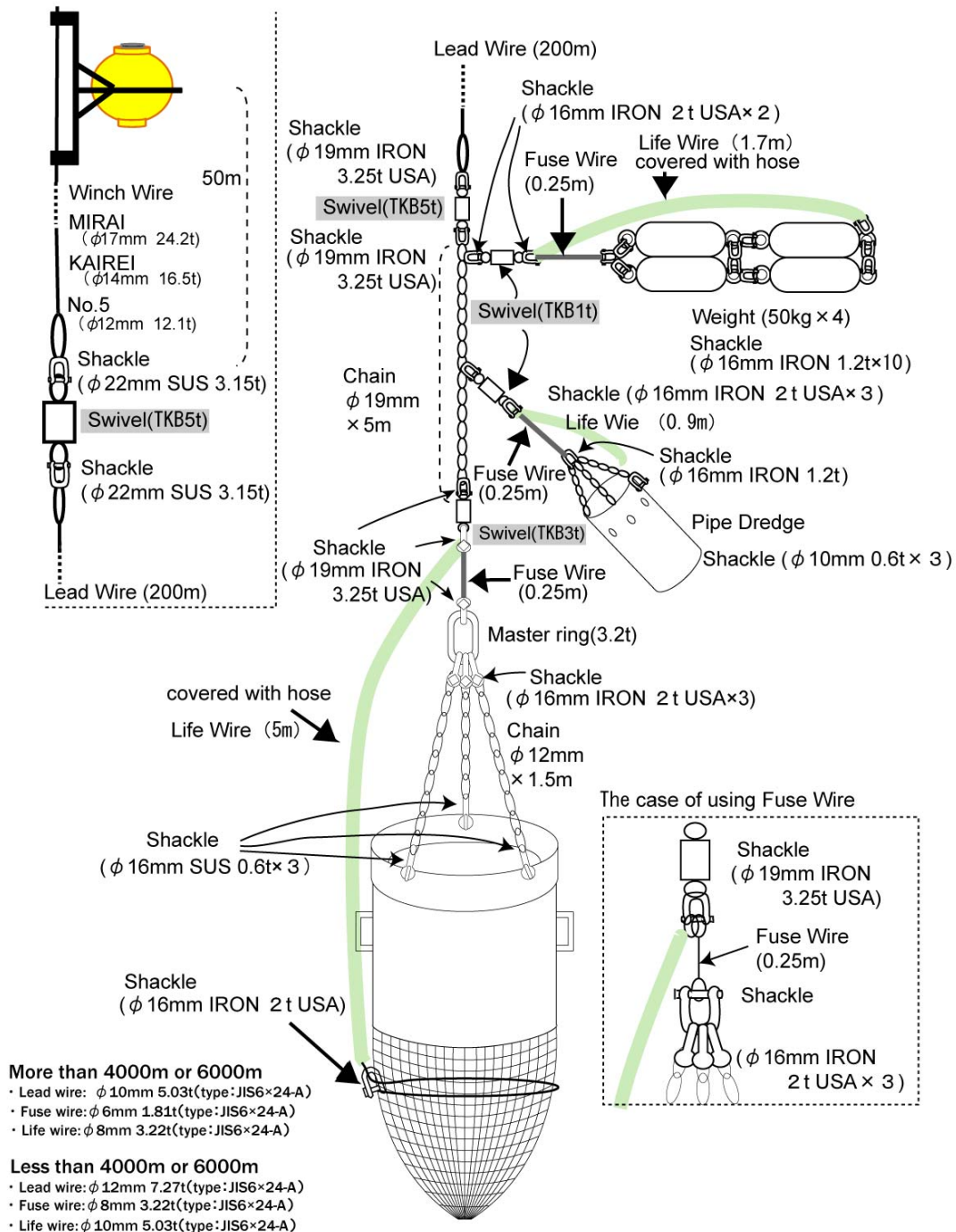


Figure 7.12-2 Dredge system with a box-type dredge.



### 大型円筒型ドレッジシステム

Figure 7.12-3 Dredge system with a cylinder-type dredge.

### (3) Results

Six dredges were conducted on the flanks of the three cones from August 6th to 8th, 2012. The dredge tracks were designed to haul the dredge on steep slopes from the bottom of the cones. The dredge tracks are shown in Figure 7.12-4. The position and depth of the dredge sites are summarized in Table 7.12-1.

#### D1 (2012/8/6)

The slope where the dredge was conducted is between two submarine ridges extending east and south on the largest cone. The dredge started at the bottom (1480 m deep) and ended halfway up of the cone. The box-type dredge was used. We had some strong bites during the dredge, although a few samples were recovered.

Recovered samples were pieces of Fe-Mn oxides and a lithic fragment. This fragment is a highly vesiculated and oxidized scoria. The maximum thickness of Fe-Mn oxides is 5 mm. Some sands with small pieces of Fe-Mn oxides were recovered in the pipe dredge.

#### D2 (2012/8/6)

The dredge was conducted on the eastern slope north of the submarine ridge extending east on the largest cone. The dredge started at the bottom (1484 m deep) and ended halfway up of the cone. The box-type dredge was used. We had some strong bites during the dredge, although a few samples were recovered again.

Recovered samples were a pillow fragment and pieces of Fe-Mn oxides. The pillow fragment is an olivine-phyric basalt with moderate visicularity. Olivines are strongly altered. The recovered sample has ~10 mm thick altered glassy margin. Mn-coat is ~5 mm thick. Some sands were also recovered in the pipe dredge.

#### D3 (2012/8/7)

The dredge was conducted on the southeastern slope of the north cone. The dredge started at the bottom (1481 m deep) and ended close to the top of the cone. The box-type dredge was used. We had some strong bites during the dredge, although a few samples were recovered, as always.

Recovered sample was Fe-Mn oxides. The maximum thickness of Fe-Mn oxides is 20 mm. A lithic fragment is included in one of Fe-Mn oxides samples. This fragment is highly altered and vesiculated. It includes altered olivines. Vesicles are filled with secondary minerals.

#### D4 (2012/8/7)

The dredge was conducted on the eastern slope of the west cone. The dredge started at the bottom (1505 m deep) and ended close to the top of the cone. The box-type dredge was used. We had some strong bites during the dredge. Finally, the dredge was stucked and the fuse wire was cut. However, samples were recovered successfully.

Recovered samples were a pumice, a volcanoclastic rock, and some pieces of Fe–Mn oxides. The pumice is highly vesiculated and altered. It may be exotic because it has no Mn-coat. The volcanoclastic rock includes some basaltic fragment that is highly vesiculated and altered. It is covered by thick Mn-coat (35mm).

#### D5 (2012/8/8)

The slope where the dredge was conducted is the same as D2 on the largest cone. The dredge started at the bottom (1478 m deep) and ended close to the top of the cone. The cylinder-type dredge was used on this day. We had some strong bites during the dredge, although a few samples were recovered, as always.

Recovered samples were a pillow fragment and a chunk of Fe–Mn oxides. The pillow fragment is an olivine-phyric basalt. Olivines are strongly altered. It is strongly vesiculated and vesicles are aligned to form some concentrated layers. Some vesicles were filled with secondary minerals. Mn-coat is 13 mm thick. The chunk of Fe–Mn oxides is 30 mm thick. It includes hyaloclastite on its edge. Some sands were also recovered in the pipe dredge.

#### D6 (2012/8/8)

The dredge was conducted on the southern slope of the largest cone. The dredge started at the bottom (1503 m deep) and ended close to the top of the cone. The cylinder-type dredge was used. We had some strong bites during the dredge. Finally, the dredge was stucked and the fuse wire was cut. However, samples were recovered successfully.

Recovered samples were some large pieces of Fe–Mn oxides and a pumice. The Fe–Mn oxides had some lithic fragments (oxidized scoria) on one side. One rock was associated with carbonates. The maximum thickness of Fe–Mn oxide fragments is 35 mm. The pumice is highly vesiculated and altered. It may be exotic because it has only very thin Mn-coat. Some sands with small pieces of Fe–Mn oxides were also recovered in the pipe dredge.

#### (4) Interpretations

Recovered samples show a wide variety of rock types, including pillow basalt, scoria,

pumice, and hyaloclastite. Pumices would be exotic as they have film (or nil) of Mn-coat. However, we suggest that scoria fragments are in-situ (either from the cones or the Nuugurigia volcano) because we recovered several samples including scoria covered by thick Fe–Mn oxides at the same dredge site (D6). Some other scoria fragments with similar texture were also recovered at other dredge sites. The presence of scoria and hyaloclastite indicates subaerial or shallow-water submarine eruption. In contrast, the cones were also formed by submarine eruption, as suggested by the emplacement of pillow lavas. The thickness of Mn-coat on these rocks varies, ranging from 5 to 35 mm. This fact may suggest multiple eruption history, although further post-cruise study is required to explore it.

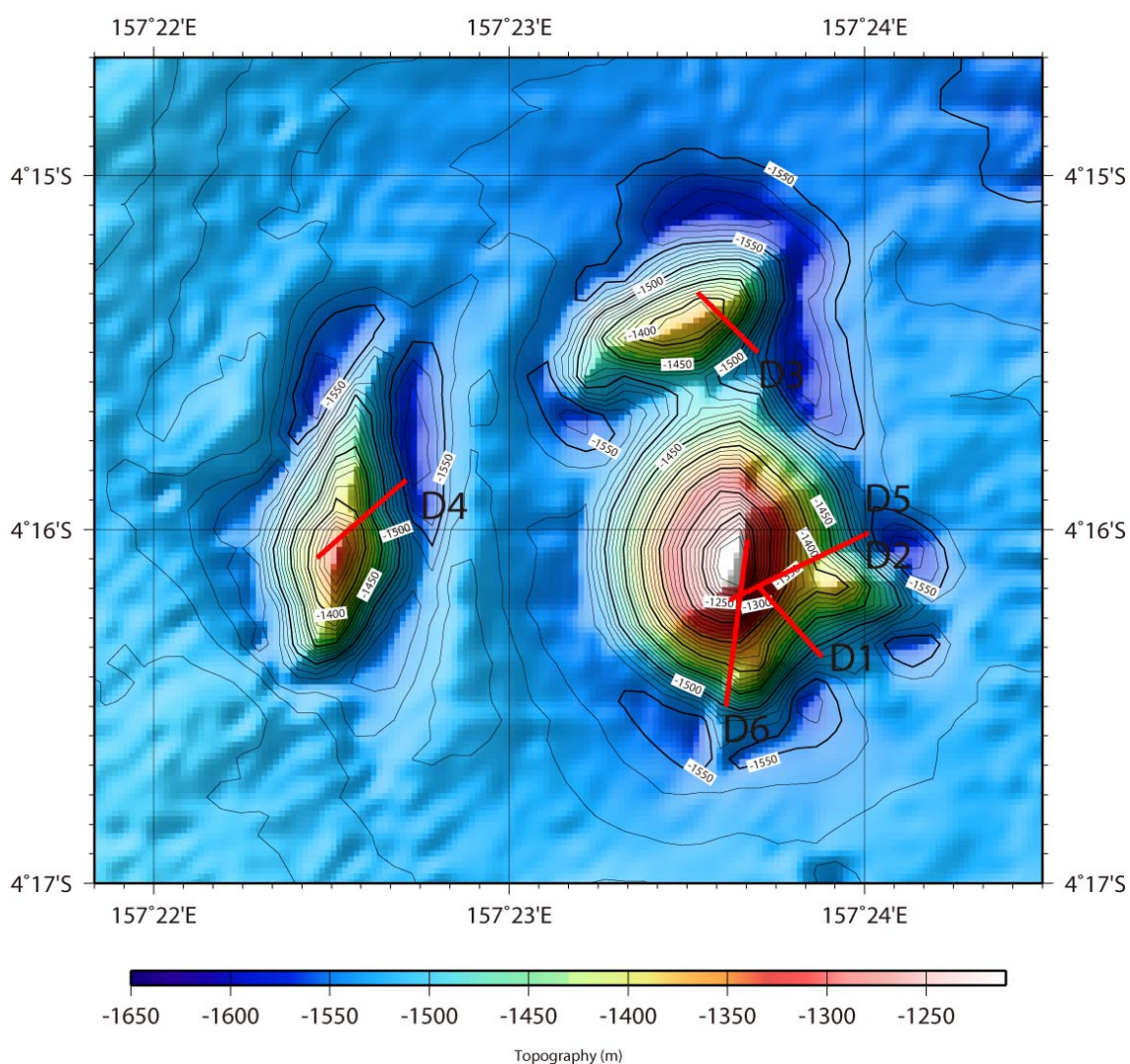


Figure 7.12-4 Bathymetric map of the studied cones. The dredge tracks are shown by red lines annotated by dredge number.

Date (UTC)	Dredge number	Location	On the bottom				Off the bottom				Depth (m)		Tension max. (t)	Survey time
			Lat. (SOQ)	Lon. (SOQ)	Lat. (SOJ)	Lon. (SOJ)	Lat. (SOQ)	Lon. (SOQ)	Lat. (SOJ)	Lon. (SOJ)	On the bottom	Off the Bottom		
2012/8/5	D1	Off northeast Nuugurigia	4-16.3557 S	157-23.8829 E	4-16.3432 S	157-23.8427 E	4-16.1770 S	157-23.7257 E	4-16.1495 S	157-23.6662 E	1,480	1,223	4.3	55min.
2012/8/6	D2	Off northeast Nuugurigia	4-16.0044 S	157-24.0136 E	4-16.0135 S	157-23.9707 E	4-16.1445 S	157-23.7463 E	4-16.1832 S	157-23.6545 E	1,484	1,232	4.5	60min.
2012/8/6	D3	Off northeast Nuugurigia	4-15.4886 S	157-23.6899 E	4-15.4722 S	157-23.6604 E	4-15.3511 S	157-23.5437 E	4-15.3119 S	157-23.4866 E	1,481	1,453	4.6	50min.
2012/8/7	D4	Off northeast Nuugurigia	4-15.8482 S	157-22.7044 E	4-15.8858 S	157-22.6799 E	4-16.0086 S	157-22.5384 E	4-16.0930 S	157-22.4590 E	1,505	1,413	4.5	57min.
2012/8/7	D5	Off northeast Nuugurigia			4-16.0344 S	157-23.9766 E			4-16.1922 S	157-23.6502 E	1,478	1,246	4.3	1h2min.
2012/8/8	D6	Off northeast Nuugurigia	4-16.5276 S	157-23.6123 E	4-16.4841 S	157-23.6111 E	4-16.2815 S	157-23.6371 E	4-16.1612 S	157-23.6529 E	1,503	1,220	4.4	1h26min.

\*SOQ = Transponder's position, SOJ = Ship's position  
\*Transponder did not work on D5.

Table 7.12-1 Summary table for six dredges in MR12-03.

Even log for dredges and night surveys around Nuugurigia.

Date	LTC (UTC+11h Narrative)
2012/8/5	approx. 13:30 Assemble dredge on rear deck (MWJ). approx. 18:00 Sub-bottom profiler on; Start underway survey from the CTD point.
2012/8/6	approx. 4:00 Pass over the cones for dredges. approx. 6:00 Pass over the cones for dredges again; Confirm strong acoustic reflection on the cones. approx. 7:30 Preparation for dredge operation. 7:57 Start operation (D1); Wire out. 8:56 Dredge on the bottom; Start the ship. 9:25 Stop the ship; Keep its position; Wire in. 9:51 Dredge off the bottom. 10:27 Dredge on deck. 12:52 Start operation (D2); Wire out. 13:46 Dredge on the bottom; Start the ship. 14:28 Stop the ship; Keep its position; Wire in. 14:46 Dredge off the bottom. 15:22 Dredge on deck. approx. 16:00 Deploy cesium magnetometer; Start underway survey.
2012/8/7	approx. 7:30 Preparation for dredge operation. 7:55 Start operation (D3); Wire out. 8:49 Dredge on the bottom; Start the ship. 9:17 Stop the ship; Keep its position; Wire in. 9:39 Dredge off the bottom. 10:19 Dredge on deck. 12:53 Start operation (D4); Wire out. 13:49 Dredge on the bottom; Start the ship. 14:27 Stop the ship; Keep its position; Wire in. 14:37 Fuse wire broken. 14:46 Dredge off the bottom. 15:32 Dredge on deck. approx. 16:00 Deploy cesium magnetometer; Start underway survey.
2012/8/8	approx. 7:30 Preparation for dredge operation. 7:53 Start operation (D5); Wire out. 8:49 Dredge on the bottom; Start the ship. 9:33 Stop the ship; Keep its position; Wire in. 9:51 Dredge off the bottom. 10:27 Dredge on deck. 12:53 Start operation (D6); Wire out. 13:13 Dredge on the bottom; Start the ship. 14:10 Stop the ship; Keep its position; Wire in. 14:43 Fuse wire broken. 14:49 Dredge off the bottom. 15:31 Dredge on deck. approx. 16:00 Disassemble dredge (MWJ); Start underway survey to the Triton buoy point.
2012/8/8	approx. 6:00 End underway survey; Stop sub-bottom profiler.

Table 7.12-2 Event log for dredges and underway geophysical survey around Nuugurigia.

(5) Remarks for topography and structure of Nuugurigia; preliminary results of underway geophysical survey

Geophysical survey was conducted during the transit into/out of the dredge sites and at night time between dredges with multi narrow beam echo sounding system, sub-bottom profiler, towing cesium magnetometer, ship-board three-component magnetometer, and gravity meter (c.f. Section 6.6). The chief objectives of underway geophysical survey are (1) to confirm the topography of the cones where we dredge, (2) to explore the submarine structure of the Nuugurigia volcano on which the cones sits, and (3) to find other cones where there are possible loci of peripheral eruptions of the volcano. The survey tracks were designed to traverse the northern and western flanks of Nuugurigia (Figure 7.12-5).

We passed over the dredge sites several times to obtain precise bathymetry, acoustic reflection, and sub-bottom profiling data for the cones. We confirmed that the cones have thin or nil sediment covers on their slopes. The largest cone has a conical shape with two ridges extending east and south. The north and west cones are different from the largest cone in terms of topography; they have a characteristic elongated shape. Orientations of the north and west cones together with the ridges on the largest cone seem to be random.

During the survey on the flanks of Nuugurigia, we found several cones that are similar to the cones, where we dredged, in terms of shape and size. They also have strong acoustic reflection, suggesting thin or nil sediments on the cones, like the cones we dredged. Although the surveyed area is limited, the cones are clustered near the dredge sites. We assume that the region around dredge sites is the place of repeated peripheral eruption on a northeast-trending submarine ridge of the Nuugurigia volcano. The cones we found in this cruise would be potential sites for future dredges and dives.

The data for gravity and geomagnetics will be processed and analyzed to explore the structure of the Nuugurigia volcano after the cruise.

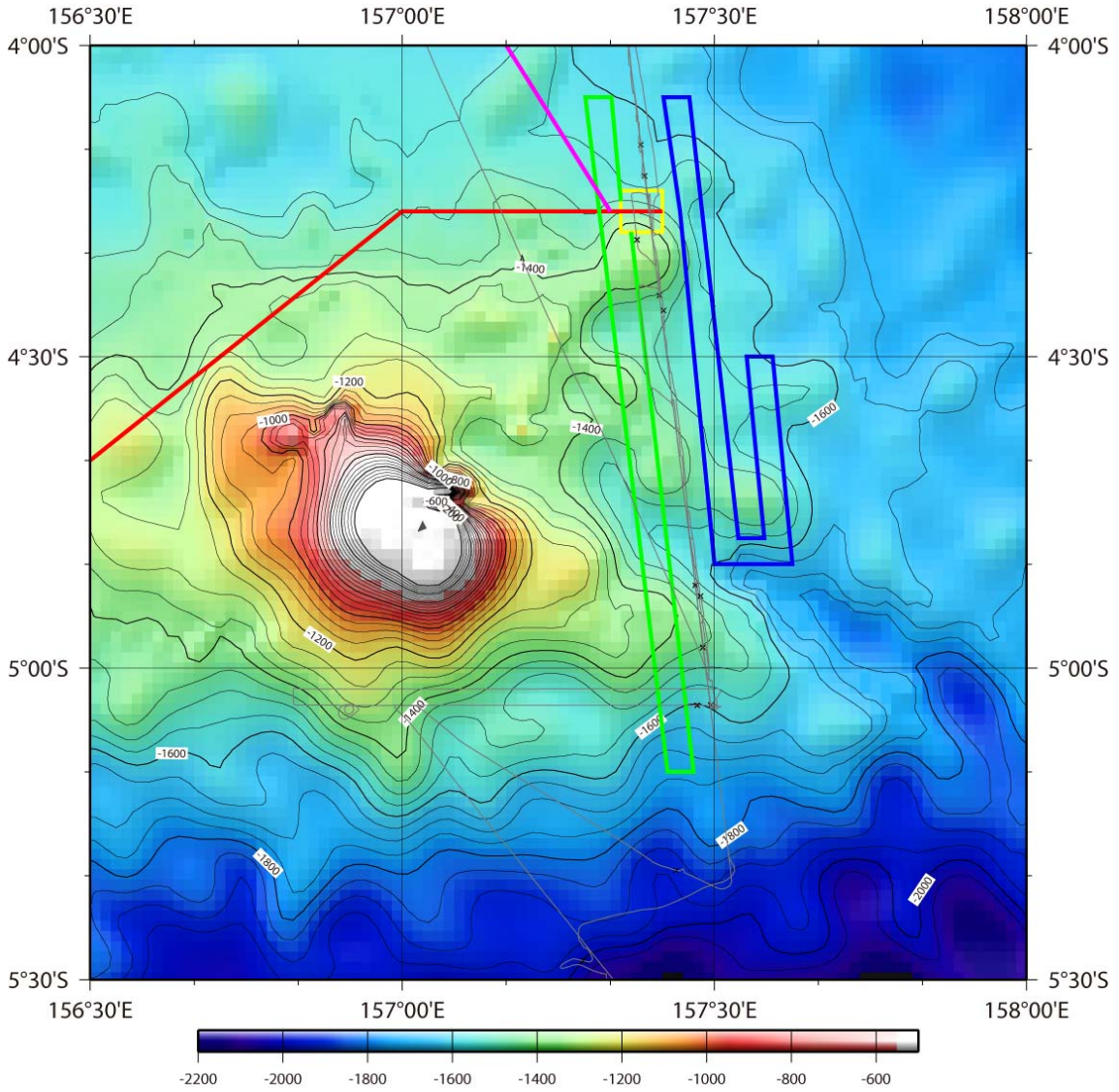


Figure 7.12-5 Bathymetric map around Nuugurigia. Tracks for underway geophysical survey are shown by colored lines: red; August 5th, green; August 6th, blue; August 7th, and pink; August 8th. Thin gray thin lines are survey tracks by previous cruises.

## References

1. Anderson, D. L., 2005. Large Igneous Provinces, delamination, and fertile mantle. *Elements* 1, 271-275.
2. Anderson, D. L., Zhang, Y-S., Tanimoto, T., 1992. Plume heads, continental lithosphere, flood basalts, and tomography. In: Storey, B. C., Alabaster, T., and Pankhurst, R. J. (eds) *Magmatism and Causes of Continental Break-up. Geol. Soc. London Spec. Pub.* 68, 99-124.
3. Campbell, I. H., 2007. Testing the plume theory. *Chem. Geol.* 241, 153-176.
4. Erba, E., Bottini, C., Weissert, H. J., and Keller, C. E., 2010. Calcareous nannoplankton response to surface-water acidification around oceanic anoxic event 1a. *Science* 329, 428-432.
5. Larson, R. L. and Erba, E., 1999. Onset of the mid-Cretaceous greenhouse in the Barremian-Aptian: igneous events and the biological, sedimentary, and geochemical responses. *Paleocean.* 14, 663-678.
6. Fitton, J. G. and Godard, M., 2004. Origin and evolution of magmas on the Ontong Java Plateau. In: Fitton, J. G., Mahoney, J. J., Wallace, P. J. and Saunders, A. D. (eds) *Origin and Evolution of the Ontong Java Plateau. Geological Society (London) Special Publication* 229, 151-178.
7. Ingle, S., Coffin, M. F., 2004. Impact origin for the greater Ontong Java Plateau? *Earth Planet. Sci. Lett.* 218, 123-134.
8. Jones, A. P., Price, G. D., Price, N. J., De Carli, P. S., Clegg, R. A., 2002. Impact induced melting and the development of large igneous provinces. *Earth Planet. Sci. Lett.* 202, 551-561.
9. Kerr, A. C. and Mahoney, J. J., 2007. Oceanic plateaus: Problematic plumes, potential paradigms. *Chem. Geol.* 241, 332-353.

10. Korenaga, J., 2004. Mantle mixing and continental breakup magmatism. *Earth Planet. Sci. Lett.* 218, 463-473.
11. Korenaga, J., 2005. Why did not the Ontong Java Plateau form subaerially? *Earth Planet. Sci. Lett.* 234, 385-399.
12. Lustrino, M., 2005. How the delamination and detachment of lower crust can influence basaltic magmatism. *Earth-Sci. Rev.* 72, 21-38.
13. Mahoney, J. J., Storey, M., Duncan, R. A., Spencer, K. J., Pringle, M., 1993. Geochemistry and geochronology of the Ontong Java Plateau. In: Pringle, M., Sager, W., Sliter, W., and Stein, S. (eds) *The Mesozoic Pacific. Geology, Tectonics, and Volcanism.* AGU Geophys. Monogr. 77, 233-261.
14. Richards, M. A., Duncan, R. A., and Courtillot, V., 1989. Flood basalts and hotspot tracks: plume heads and tails. *Science* 246, 103-107.
15. Rogers, G. C., 1982. Oceanic plateaus as meteorite impact signatures. *Nature* 299, 341-342.
16. Tarduno, J. A., Brinkman, D. B., Renne, P. R., Cottrell, R. D., Scher, H. and Castillo, P., 1998. Evidence for extreme climatic warmth from Late Cretaceous Arctic vertebrates. *Science* 282, 2241-2244.
17. Tejada, M. L. G., J. J. Mahoney, C. R. Neal, R. A. Duncan, and M. G. Petterson, 2002. Basement geochemistry and geochronology of Central Malaita, Solomon Islands, with implications for the origin and evolution of the Ontong Java Plateau. *J. Petrol.* 43, 449-484.
18. Tejada, M. L. G., J. J. Mahoney, P. R. Castillo, S. P. Ingle, H. C. Sheth, and D. Weis, 2004. Pin-pricking the elephant: Evidence on the origin of the Ontong Java Plateau from Pb-Sr-Hf-Nd isotopic characteristics of ODP Leg 192 basalts. In: Fitton, J. G. et al. (eds) *Origin and Evolution of the Ontong Java Plateau.* Geol. Soc.(London) Spe. Pub. 229, 133-150.

19. Tejada, M. L. G., Suzuki, K., Kuroda, J., Coccioni, R., Mahoney, J. J., Ohkouchi, N., Sakamoto, T., and Tatsumi, Y., 2009. Ontong Java Plateau eruption as a trigger for the Early Aptian oceanic event. *Geology* 37, 855-858.